

AN INVESTIGATION OF ELECTROANALYTICAL
TECHNIQUES APPLICABLE TO ELECTROLYTIC POLYMERIZATIONS.

A Thesis

Presented to

The Faculty of Graduate Studies and Research

The University of Manitoba

In Partial Fulfillment

of the Requirements for the Degree

Doctor of Philosophy

by

Derek Geoffrey Gray

April 1968



ACKNOWLEDGMENTS

The author wishes to thank most sincerely, Dr. B. L. Funt for his encouragement and help at all stages in the preparation of this thesis.

The financial support of Chemcell Limited in the form of a Chemcell Graduate Fellowship, 1966-1968, is gratefully acknowledged.

Thanks are also due to Mr. George Epp for his skilled glass-blowing, and to the electronics shop of the Physics Department, University of Manitoba for constructing some electronic equipment.

Not least, the author would like to thank all those staff and graduate students in the Department of Chemistry, University of Manitoba who freely offered much friendly assistance.

ABSTRACT

Electrolytically initiated polymerizations have in general been performed either with constant current or constant voltage. The purpose of this thesis was to investigate controlled electrode potential techniques for the study of electrochemical polymerizations. Styrene and methyl methacrylate were electrolysed at a controlled cathode potential in dimethylformamide with tetrabutylammonium salts as supporting electrolytes. Polymer was isolated when the monomer concentration was sufficiently high; the chain initiation was shown to involve direct electron transfer to monomer. Product analysis, coulometry and voltammetric measurements at a stationary platinum electrode showed that the nature of the products formed by electrolysis depended on the relative concentrations of monomer and supporting electrolyte.

The feasibility of using cyclic voltammetry to study electron transfer mechanisms in tetrahydrofuran under vacuum conditions was demonstrated using diphenylpicrylhydrazyl as a model electroactive substance. In this system, voltammograms indicated that a relatively stable cation, radical, anion, dianion radical and trianion were formed in an unusual series of reversible electron transfer steps. Cyclic voltammetry under similar conditions was used to study the electrolytic reduction of acenaphthylene, acenaphthene, 1,1-biacenaphthylidene, 1,1-diacenaphthenylidene, tetraphenylethylene, triphenylethylene, stilbene, 1,1-diphenylethylene and styrene. The

anodic scan data provided evidence for the electrolytic reoxidation of carbanionic species derived from the primary reduction products, and helped to clarify the reduction processes. The various reduction mechanisms were related to hydrocarbon structure; results relevant to electroinitiated anionic polymerizations were indicated. Application of the voltammetric technique to novel solvent/electrolyte systems, to electrolyte discharge and to the electrolytic generation of monomer were briefly examined.

TABLE OF CONTENTS

INTRODUCTION

Page

ELECTROLYTICALLY CONTROLLED POLYMERIZATIONS

Anodic Free Radical Initiation.....	1
Cathodic Free Radical Initiation.....	3
Ionic Polymerizations.....	5
Electro-initiated Anionic Polymerization of Acrylonitrile.....	6
Other Electroinitiated Ionic Polymerizations.....	8
Electrolytic Control of Chain Propagation.....	12
Electrolytic Polymerizations - Conclusions.....	14

ELECTROCHEMICAL METHODS

Introduction.....	15
Methods Applicable to this Investigation.....	18
Some Theoretical Considerations.....	18
Controlled Potential Electrolysis.....	20
Current-Potential Curves.....	27
Voltammetric Methods; Reversible Processes.....	32
Irreversible Processes.....	39
Quasi-reversible Processes.....	40
Coupled Chemical Reaction.....	41
Non-Faradaic Effects.....	43
Summary.....	44

EXPERIMENTAL METHODS

Materials.....	45
Apparatus.....	46
Method.....	50
Accuracy of Voltammograms.....	52

RESULTS AND DISCUSSION

CONTROLLED-POTENTIAL ELECTROLYSES.....	53
VOLTAMMETRY AND MONOMER CONCENTRATION.....	62
A DETAILED STUDY OF SELECTED ELECTROLYTIC REACTIONS USING CYCLIC VOLTAMMETRY.....	67

	Page	
The Redox Behavior of Diphenylpicrylhydrazyl.....	67	
Cyclic Voltammetry of Acenaphthylene, a Model Polymerizable Compound.....	72	
Application of Cyclic Voltammetry to the Reduction of Phenyl-substituted Ethylenes.....	81	
INVESTIGATION OF ALTERNATIVE ELECTROLYTE SYSTEMS		
Acenaphthylene Reduction in Tetrahydrofuran with Sodium Tetraphenylboride as Electrolyte.....	92	
α -Methylstyrene Reduction in Hexamethylphosphoramide with Tetramethylammonium Tetraphenylboride as Electrolyte.....	97	
OTHER APPLICATIONS OF CYCLIC VOLTAMMETRY TO ELECTROPOLYMERIZATIONS		
Mechanism of Salt Discharge.....	100	
Electrolytic Formation of Highly Reactive Monomer.....	100	
CONCLUSIONS.....		102
REFERENCES.....		105

LIST OF FIGURES

Figure		Page
1	Operating Principle of the Wenking Electronic Potentiostat..	22a
2	Idealized Current-potential Curves.....	32a
3	Single Cycle Voltammogram for a Reversible Electron Transfer.....	33a
4	Theoretical Voltammetric Curves.....	37a
5	Arrangement of Apparatus for Cyclic Voltammetry.....	48a
6	Cell for Controlled Potential Electrolysis.....	49a
7	Cell for Cyclic Voltammetry.....	49b
8	Cell for esr Measurements.....	50a
9	Current/Potential Plots for the Reduction of Methyl Methacrylate and Styrene at a Platinum Electrode.....	55a
10	Current/Potential Plots for α -Methylstyrene in Sodium Tetrphenylboride Solution.....	56a
11	The Effect of Monomer Concentration on Current/Potential Plots.....	56a
12	Graph of the Decrease in Monomer Concentration with Amount of Electricity Passed during the Controlled-Potential Polymerization of Styrene and Methyl Methacrylate.....	57a
13	Controlled Potential Electrolysis of Styrene at Low Concentration in Anhydrous Dimethylformamide: (a) Graph of Electrolysis Current versus Electrolysis time; (b) Graph of Amount of Styrene in the Catholyte versus quantity of Electricity Consumed.....	60a
14	Variation of Voltammetric Peak Current Density with Monomer Concentration; Effect of Salt Concentration.....	63a
15	Variation of Voltammetric Peak Current with Monomer Concentration; Low Concentration Data from Figure 14 Replotted on a Larger Scale.....	65a

Figure

Page

16	Cyclic Voltammogram for Diphenylpicrylhydrazyl.....	68a
17	Effect of Scan Rate Increase on the Voltammetric Peak for the Process $\text{DPPH} \cdot + e = \text{DPPH}^-$	69a
18	Cyclic Voltammogram for the First Reduction Step of Acenaphthylene.....	73a
19	Cyclic Voltammogram for Acenaphthylene Reduction Showing the Four Electron Transfer Steps Involved.....	74a
20	The Variation of Acenaphthylene Peak Currents with the Square Root of the Scan Rate.....	74b
21	Possible Mechanisms for the Electrolytic Reduction of Acenaphthylene.....	75a
22	Cyclic Voltammograms with Asymmetric Potential Scan for Acenaphthylene.....	76a
23	Variation of Acenaphthylene Peak Current with the Square Root of the Reverse Scan Rate.....	76b
24	Asymmetric Scan Voltammogram for 1,1-Diacenaphthenylidene..	79a
25	Cyclic Voltammogram for the Reduction of Tetraphenylethylene	82a
26	Cyclic Voltammogram for the Reduction of Triphenylethylene..	83a
27	The Rate of Change of Cathodic and Anodic Peak Heights with the Square Root of the Scan Rate for Triphenylethylene.	85a
28	Cyclic Voltammogram for Trans-stilbene.....	86a
29	Cyclic Voltammogram with Asymmetric Potential Scan for 1,1-Diphenylethylene.....	87a
30	Cyclic Voltammogram for the Reduction of Styrene.....	88a
31	A Comparison of Cyclic Voltammograms for Phenyl- substituted Ethylenes.....	88b
32	Theoretical Variation of Peak Potential with Peak Current as the Scan Rate is Increased.....	90a
33	Cyclic Voltammogram of Acenaphthylene in Sodium Tetraphenylboride-tetrahydrofuran Solution.....	93a

Figure	Page
34 Cyclic Voltammograms for α -Methylstyrene in Hexamethyl- Phosphoramide with Tetramethylammonium Tetrphenylboride as Supporting Electrolyte.....	97a
35 Cyclic Voltammogram for α,α' -Dibromo-p-xylene in Dimethylformamide.....	101a

LIST OF TABLES

Table		Page
I	Voltammetric Data for Diphenylpicrylhydrazyl.....	69b
II	Cyclic Voltammetric Data for Acenaphthylene and Related Compounds.....	77a
III	Cyclic Voltammetric Data for Phenyl-substituted Ethylenes.....	88c
IV	A Summary of the Relative Stabilities of the Anionic Species Derived from Phenyl-substituted Ethylenes under Voltammetric Conditions.....	91a

INTRODUCTION

The controlled initiation of polymerizations by electrolytic means has been demonstrated for a variety of systems. In most studies, the emphasis has been on the polymerization phenomena; less attention has been paid to the nature of the electrode processes and the initial interactions of the species formed. This thesis is concerned with the development of suitable electrochemical methods, and their application to some polymerization reactions. It is hoped that such studies will broaden the scope of electrolytically controlled polymerizations.

In this introduction, a brief survey of previous electrolytic polymerizations will be given. This will be followed by a development of the theory relevant to electrochemical methods used in this investigation.

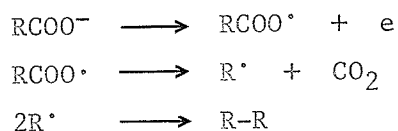
ELECTROLYTICALLY CONTROLLED POLYMERIZATIONS

The field of electrolytically controlled polymerizations has been reviewed recently (1,2,3,4) so that detailed treatment in this thesis is unnecessary. However, the electrolytic processes used to produce polymerization will be outlined, with special reference to electrochemical investigations of the mechanisms involved. Recent developments in the field will be introduced. Electrochemical methods used to determine the kinetics of conventionally initiated polymerizations (5,6) will not be considered here.

Anodic Free Radical Initiation.

One of the earliest electro-organic synthetic procedures was

developed by Kolb  in 1849. The reaction involved the discharge of an aliphatic carboxylate anion to give a hydrocarbon; the generally accepted mechanism may be written:



The free radical intermediates may function as initiators for vinyl polymerization (7); acetate ions have been employed most frequently for this purpose. Although some polymerization does occur in aqueous, essentially heterogeneous systems (8), it is advantageous to use homogeneous systems where the monomer and polymer are both readily soluble. Thus a high monomer concentration in solution favours chain initiation and propagation over radical side reactions, and if the polymer is readily soluble, the formation of an insulating polymeric coating on the electrode is less likely.

Homogeneous polymerization systems may be achieved by electrolysis of water-soluble monomers such as acrylic acid in aqueous acetate solutions (9,10). Alternatively, homogeneity may be produced by using solvent mixtures in which monomer, polymer and electrolyte are soluble. For example, Funt and Yu (11) studied the polymerization of methyl methacrylate initiated by the electrolysis of a variety of acetate salts in dimethylsulphoxide. The same monomer was used by Tsvetkov and Koval'chuk (12) in water and aqueous ethanol, methanol, acetone and glycol. Only in aqueous glycol did they report good yields of polymer. Shapoval (13) studied the effect of some inhibitors on the electrolytic polymerization of acrylonitrile in dimethylformamide with sodium acetate as electrolyte.

Little attempt has been made to investigate the initiating mechanism electrochemically because of the complexity of the processes in these systems. Indeed, the mechanism of the simple Kolb  reaction, without added monomer, is still a subject of controversy (14). The importance of species adsorbed on the electrode has been stressed in a recent review by Vijn and Conway on the electrode kinetic aspects of the Kolb  reaction (15). The results of a variety of electrochemical techniques lead the authors to conclude that the radicals form and react on the electrode surface rather than desorb and diffuse into the bulk of the solution before reaction. It is unclear in this case how polymerization takes place.

Some caution is necessary in interpreting the results of polymerizations initiated by the electrolysis of acetate salts. Das and Palit (16) and recently Tidswell (17) electrolysed alkali metal acetates in the presence of methyl methacrylate. In both cases, polymer formation occurred at the cathode rather than by the expected anodic Kolb  process.

Cathodic Free Radical Initiation.

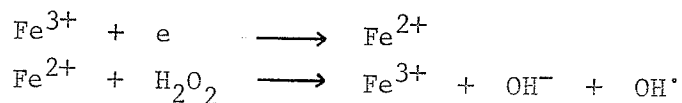
Following the early reports of electroinitiated polymerization by Wilson et al. (18), it was found that many monomers polymerized by a free radical mechanism initiated in acidic aqueous solutions at the cathode (19,20,21,22). Under the experimental conditions used, it was assumed that the cathodic discharge of hydronium ions produced hydrogen atoms which initiated polymerization. This hypothesis was supported by the relationship between the hydrogen overpotential of the

cathode metal and its efficiency in initiating polymerization; hydrogen adsorbed, presumably as atoms, on metal surfaces was shown to initiate polymerization. Hydrogen atom initiation was also proposed for the electrolytic polymerization of methyl methacrylate using an alternating current (23).

Fedorova et al. (24,25) criticized the experimental basis for these results because, in common with most electrolytic polymerizations to date, no attempt was made to measure or control the electrode potential, and oxygen was not rigorously excluded from the reaction cell. Using polarography, controlled potential electrolyses, and careful purification procedures, these workers concluded that the electrolytic reduction of oxides or of peroxides, formed by exposure of the monomer to air, was in fact necessary for the initiation of these polymerizations. However, the presence of oxygen also inhibited the chain propagation step. Discrepancies remain among results reported for these systems, and further studies, paying due attention to the control of electrochemical variables are necessary.

Several other cathodic processes have been used to generate free radicals for polymer chain initiation. In a recent paper, Fedorova and Vasina (26) reported that during the reduction of pyridine in acid solution, an insoluble polymer formed by a free radical ring-opening reaction. No details of yields or electrical efficiencies were presented. Kolthoff and Ferstandig (27) used both the electrolytic reduction of persulphate ion and the electrolytic regeneration of Fenton's reagent to initiate the polymerization of acrylonitrile.

The initiation using Fenton's reagent:



apparently produced a high yield of polymer at a current efficiency of 1,300 moles of acrylonitrile polymerized per mole of ferrous ions produced. This was several orders of magnitude higher than that usually found in free radical systems. Polarization curves were determined for these electrolyses, and an attempt was made to correlate the electrochemical data with the yields of polymer obtained.

The low electrical efficiency of most free radical systems deserves some comment. It stems in general from the wide variety of side reactions that free radicals may undergo, especially when formed at high concentrations close to the electrode or in the adsorbed state. Dimerization, disproportionation, solvent attack or reaction with the electrode metal are all possibilities which interfere with chain initiation and propagation. In the one reported case where highly efficient initiation took place, mentioned above, the initiating hydroxyl radical is formed in the bulk of the solution rather than in the primary electrochemical step.

Ionic Polymerizations.

A higher degree of electrical efficiency would be expected for polymerizations occurring by ionic chain mechanisms because the bimolecular side reactions of free radicals cannot occur with ionic species. In addition, the initiating step for ionic polymerizations involves in general the formation of a charged rather than a neutral

species at the electrode surface. The resultant electrostatic repulsion between the electrode surface and the ionic species formed makes adsorption less favourable, and so promotes homogeneous polymerization. The potentialities of initiating both anionic and cationic polymerizations electrolytically were first demonstrated by Breitenbach (28) using strictly non-aqueous solvents and a variety of tetra-alkylammonium salts. The nature of the polymerization was determined using inhibitors and copolymerization studies.

Electro-initiated Anionic Polymerization of Acrylonitrile.

Breitenbach (28) briefly investigated the anionic polymerization of acrylonitrile in dimethyl-formamide initiated by the electrolysis of tetra-alkylammonium salts. Closely related systems were investigated from different viewpoints by three other groups of workers. A brief consideration of their results and conclusions is relevant; the system has been investigated more fully than any other, using a variety of electrochemical techniques, and the proposed mechanisms for initiation are possible in other anionic polymerizations. Murphy et al. (29) first attempted an investigation of the reduction of acrylonitrile at a mercury cathode in dimethyl-formamide. In the presence of small quantities of water, well-defined polarograms were obtained; in pure dimethyl-formamide the polarograms were distorted, and of smaller wave height. Controlled potential electrolysis in dry dimethyl-formamide indicated that between 5 and 10 acrylonitrile molecules reacted for each electron passed. This result was attributed to reaction between the carbanion formed initially and further monomer

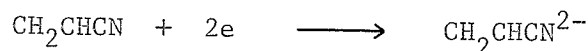
molecules in solution, but neither the nature of the carbanion formed electrolytically nor the yields of polymer were discussed.

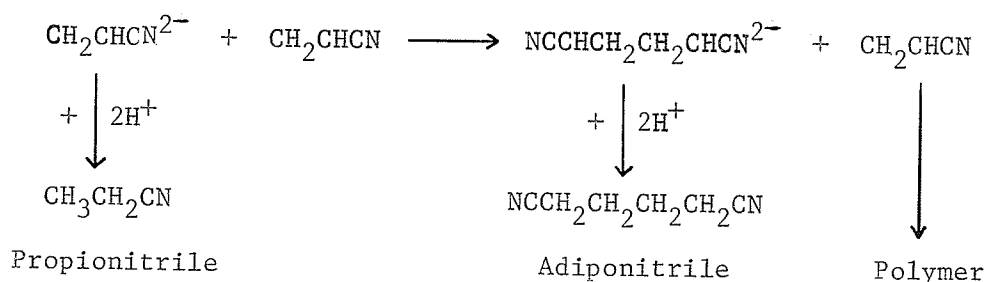
Funt and Williams (30) studied the polymerization process in more detail. Acrylonitrile was polymerized in dimethyl-formamide using a variety of salts, and kinetic and copolymerization experiments were conducted. The initiating mechanism proposed involved the dimerization of a radical anion of acrylonitrile that had been formed by direct electron transfer from the electrode. This may be written:-



Polymerization was initiated by the dimeric dianion. The polarographic evidence presented for this mechanism was somewhat equivocal, but a similar mechanism has been proposed for the anionic polymerization of acrylamide under similar conditions (31).

The electrolytic reduction of acrylonitrile was studied by Baizer and coworkers (32,33,34) as a route to the synthesis of adiponitrile, a key intermediate in the production of nylon 66. The conditions that favoured polymerization rather than the desired hydrodimerization were investigated. The yield of polymer formed by the electrolysis of a tetra-alkylammonium salt in dimethyl-formamide/water solution was found to depend on the relative amounts of water and acrylonitrile present. The proposed mechanism involved the initial formation of a monomeric dianion:-





Subsequent reactions of the dianion depended on the concentrations of water and acrylonitrile. Propionitrile, adiponitrile and polymeric products may be formed as indicated above.

A similar reaction scheme, formulated in terms of the proton donating ability of the solution was presented by Feoktistov et al. (35) and again in more detail by Tomilov and Klimov (36). Arad and co-workers recently considered possible specific effects of the tetra-alkylammonium cations on the course of the reaction (37).

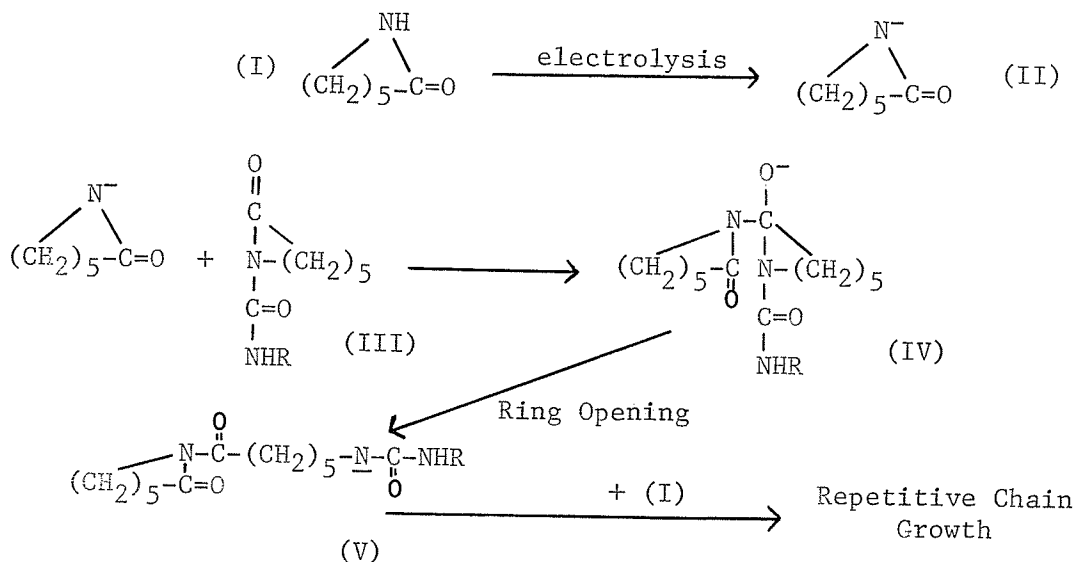
The electrochemistry of the initiating step for the polymerization of acrylonitrile in very dry dimethyl-formamide was examined by Lazarov et al. (38). From polarographic, microcoulometric and galvanostatic measurements, they deduced that at very low acrylonitrile concentrations, two electrons were transferred simultaneously to give a monomeric dianion. At higher acrylonitrile concentrations, the number of electrons transferred per molecule reduced dropped to a fractional value, and the polarographic curves became distorted. An explanation of these effects in terms of polymer formation was presented.

Other Electro-initiated Ionic Polymerizations.

Although the electrochemistry of the reduction polymerization of acrylonitrile has attracted most attention, other electrolytically initiated anionic systems have been studied. In general, the factors

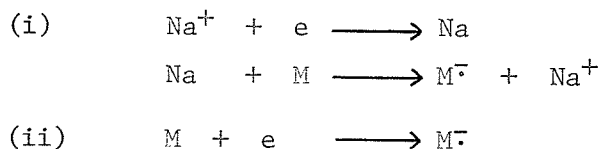
affecting the yield and molecular weight of the polymer have been emphasized, rather than the detailed initiation mechanisms. Funt and coworkers (39,40) studied the polymerization of styrene in dimethylformamide with a variety of salts. Methyl methacrylate polymerizations under similar conditions were examined (41). The polymerizations of these vinyl monomers were carried out at constant current, and the reactions were shown to be first order in monomer.

A very different type of electrolytically initiated anionic polymerization has been reported recently by Gilch and Michael (42) as a possible method to coat electrical conductors with nylon 6. The method is based on the discovery that in the presence of an acylating agent as activator, lactams undergo base catalysed ring-opening polymerization in the melt. Gilch electrolysed sodium benzoate in a caprolactam (I) melt at 160°C. to form the chain-initiating base (II). The subsequent reaction steps may be indicated thus:-



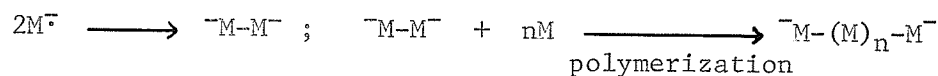
The base (II) attacks an acylated caprolactam molecule (III) (in this case an isocyanate was used as activator) to produce (IV). This species undergoes ring opening to form the base (V) which abstracts a proton from another caprolactam to regenerate the anion (II). Thus the ring opening process may be repeated. The effects of temperature, activator concentration, electrolyte concentration, current density and amount of current passed on the yields and viscosities of the polymer formed were examined. For example, it was found that for a given total amount of electricity passed, the yield of polymer reached a maximum at an intermediate current density. This yield corresponded to about 85 caprolactam molecules polymerized per electron, and was approximately independent of the total current pass; inexplicably, the degree of polymerization was apparently much higher than this value would suggest. In common with some free radical systems, polymerization continued for a time after the current flow had ceased.

One of the most interesting developments in electroinitiated polymerization was the recent electrolytic formation of "living polymers" (43). α -Methyl styrene was polymerized in dry tetrahydrofuran using LiAlH_4 or NaAlR_4 as electrolytes. Of the two possible initiating mechanisms:-



the second, involving direct electron transfer from the electrode, was preferred on the basis of current-voltage curves. The reaction is then presumed to proceed according to the mechanism proposed by Szwarc (44)

for conventional living polymerization.



This process goes to completion in the absence of chain terminating agents so that all the monomer is consumed, and the number average molecular weight \bar{M}_n is given by:-

$$\bar{M}_n = \frac{\text{initial amount of monomer (g.)}}{\frac{1}{2} \times \text{quantity of current passed, (Faradays)}}$$

This simple relationship between current passed and molecular weight provided Funt and coworkers (45,46) with a unique method for the preparation of polymer samples with defined molecular weight distributions. These workers found that sodium tetraphenylboride, $NaB(Ph)_4$, served as a stable easily handled electrolyte, and that controlled termination of growing polymer chains could be achieved stoichiometrically by simply reversing the current. At present, non-terminating anionic polymerizations and copolymerizations (47) are being actively studied, both from the point of view of the chemistry and electrochemistry of the reactions involved, and also as a method of tailoring molecular weight distributions.

The electrochemical polymerization of 4-vinyl-pyridine in liquid ammonia recently reported by Laurin and Parravano (48) also apparently involves "living" anions, but chain transfer reactions with the solvent occur, interfering with the molecular weight distribution.

Much less work has been performed on electrolytically initiated cationic polymerizations. Breitenbach (28) reported that styrene,

isobutyl vinyl ether and N-vinyl carbazole polymerizations could be effected by the anodic discharge of perchlorate and tetrafluoroborate ions. Funt and coworkers in some unpublished results found that tetrahydrofuran may be polymerized by a cationic ring-opening mechanism initiated electrolytically. However, reproducible kinetic results proved to be difficult to obtain in these cationic systems.

Electrolytic Control of Chain Propagation.

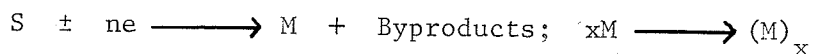
In all cases mentioned so far, the electrolytic process has been instrumental in the initiating stage of polymerization alone. One exception is the control of termination effected electrolytically in some "living" anionic systems. However, it would be of great interest to develop a method to control the chain propagation steps electrolytically. Theoretically, this might be achieved by using any difunctional species with substituents that undergo electrolytic coupling. The propagation step might be represented thus:-



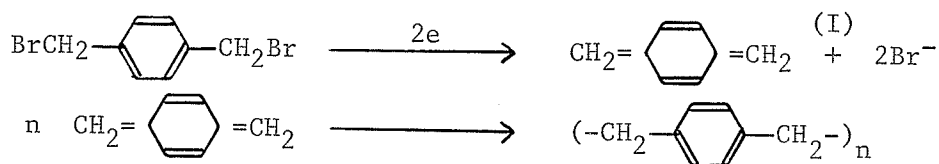
Here, X and Y represent two functional groups which may couple with the exchange of z electrons, and U represents the repeating unit of the polymer chain. Thus, for example, a repetitive Kolb  reaction, where X and Y would be carboxylate groups, might be expected to give polymeric material in this manner. (This case should be distinguished from those in which the Kolb  reaction provides the initiating free radical, and vinyl monomers are polymerized by the usual chain propagation steps.) However, attempts to produce polymer in this manner have not as yet been successful (1). Failure apparently stems from the fact that a

very high coupling efficiency with the absence of side reactions is necessary if high molecular weights are to be attained, in analogy with the requirements for condensation polymerization. Such efficiencies are not in general found in electrolytic coupling reactions, and in addition competitive intramolecular coupling would be expected for difunctional species.

An alternative method for exerting control of chain propagation would be to generate the monomer electrolytically. Such a polymerization may be represented schematically thus:-



where S is a non-polymerizable electroactive substrate and M is some monomeric species. Recently, the formation of polypara-xylylenes by this type of reaction has been reported. The electrolytic reduction of a number of α, α' -dihalo-p-xylenes at controlled cathode potentials was performed by Gilch (49), and the process was investigated by a variety of electrochemical means by Covitz (50). For the polymerization of α, α' -dibromo-p-xylene, the following mechanism was proposed:-



p-Xylylene (I) was also postulated as the intermediate in a related electrolytic process for coating aluminium with poly-p-xylylene (51). In this case, p-xylylene was produced by the discharge of p-xylylenebis (trialkylammonium salt) or p-xylylenebis (triphenylphosphonium salt):-



The p-xylylene (I) produced exhibits marked diradical character, and polymerizes very readily to give poly-p-xylylene, presumably by a rapid stepwise radical-coupling process.

Electrolytic Polymerizations; Conclusions.

In this brief summary, a wide variety of electrochemically controlled polymerizations have been outlined. Of these, the anionic chain polymerizations have attracted the most attention, firstly because of the good yields and high electrical efficiencies achieved, and secondly because of the facile molecular weight control possible in living anionic systems. In general, the emphasis in the reported work has been on polymer yields and propagation mechanisms. In order to improve the degree of control of the chain initiation and termination steps, a more detailed study of the electrochemistry of these reactions is required. Such a study might also help to interpret some anomalous data on propagation mechanisms which were obtained from inhibitor and copolymerization studies.

ELECTROCHEMICAL METHODS

Introduction

Before examining specific electrochemical methods which might be applied to a study of electropolymerizations, a very brief outline of the development and scope of electrochemistry will be presented.

The chemical effects of electrical current were discovered at the beginning of the nineteenth century. Nicholson and Carlisle demonstrated the decomposition of water by electricity in 1800, and Davy in 1807 isolated metallic sodium and potassium by electrolysis of their fused hydroxides. Faraday (1834) discovered the quantitative relationship between the amount of current passed and amount of substance transformed. Until the studies of conductance by Kohlrausch (1868) and Arrhenius (1889), electrochemistry remained basically phenomenological; no distinction was made between processes occurring in the bulk of the solution and those occurring at the electrode. However, following the development of conductometry, the subject has tended to separate into two main divisions, "ionics" and "electrodics" (52).

"Ionics" deals with the nature and properties of ions in solution and in the molten state, and is based primarily on conductance measurements. Thus, following the classical Arrhenius dissociation theory of electrolytic solutions, which was adequate for weak electrolytes, Debye and Huckel (1923) and Onsager (1926) developed a theoretical approach to dilute solutions of strong electrolytes based on the interplay of electrostatic forces with thermal motion. More recently, quasi-matrix

models have been proposed to describe more concentrated ionic solutions (53). The thermodynamics of ions in solution may be considered as a further branch of ionics. The foundation of this aspect of electrochemistry was laid by Nernst (1889) with his equation relating the equilibrium electrode potential to the activities of ions in solution. This relationship has been of great value in chemical thermodynamics because, with suitable electrochemical cells, potentiometric measurements enable ionic activities in solution to be determined. The utility of potentiometry in electroanalytical chemistry has recently been enhanced by the development of a wide range of cation- and anion-sensitive glass membrane electrodes in addition to the hydrogen-ion sensitive variety.

The second, and at present more active branch of electrochemistry has been termed "electrodics". This encompasses those processes taking place at the electrode. The importance of the electrode potential in governing the yields and products of electrochemical reactions was first stressed by Haber (1898) in his work on the electrolytic preparation of organic compounds. The possibility of selectively depositing a given metal ion from a mixture in solution by controlling the electrode potential was first realized by Sand and Fisher (1907). The development of polarography by Heyrovsky (1922) first engendered widespread interest in electrochemistry and its application to inorganic and organic analysis. The form of the polarographic current/potential curves obtained using the dropping mercury electrode was governed by the mass transfer processes which transport the electroactive material to and from the electrode surface. In some cases, the shape of the polarogram was also

affected by the kinetics of the heterogeneous electron transfer steps taking place at the electrode. The study of "irreversible" processes involving slow electron transfer steps has become an important branch of electrochemistry. The accepted theoretical treatment of the kinetics of electron transfer was developed by Butler (1924) and Erdey-Gruz and Volmer (1930), although the concept of overpotential had already been introduced by Tafel (1905).

Experimental methods used to determine electrode kinetics include modification of classical polarography such as oscillographic and alternating current polarography. In the last twenty years, a further range of electrochemical relaxation techniques has been used to study relatively fast heterogeneous electron transfer reactions. The techniques generally involve time-dependent rates of mass transfer, controlled by diffusion to a solid or dropping mercury electrode. Steady state mass transfer methods have also grown in importance. In particular, the rotating disc electrode developed by Levich (1942) enables moderately fast electrode processes to be studied under well-defined hydrodynamic conditions (54).

The kinetics of electrode processes are intimately linked with the structure of the electrode double layer. The development of a satisfactory double layer model has been slow due to both experimental and theoretical difficulties, and this is at present an active area of research in electrostatics (52,55). However, it will be shown that such complications are of minor importance in the work presented in this thesis.

Methods Applicable to this Investigation.

As mentioned previously, a study of the electrolytic processes taking place in anionic polymerization systems is of primary interest. Thus electrochemical techniques compatible with the rigorous purity necessary for anionic polymerizations are required.

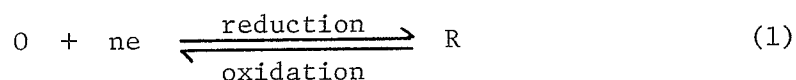
As a first step, the effect of the electrode potential on the course of the reaction may be investigated by electrolysing monomer solutions at a constant electrode potential, and examining the products. Controlled potential coulometry is a useful extension of this method; the amount of current required for a specific electrochemical reaction is measured. Polarography is another very useful tool in the study of electrochemical processes. However, the use of a dropping mercury electrode in organic solutions of high resistance under conditions similar to those necessary for anionic polymerizations raises severe experimental problems. The use of a platinum microelectrode appears more attractive because the design of cells for vacuum-line transfer of solvents is simpler, and also most electropolymerizations have been performed with platinum electrodes. Of the possible electrochemical methods for examining organic reactions at a platinum microelectrode, cyclic voltammetry seems the most promising. However, before describing these methods in more detail, some relevant electrochemical theory must be considered.

Some Theoretical Considerations.

No attempt will be made to give a full or rigorous derivation of the theory of the electrochemical methods used. However, an

indication of the concepts involved and the assumptions made in deriving the relationships employed later in the thesis will be presented. A comprehensive modern treatment of the fundamentals of electrochemistry is given by Kortum (56). Delahay discussed a wide variety of instrumental electrochemical methods and derived the applicable theory in useful form (57). His approach is used in parts of the following treatment.

Consider a simple oxidation-reduction equilibrium maintained between an electrode and an electro-active compound in the surrounding solution:-



For this "redox couple", O and R represent the oxidized and reduced forms of the reactant, and n is the number of electrons, e, involved in the reaction. An equilibrium constant, K, may be written:-

$$K = \frac{a_r}{a_o (a_e)^n} \quad (2)$$

where a_r and a_o refer to the activities of the reduced and oxidized forms at the electrode surface. If the solution is dilute and no specific adsorption occurs at the electrode, the surface activities may be approximated by the bulk concentrations. The standard free energy change G° for the process is related to the equilibrium constant and to E° , the standard half-cell potential:-

$$G^\circ = -RT \ln K = -nFE^\circ \quad (3)$$

$$E^{\circ} = \frac{RT}{nF} \ln K = \frac{RT}{nF} \ln \frac{a_r}{a_o} - \frac{RT}{F} \ln a_e \quad (4)$$

For a solution initially at equilibrium, if the electron activity a_e is increased, then the ratio a_r/a_o must also increase to maintain equilibrium. The term $-(RT/F) \ln a_e$ may be written as E , the potential of the working electrode. Making this substitution in equation (4), the Nernst equation, giving the equilibrium potential of an electrode in contact with a redox couple, is obtained:-

$$E = E^{\circ} - (RT/nF) \ln(a_r/a_o) \quad (5)$$

Evaluating the constants at 25°C. and changing the logarithmic base, this equation becomes:-

$$E = E^{\circ} + 0.059/n \log_{10}(a_o/a_r) \quad (6)$$

Thus, an increase in the electrode potential results in an increase in the activity of the oxidized species relative to the reduced species. Experimentally, only differences in E or a_e can be determined, so it is necessary to choose a standard state; the normal hydrogen electrode provides the defined zero of potential at all temperatures. More conveniently, electrode potentials are usually referred to those of the saturated calomel, the silver/silver halide, or some other non-polarizable reference electrode with constant half-cell potential (58).

Controlled Potential Electrolysis.

In order to bring about electrolytic reactions, a dc voltage, sufficient to cause a current to pass, is applied to a cell consisting of two electrodes in contact with a solution of electroactive and ionic species. Electrons flow through the external circuit from the anode to

the cathode. At the cathode surface, electrons are transferred to some electroactive substance in solution, which is thereby reduced. Simultaneously at the anode, electrons are transferred from some species in solution to the electrode. The species involved thus is oxidized. The electrical current flowing through the bulk of the solution results from the migration of ionic species under the influence of the impressed electromotive force. The solution exhibits a resistance R , whose magnitude depends on (i) the nature of the solvent, (ii) the concentrations and mobilities of each of the ionic species present, (iii) the areas of the electrodes and the distance between them, (iv) the nature of the electrode reactions, and (v) the type of barrier used to prevent mixing of the anodic and cathodic products.

The total impressed voltage, V , across an electrolysis cell may be divided in the following manner:-

$$V = E_a + E_c + iR \quad (7)$$

where E_a and E_c are the potentials of the anode and cathode referred to some reference electrode, R is the resistance of the solution, and i is the current flowing through the cell. In simple electrolyses, either the applied voltage V , or the current i remains constant for the duration of the experiment. However, because the electroactive substances are removed by electrolysis, the solution resistance and the potentials of the anode and cathode may alter with time. To avoid this, electrolysis may be performed at a controlled electrode potential (59,60).

Consider the electrolytic reduction of a given electroactive substance present in the solution at the cathode. (In this case, the cathode may be termed the "working electrode" and the anode may be termed the "counter electrode". These names are reversed for an oxidation process.) It may be determined, using methods described later in the thesis, that the required reduction takes place when the working electrode is at some optimum potential, E_c . The essential feature of electrolysis at controlled potential is that the electrode potential is maintained at E_c , despite changes in the solution composition and resistance, by altering the total voltage V applied to the electrolysis cell. This may be accomplished automatically using a "potentiostat"; the operating principle of an electronic potentiostat is outlined in Figure 1.

By this means, the reaction at the cathode may be restricted to the reduction occurring at potential E_c , even in the presence of other species in solution which are reduced at more cathodic potentials. Thus, this process is much more selective than electrolysis at constant current or constant voltage. It is generally possible to plate out a given metal ion from a solution containing a number of metal ions, or to produce a variety of oxidation or reduction products from a given electroactive organic substrate by choosing suitable potentials. Because the electrolysis is selective, the current will drop to zero when all the starting material has been electrolysed. The total quantity of electricity Q , consumed in the process will be:-

$$Q = \int_0^{\infty} i \, dt = nFN \quad (8)$$

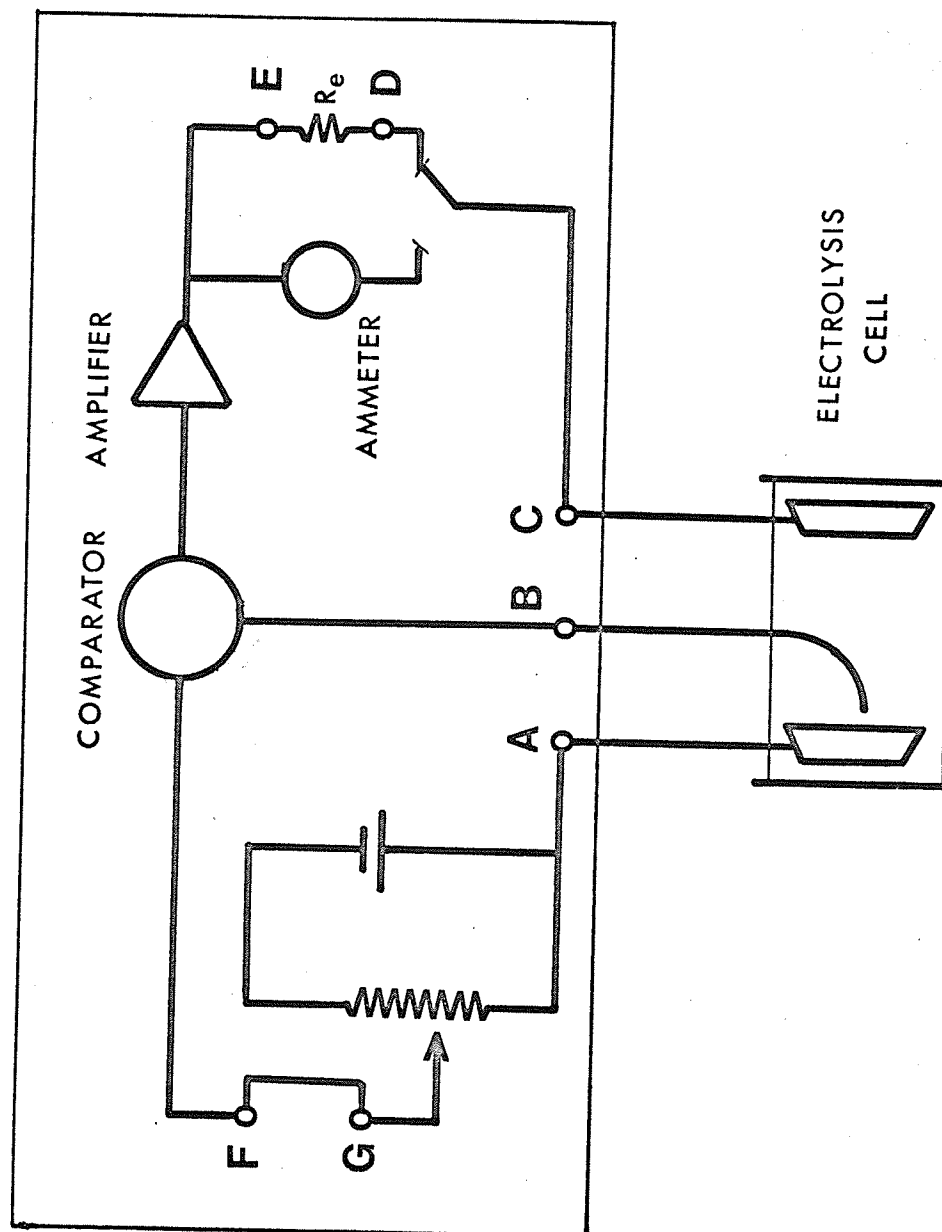
FIGURE 1.

OPERATING PRINCIPLE OF THE WENKING ELECTRONIC POTENTIOSTAT.

TERMINALS LABELLED AS FOLLOWS:

- A. WORKING ELECTRODE.
- B. REFERENCE ELECTRODE.
- C. COUNTER ELECTRODE.
- D,E. EXTERNAL CURRENT RECORDER, ACROSS RESISTANCE R_e .
- F,G. EXTERNAL VOLTAGE SOURCE.

FIGURE 1.



where N is the number of moles of starting material, n is the number of electrons involved in the electrolysis step per molecule, and F is Faraday's constant. Thus, if the number of moles of starting material is known, the number of electrons transferred in the reduction or oxidation step is easily found from Q .

As electrolysis proceeds, the amount of electroactive substrate is depleted, and the electrolysis current decreases. The variation of current with time during controlled potential electrolysis will now be considered (61,62). As an example, for the half-cell reaction $O + ne \longrightarrow R$, proceeding at a suitable constant cathode potential, the oxidized compound O becomes depleted in the region near the electrode. It may be replaced in three ways:-

- (i) Diffusion; this may be regarded as mass transfer due to concentration gradients around the electrode.
- (ii) Convection; this is the mass transfer process resulting from mechanical or thermal agitation of the solution.
- (iii) Migration; this term refers to ionic movements caused by electrical gradients whereby ions are attracted by the electrode of opposite charge.

The effect of migration in all the systems considered in this thesis is almost eliminated by the use of a "supporting electrolyte". This is a salt which is electrochemically more inert than the substance under study, and is present in much higher concentrations, so that it transports most of the current.

Most controlled potential electrolyses are carried out in

stirred solutions, because forced convection increases the rate of reaction. Thus, the current flowing at any time depends on the rate of stirring. The rigorous mathematical analysis of mass transfer processes in stirred solutions therefore involves both diffusion and convection, and is very involved. However, a useful approximation based on the concept of the diffusion layer was developed by Nernst (63). It is assumed that at the electrode surface there exists a diffusion layer of thickness d_o in which the solution is stationary. The reacting species, O, is brought to this layer by stirring. Within the layer, mass transfer occurs by diffusion, and it is assumed that the concentration of the reacting species varies linearly with perpendicular distance from the electrode. Hence, the concentration gradient at the electrode surface is given by:

$$\left(\frac{\delta C_o(x)}{\delta x} \right)_{x=0} = \left(\frac{C_o^b - C_o(0)}{d_o} \right) \quad (9)$$

where x is the perpendicular distance from the planar electrode,

$C_o(x)$ is the concentration of substance O at distance x from the electrode,

$C_o(0)$ is the concentration of O at the electrode surface,

C_o^b is the concentration of O in the bulk of the solution,

d_o is the thickness of the diffusion layer.

If the electrode reaction is fast, then the concentration at the electrode surface, C_o^b , is effectively zero, so that

$$\left(\frac{\delta C_o(x)}{\delta x} \right)_{x=0} = C_o^b / d_o \quad (10)$$

To examine the diffusion process, Fick's first law of diffusion may be used. For a solution extending semi-infinitely in a direction perpendicular to a planar electrode, this states that the number of moles of O, diffusing through a plane parallel to the electrode and at a distance x from it, is proportional to the concentration gradient of substance O at the distance x from the electrode. This may be written:

$$q(x,t) = D_0 \left(\frac{\delta C_0(x,t)}{\delta x} \right) \quad (11)$$

where $q(x,t)$ is the rate of diffusion per unit area (the "flux") of substance O at distance x from the electrode, and perpendicular to it.

D_0 is a proportionality constant, the "diffusion coefficient".

$C_0(x,t)$ is the concentration of O at distance x from the electrode at time t after the start of electrolysis.

The electrolysis current is equal to the product of the flux of substance O at the electrode surface, and the charge necessary to reduce one mole of O. Thus, at a plane electrode, of area A :

$$i = nFA \cdot q(0,t) \quad (12)$$

Substituting this expression into equation (11)

$$i = nFAD_0 \left(\frac{\delta C_0(x,t)}{\delta x} \right)_{x=0} \quad (13)$$

By introducing the concept of the diffusion layer using equation (10), the current flowing in a stirred solution may be written:-

$$i(t) = nFAD_0 \frac{C_0^b(t)}{d_0} \quad (14)$$

C_O^b is written as a function of t because during electrolysis the bulk concentration of O will decrease with time. The current i at time t may also be related to the number of moles of O being reduced per unit time:-

$$i(t) = -nF \frac{dN(t)}{dt} \quad (15)$$

Here, $N(t)$ is the number of moles of O present in the solution at time t ; if the volume of solution is V , then $C_O^b = N(t)/V$, and so:-

$$i(t) = -nFV \frac{dC_O^b(t)}{dt} \quad (16)$$

Equating (16) and (14), solving the resultant differential equation for C_O^b , and resubstituting, the following equation for the variation of the current with time is obtained:-

$$i(t) = nFAD_O \frac{C_O^b(0)}{d_O} \exp\left(-\frac{D_O A}{Vd_O} t\right) \quad (17)$$

where $C_O^b(0)$ is the bulk concentration of O before electrolysis commences (that is, for $t=0$). This equation indicates that for a simple oxidation or reduction process performed at constant potential in a stirred solution, the current decreases exponentially with time. Thus, a controlled potential electrolysis never goes to completion; however, the exponential current decay means that in general high yields may be achieved in reasonable times. If the changes in the cell resistance and the counter electrode potential are small, then the total potential applied to the cell, V , also decreases almost exponentially with time. This constant change in applied voltage which is consequently necessary in controlled potential electrolyses prevented

widespread application of the method until recently. Manual voltage adjustment was time-consuming, difficult to perform during the initial sharp voltage decrease. However, the recent development of automatic electromechanical and electronic devices for maintaining a fixed electrode potential has increased the usefulness of this method of electrolysis. It has been applied to the analysis of mixtures of metallic ions in solution, as a tool for investigating electrochemical mechanisms, and in preparative organic and inorganic chemistry (59,60).

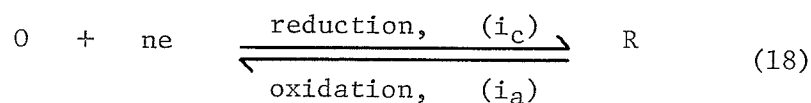
Current-Potential Curves.

In order to apply controlled potential electrolyses effectively, it is necessary to determine the current-potential relationship for the system under study. Furthermore, this "voltammetric" information often aids interpretation of the mechanisms involved in the electrolytic process. Polarography at the dropping mercury electrode is the best-known technique for finding this information, but other methods are available. However, before examining practical voltammetric methods, some general features of electrode kinetics must be discussed.

In the derivation of the Nernst equation (equation 6), it was assumed that electrochemical equilibrium existed between the electrode and the electroactive species in solution. This assumption is generally valid for many inorganic redox couples, when the rate of potential change is moderate. Nevertheless, other situations where the kinetic approach to equilibrium must be considered.

A general unimolecular oxidation-reduction reaction may be

represented thus:-



The following idealized conditions are assumed to apply to the system. Firstly, the electrode process is assumed to involve two soluble substances. Secondly, the concentrations of the substances reacting at the electrode are constant; this implies that the rate of mass transfer is much greater than the rate of electrochemical reaction. The third assumption is that the working electrode potential may be measured relative to a stable reference electrode, and that the flow of current introduces no error in the potential.

Equation (18) describes a reaction whose rate depends on the rates at which electrons are transferred between the electrode and the electroactive species. These rates of electron transfer are represented as the currents i_c and i_a , due to the reduction and oxidation processes respectively. By convention, cathodic currents are positive and anodic currents are negative. The overall, measurable current at the electrode will thus be:-

$$i = i_c + i_a \quad (19)$$

When the electrode is in equilibrium with the solution at a potential E_{eq} , then $i_c = i_a$, and no net current flows. If a potential different from E_{eq} is applied to the electrode, then electrolysis takes place until a new equilibrium is achieved. However, there exists an energy barrier to electrolysis, the magnitude of which determines the rate of

of transformation of O to R. The net rate of transformation (in moles.sec.⁻¹cm.⁻²) is given by:-

$$-\frac{dN_O}{dt} = \frac{dN_R}{dt} = k_{c,h} C_O - k_{a,h} C_R \quad (20)$$

where $k_{c,h}$ and $k_{a,h}$ are the heterogeneous rate constants for the forward (cathodic) and backward (anodic) processes respectively. The units for first order heterogeneous rate constants are centimeters per second, and their magnitude for a given reaction depends on the potential of the electrode.

By analogy with chemical reactions, $k_{c,h}$ for a reaction which is n^{th} order in electrons should be proportional to $(a_e)^n$, and $k_{a,h}$ should be independent of a_e . However, this is not so; as the potential E is made more negative (i.e. as a_e is increased) the rate of the anodic reaction will decrease because the electric field at the electrode hinders the transfer of electrons from R to the electrode. The transfer coefficient, α , allows for that fraction of the increase in $-E$ that favours the reduction, while $(1-\alpha)$ must be that fraction which hinders the oxidation. Then the dependence of the rate constants on electrode potential is given by:-

$$k_{c,h} = k_{c,h}^0 (a_e)^{\alpha n} = k_{c,h}^0 \exp(-\alpha n F E / RT) \quad (21)$$

$$k_{a,h} = k_{a,h}^0 (a_e)^{-(1-\alpha)n} = k_{a,h}^0 \exp((1-\alpha)n F E / RT) \quad (22)$$

Here the k^0 terms are the rate constants under standard conditions, where a_e is unity, and hence E , as defined in equations (4) and (5), is zero. The transfer coefficient, α , in electrochemical kinetics may be

considered analogous to the more familiar Bronstead α of general acid catalysis. For most electrode processes its value apparently lies close to 0.5. The concept of the transfer coefficient has recently been reviewed critically by Bauer (64).

Substituting expressions (21) and (22) for the rate constants into the rate expression (20), an equation giving the current may be obtained by multiplying the rate by the product of the electrode area, A , and the charge involved per mole of O reduced, nF :-

$$i = nFA \left\{ C_O k_{C,h}^O \exp(-\alpha nFE/RT) - C_R k_{a,h}^O \exp((1-\alpha)nFE/RT) \right\} \quad (23)$$

At the equilibrium electrode potential, the overall current flowing, i , is zero, and equation (23) may be simplified to give the Nernst equation, with the standard electrode potential expressed in terms of the formal rate constants.

The potential dependence of the heterogeneous rate constants in equation (23) may be eliminated by rewriting it in terms of the standard electrode potential:-

$$i = nFA k_{s,h} \left\{ C_O \exp(-\alpha nF(E-E_C^O)/RT) - C_R \exp((1-\alpha)nF(E-E_C^O)/RT) \right\} \quad (24)$$

Here, $k_{s,h}$ is a rate constant characteristic of the electrode process,

E_C^O is the formal standard electrode potential for the process.

It is defined identically to the standard electrode potential, E^O according to equations (2) and (4), except that concentrations replace activities. Little error is introduced by using E^O for E_C^O .

Thus, to summarize the argument to this point, for a simple

electrode process where mass transfer is fast enough to maintain a constant concentration of electroactive substance at the electrode, the kinetics of the electron transfer may be described according to equation (24) by two parameters, E_C^0 and $k_{s,h}$. The relationship between these parameters and the more familiar electrochemical concepts of overpotential and reversibility will now be considered.

E^0 is the standard electrode potential for the redox couple involved, measured relative to the normal hydrogen electrode. At this potential, $E = E^0 \rightleftharpoons E_C^0$, and the total current flowing is zero. However, the anodic and cathodic currents, i_a and i_c , are not zero, but are equal to the "exchange current", i_0 whose magnitude depends on $k_{s,h}$ thus:-

$$i_0 = nFAk_{s,h} C_O = nFAk_{s,h} C_R \quad (25)$$

These values for i_0 were obtained by substituting the values of i and E at the standard electrode potential into equation (24). If the electron transfer rate is very fast, then i_0 and $k_{s,h}$ will both be large. This implies that the energy barrier which must be overcome is very small. This situation corresponds to a "reversible" electrode process. Conversely, an irreversible process will have a low value for $k_{s,h}$.

In many polarographic and voltammetric systems, only one component is present. Thus, if only O is present initially, then C_R is effectively zero, and the second term in equation (24) disappears. In this case, the current becomes a simple exponential function of potential. The "overpotential" or "overvoltage" is

defined as the potential which must be added to the reversible (equilibrium) potential to produce a given current. For example, from equation (24), when the current is i , the corresponding overpotential $\eta = (E - E_c^0)$. The overpotential is negative for a cathodic process, and its value is dependent on $k_{s,h}$, α , and the current flowing. For an irreversible system, the overpotential will decrease with increasing $k_{s,h}$, effectively reaching zero when the system becomes reversible. On this basis, it is obvious that the degree of reversibility or irreversibility of an electrode reaction depends on the conditions. The relationship between current flowing and electrode potential in an idealized system where the rate of mass transfer is very large compared with the electrochemical rate is indicated graphically in Figure 2.

Voltammetric Methods.

In the above discussion of the kinetics of electron transfer at an electrode, it is assumed that the rate of transfer of reactants to the electrode and products from the electrode is sufficiently large to allow the rate of electron transfer to control the current flow. However, in practical systems, the exponential increase in current as the applied potential is increased is limited by the inability of sufficient electroactive material to diffuse to the electrode. If the experimental conditions are chosen so that migration and convection are eliminated as a means of transporting electroactive species to the electrode, then the current is said to be diffusion controlled.

Diffusion control of the electrolytic current is fundamental

FIGURE 2.

IDEALIZED CURRENT-POTENTIAL CURVES.

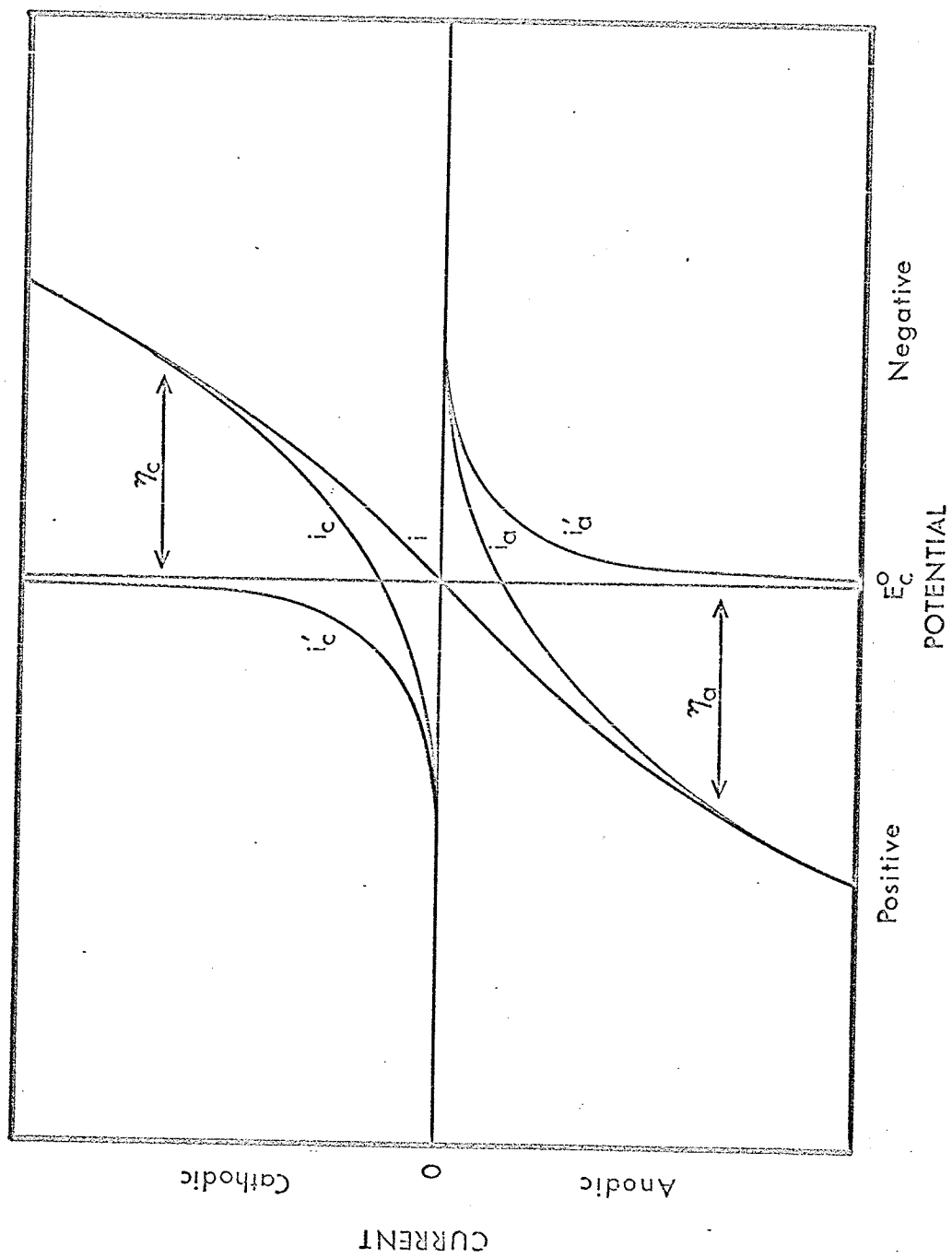
Currents i'_c and i'_a are the cathodic and anodic currents for a fast (reversible) electron transfer.

Current i is the algebraic sum of i_c and i_a , the cathodic and anodic currents for a slow electron transfer.

E_c^0 is the formal standard electrode potential for the processes.

η_c and η_a are the cathodic and anodic overpotentials for the slow electron transfer at the indicated currents.

FIGURE 2:



to many electroanalytical techniques. One such technique is "cyclic voltammetry", which, for the reasons mentioned previously, was employed in this study. It will now be examined in more detail.

Basically, cyclic voltammetry involves the determination of current-potential curves at a fixed electrode in unstirred solution. A typical voltammogram for the simple reduction $O + ne = R$ may be obtained by increasing the potential of the electrode linearly with time in a cathodic direction. When a sufficiently cathodic potential has been reached, an electrolysis current begins to flow. At first, the current increases approximately exponentially, but is soon limited by the rate of diffusion of electroactive material to the electrode, resulting in a peak in the current-potential curve. At a suitable potential, known as the "switching potential", the direction of potential scan is reversed, so that the electrode now becomes more anodic with time. For a reversible electron transfer, a current-potential curve similar to that for the cathodic scan, but inverted, will be found on the anodic scan. This is illustrated in Figure 3.

The detailed theoretical treatment of the shape of voltammograms obtained with linearly varying potential is relatively complicated mathematically. A theoretical treatment for the simplest case of a single scan for a reversible reaction at a plane electrode was given first by Randles (65) and Sevcik (66). This treatment was extended to cylindrical (67) and spherical (68) electrodes. Delahay (69) derived the theory for totally irreversible electrodes. Matsuda (70) considered in detail the shape of cyclic voltammograms obtained for multisweep voltage scans. Nicholson and Shain (71) reviewed the theory of cyclic

FIGURE 3.

SINGLE CYCLE VOLTAMMOGRAM FOR A REVERSIBLE ELECTRON TRANSFER.

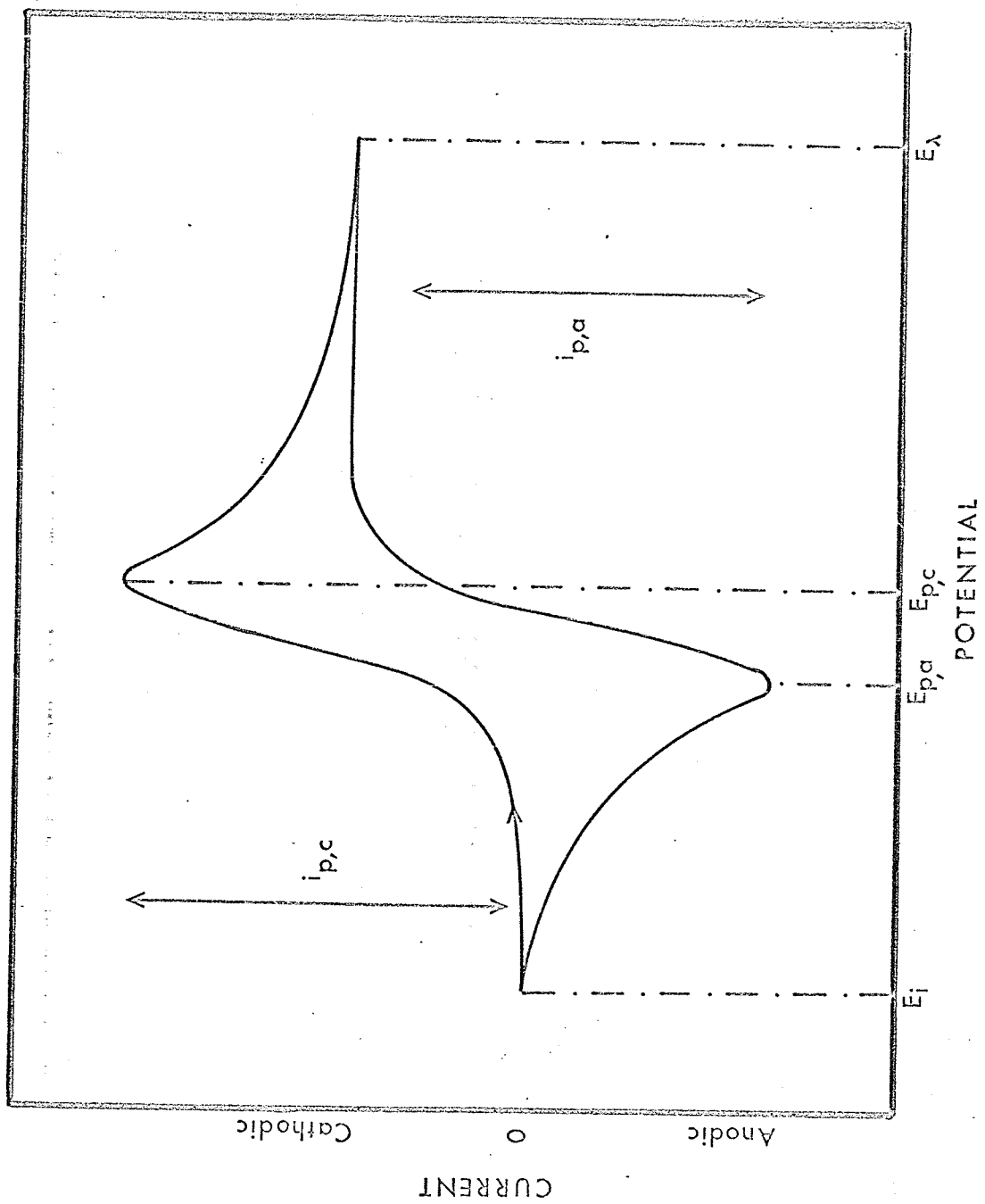
$E_{p,c}$ and $E_{p,a}$ are the cathodic and anodic peak potentials.

$i_{p,c}$ and $i_{p,a}$ are the cathodic and anodic peak currents.

E_i is the initial potential at the start of the potential scan.

E_λ is the switching potential.

FIGURE 3.



voltammetry involving simultaneous homogeneous chemical reactions, and presented further data in a useful form. Extensions of the theory to multistep charge transfers (72,73) and to the evaluation of heterogeneous rate constants (74) have been reported. Saveant (75) recently described the application of asymmetrical potential scan techniques to the study of chemical reactions subsequent to electron transfer.

The general approach to the theoretical derivation of the shape of voltammetric curves will now be outlined. As in the previous treatment of the diffusion layer concept, Fick's first law of diffusion provides the starting point. For substance O diffusing to a plane electrode:-

$$q(x,t) = D_0 \frac{\delta C_0(x,t)}{\delta x} \quad (11)$$

where $q(x,t)$ is the flux of substance O at distance x from the electrode at time t . D_0 is the diffusion coefficient of O, and $C_0(x,t)$ is the concentration of O at position x and time t .

At a distance $x + dx$ from the electrode, the flux is:-

$$q(x,t) + \left(\frac{\delta q(x,t)}{\delta x} \right) dx$$

Hence, the rate of change of concentration of O between two planes parallel to, and at distances x and $x + dx$ from the electrode is given by:-

$$\frac{\delta C_0(x,t)}{\delta t} = \frac{\delta}{\delta x} D_0 \left(\frac{\delta C_0(x,t)}{\delta x} \right) \quad (26)$$

It is usually assumed in electrolytic processes that the diffusion

coefficient D_O is independent of x ; in this case, equation (26) simplifies to give:-

$$\frac{\delta C_O(x,t)}{\delta t} = D_O \frac{\delta^2 C_O(x,t)}{\delta x^2} \quad (27)$$

The fundamental problem in diffusion controlled electroanalytical methods is to solve this equation for the initial and boundary conditions applicable to the physical problem under study. Thus, for a simple reversible reaction, $O + ne = R$, taking place at a plane electrode, the physical situation may be represented as follows:-

$$\frac{\delta C_O(x,t)}{\delta t} = D_O \frac{\delta^2 C_O(x,t)}{\delta x^2} \quad (27)$$

$$\frac{\delta C_R(x,t)}{\delta t} = D_R \frac{\delta^2 C_O(x,t)}{\delta x^2} \quad (28)$$

The initial conditions, at $t = 0$, for all distances from the electrode ($x > 0$), are:-

$$C_O = C_O^b, \quad C_R = C_R^b \approx 0 \quad (29)$$

where C_O^b , C_R^b are the concentrations of O and R in the bulk of the solution. In this case, it is assumed that initially no R is present in solution.

$$\text{At all times, for } x \rightarrow \infty, C_O \rightarrow C_O^b \text{ and } C_R \rightarrow 0 \quad (30)$$

There are two boundary conditions. Firstly, all substance O reaching the electrode surface is converted to R , so that at the surface, where $x = 0$, the sum of the fluxes of O and R is zero:-

$$D_o \left(\frac{\delta C_o(x,t)}{\delta x} \right)_{x=0} + D_r \left(\frac{\delta C_r(x,t)}{\delta x} \right)_{x=0} = 0 \quad (31)$$

The second boundary condition is given by the Nernst equation (5) relating the activities of O and R at the electrode surface to the electrode potential E. By rearranging equation (5) and substituting concentrations for activities, the Nernst equation may be written:-

$$\frac{C_o(0,t)}{C_r(0,t)} = \exp \left[(nF/RT) (E(t) - E^0) \right] \quad (32)$$

where the electrode potential E(t) is some function of t. For cyclic voltammetry with linear potential scan, the variation of E with t is given by:-

$$\begin{aligned} E(t) &= E_i - vt & \text{for } 0 < t \leq \lambda \\ E(t) &= E_i - 2v\lambda + vt & \text{for } \lambda \leq t \end{aligned} \quad (33)$$

where E_i is the initial electrode potential when $t = 0$,

v is the rate of potential scan,

λ is the time at which the direction of potential is reversed.

Methods of solution of equations (27) and (28) under the initial and boundary conditions given by equations (29) to (33) have been outlined by Delahay (55) and Nicholson and Shain (71). The solution gives the flux of O at the electrode surface as a complex function of time or potential. Using equation (13), the current corresponding to a given flux of O may be found, and hence the current-potential relationship for a reversible electron transfer may be determined.

The most general methods of solution require numerical

evaluation at some stage. Results are therefore presented in the form:- $i = Z \cdot \phi(E)$, where Z is some defined function of the experimental parameters, and $\phi(E)$ is a complicated function of the applied potential which has been evaluated numerically, and is presented either graphically or in tabular form. For example, Nicholson and Shain (71) express the theoretical current-potential relationship at a planar electrode as follows:-

$$i = nFAC_0^b (aD_0\pi)^{1/2} \cdot \chi(at) \quad (34)$$

where $at = nFvt/RT = nF(E_i - E)/RT$ and, as previously indicated, n is the number of electrons transferred, F is Faraday's constant, A is the electrode area, C_0^b is the bulk concentration of O , D_0 is the diffusion coefficient, t is the time elapsed since the start of the potential scan, v is the rate of potential scan, and E_i is the potential at the start of the scan. The values of the function $\sqrt{\pi} \chi(at)$ are presented in a table with the corresponding values of $(E - E_{1/2})n$. Figure 4 includes a plot of such values for a simple reversible electron transfer. The resultant curve has a maximum at a potential E_p which is 0.028 volts more cathodic than $E_{1/2}$, the polarographic half-wave potential, for the same process. (For a reversible process, $E_{1/2}$ is related to E^0 thus:-

$$E_{1/2} = E^0 - (RT/nF) \ln(f_r/f_o) (D_o/D_r)^{1/2}$$

where f_o and f_r are the activity coefficients of O and R .

$E_{1/2}$ is thus close to E^0 under the usual conditions.)

At E_p , the current function $\sqrt{\pi} \chi(at)$ reaches a maximum value of 0.446. The peak current i_p corresponding to this value may be

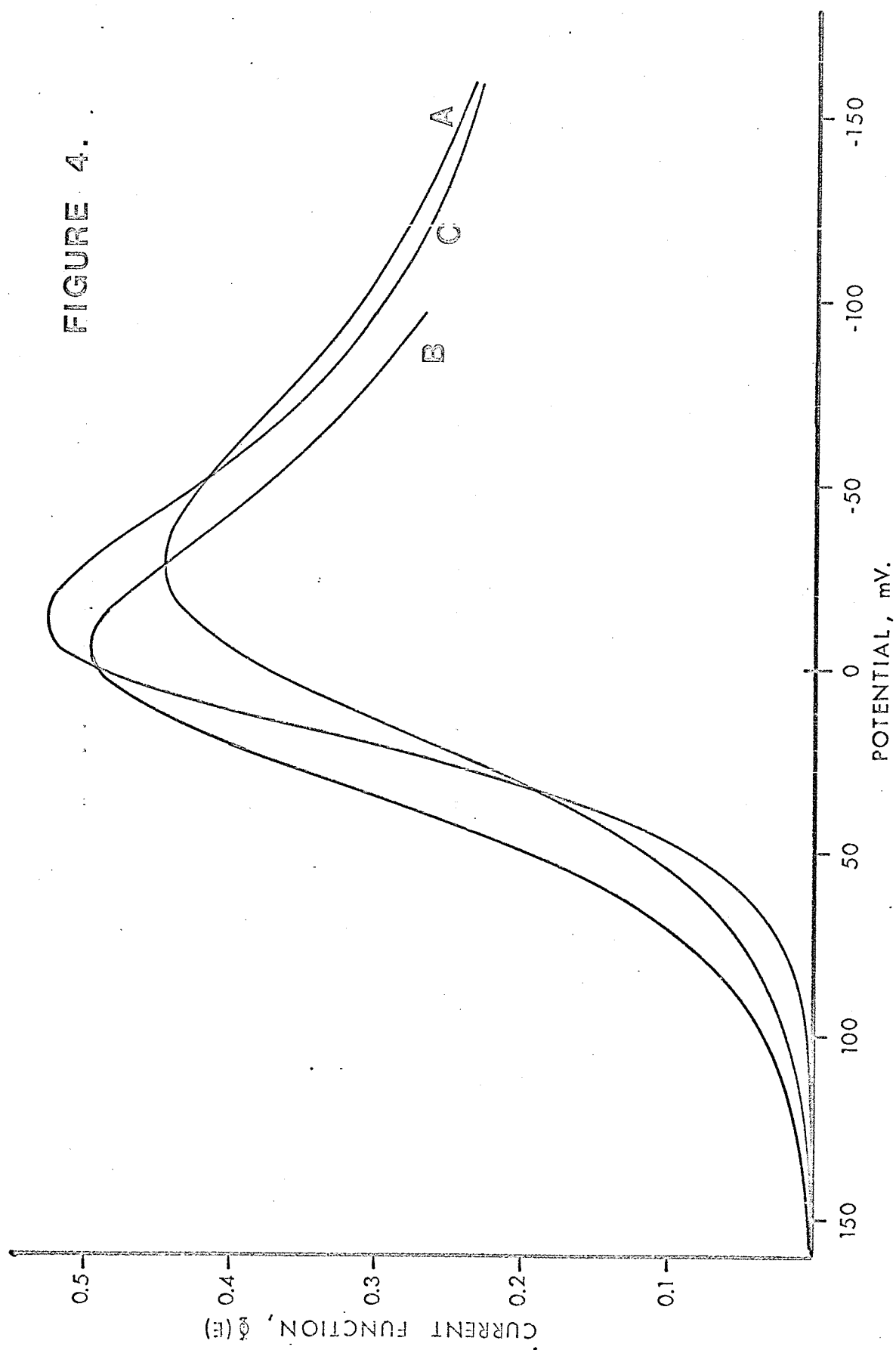
FIGURE 4.

THEORETICAL VOLTAMMETRIC CURVES.

- A. Reversible electron transfer.
- B. Reversible electron transfer followed by fast first order chemical reaction of product.
- C. Reversible reaction followed by fast dimerization of product.

The curves are plotted from data presented in references (71) and (77). The current is given by $i = Z\phi(E)$ where $Z = nFAC_o^b(aD_o)^{1/2}$.

FIGURE 4.



obtained by substitution in equation (34). Evaluating the constants at 25°C, the peak current is given by:-

$$i_p = 2.69 \times 10^5 n^{3/2} A D_o^{1/2} C_o^b v^{1/2} \quad (35)$$

with i_p in amp., A in cm.², C_o^b in mol. cm.³, D_o in cm.²sec.⁻¹ and v in volt. sec.⁻¹. The peak height of the voltammetric curve therefore varies linearly with the bulk concentration of electro-active material, and also with the square root of the scan rate.

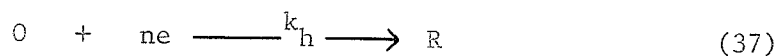
The shape of the reverse portion of the cyclic voltammogram, where the potential is being scanned from cathodic to anodic values, is found to depend on the switching potential (71). However, for switching potentials, E_λ more than 40/n millivolts cathodic of the peak potential $(E_p)_c$, an anodic curve similar in shape to the inverted cathodic peak results (Figure 3). Furthermore, if the extension of the cathodic curve is used as a base line from which to measure the anodic peak height $(i_p)_a$, it is found that for a reversible system, $(i_p)_a = (i_p)_c$. The problems of determining base lines are discussed by Nicholson (71) and by Polcyn and Shain (72). The separation between the anodic and cathodic peak potentials is an important parameter in cyclic voltammetry. As mentioned previously, the cathodic peak potential for a reversible electron transfer is given by $(E_p)_c = E_{1/2} - 0.028/n$. On this basis, the anodic peak on reverse scan would be expected to occur at $(E_p)_a = E_{1/2} + 0.028/n$, leading to a peak separation of $(E_p)_a - (E_p)_c = 0.056/n$ volts. However, because of the effect of the switching potential on $(E_p)_a$, the peak separation is usually assumed to be 60/n millivolts. Thus, one voltammetric criterion of a reversible electrode process is given by:-

$$(E_p)_a - (E_p)_c = \Delta E_p = 0.060/n \text{ volts} \quad (36)$$

Figure 3 indicates the shape expected for a simple reversible oxidation-reduction process, $O + ne = R$. Deviations from this shape may be explained in terms of an irreversible electron transfer step, or as a result of complicating chemical or electrochemical reactions. These effects will now be examined.

Irreversible Processes.

The case where the electrochemical electrode reaction is totally irreversible will be considered first. For the reduction of substance O to give R in a single rate-determining step, the reaction may be represented as:-



where the reverse reaction is ignored. The initial and boundary conditions in this case resemble those for the reversible case. Equations (27, (29) and (30) are still valid if the terms involving R are ignored. However, the flux of O at the electrode surface is given by:-

$$D_o \left(\frac{\delta C_o(x,t)}{\delta x} \right)_{x=0} = k_h C_o \quad (38)$$

where k_h , the heterogeneous rate constant at potential E , is related to the standard heterogeneous rate constant for the process $k_{h,s}$ as follows:-

$$k_h = k_{h,s} \exp \left[(-\alpha n_a F/RT) (E - E^0) \right] \quad (39)$$

where n_a is the number of electrons transferred in the rate-determining step. The boundary conditions of the diffusion problem for the totally irreversible case therefore involve the transfer coefficient α and the standard rate constant for the process. The solution may be expressed in a form similar to that for the reversible case given in equation (34).

$$i = nFA C_O^b (bD_O\pi)^{1/2} \chi(bt) \quad (40)$$

Here, $bt = (\alpha n_a F/RT)(E_1 - E) = (\alpha n_a Fvt)/RT$ and the other symbols are as defined previously. Values of $(\pi)^{1/2} \chi(bt)$ as a function of the electrode potential have been calculated by Delahay (69), Matsuda and Ayabe (76) and Nicholson and Shain (71). Substituting for $\chi(bt)$ in equation (40) and evaluating the constants at 25°C, the following expression for the peak current is obtained:-

$$i_p = 2.99 \times 10^5 n(\alpha n_a)^{1/2} A C_O^b (D_O v)^{1/2} \quad (41)$$

where the units and symbols are the same as in equation (35).

Because the reaction is irreversible, there is no anodic peak. A further difference from the reversible case is that the peak potential varies with the scan rate; for two scan rates v' and v'' , the difference in peak potentials is found to be:-

$$(E_p)''_c - (E_p)'_c = (RT/\alpha n_a F) \ln(v'/v'')^{1/2} \quad (42)$$

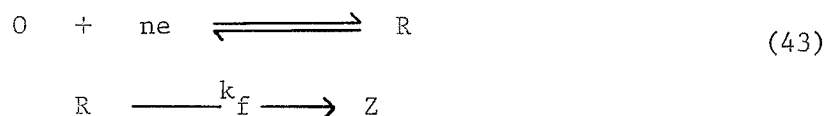
Quasi-reversible Processes.

In the preceding discussion of cyclic voltammetry, it has been assumed that the electrode reaction is either reversible or totally irreversible. However, intermediate quasi-reversible transfer processes also occur. In fact, any system which is reversible at one

scan rate would be expected to display kinetic behaviour if the scan rate is increased sufficiently. Such kinetic behaviour is indicated by a decrease in the anodic peak height relative to the cathodic as the scan rate is increased. Simultaneously, the separation of the anodic and cathodic peak potentials $(E_p)_a - (E_p)_c$ increases from the value of $0.060/n$ volts expected for a reversible system. As the scan rate is increased further, the voltammogram shape becomes identical to that described for totally irreversible electron transfer. The variation of peak separation with scan rate provides a convenient method for estimating the rate constant $k_{h,s}$ for the process (74).

Coupled Chemical Reactions

The discussion so far has been confined to simple electron transfer processes occurring at the electrode. Recently it has become apparent that cyclic voltammetry provides a powerful method to study homogeneous chemical reactions coupled to heterogeneous electrode processes. The coupled chemical reaction often causes marked changes in the shape of the voltammogram, thus enabling an estimation of the homogeneous kinetic parameters to be made. A typical example of a coupled chemical reaction involves the pseudo first order reaction of the product of a reversible reduction process with the solvent or electrolyte. This may be represented thus:-



where k_f is the homogeneous rate constant for the reaction, and Z

is a non-electroactive product.

The homogeneous reaction will alter the flux of R at the electrode surface, so that the diffusion equations now become

$$\frac{\delta C_o}{\delta t} = D_o \left(\frac{\delta^2 C_o}{\delta x^2} \right) \quad \text{and} \quad \frac{\delta C_r}{\delta t} = D_r \left(\frac{\delta^2 C_r}{\delta x^2} \right) - k_f C_r \quad (44)$$

The initial conditions remain, for $t = 0$, $x \approx 0$,

$$C_o = C_o^b, \quad C_r = C_r^b = 0 \quad (45)$$

The boundary conditions also remain the same as those for uncomplicated reversible electron transfer (equations 30 to 33).

As in previous cases, the solution to the problem may be expressed as a numerical current function corresponding to a given potential. However, in this problem the current function is also dependent on the value of k_f , the rate constant for the coupled chemical reaction. Values of the current function have been tabulated (71) for different values of k_f/a where $a = nFv/RT$. For low values of k_f/a (i.e. for slow homogeneous reactions or fast scan rates) the shape of the current-potential curve is indistinguishable from that for an uncomplicated reversible electron transfer. As k_f/a is increased, the curve shape approaches that expected for a totally irreversible electrode reaction. In the intermediate range, the ratio of anodic to cathodic peak heights may be used to determine the rate constant k_f for the coupled chemical reaction.

A similar approach has been employed to study the effects of preceeding, catalytic and subsequent homogenous chemical reactions on

both reversible and irreversible electron transfer processes (71,73). Electron transfer followed by dimerization of products (77,78) and two electron transfer reactions coupled to a homogeneous chemical reaction (79) have also been examined theoretically. Accurate current-potential curves for reversible electron transfer followed by fast first and second order reactions are shown in Figure 4.

Non-Faradaic Effects.

The shape of voltammograms may be influenced by factors other than the electrochemical and coupled chemical reactions of the depolarizing species. Two such factors must be mentioned. Although the use of a three electrode system removes the major effects of solution resistance on current/potential curves, the problem of uncompensated ohmic resistance remains. There will always be a small resistance R_u , dependent on the solution resistance and the geometry of the cell, between the working and the reference electrode. If a current i is flowing between the working electrode and the counter electrode, then an error, iR_u is introduced into the apparent potential of the working electrode measured relative to the reference electrode. The effects on the voltammogram are twofold (77); firstly, the current potential curves are displaced along the potential axis (in a cathodic direction for a cathodic scan) by an amount iR_u . Secondly, the effective potential scan rate becomes nonlinear with time, as an error iR_u is introduced into the effective potential applied to the working electrode. The rate, therefore, decreases continually before the peak and increases after the peak. The combined effect on

the voltammogram is a displacement of potential linearly dependent on the current flowing, coupled with a lowering and broadening of the peak. The distortion will be greatest at high scan rates (large i) or in solutions of high resistance (large R_u).

In deriving the theoretical shapes of voltammograms, it was assumed that diffusion or chemical reaction alone controlled the amount of electroactive substance at the electrode surface. However, adsorption of electroactive material on the electrode surface plays an important role in many electrochemical systems. In a recent theoretical study of the effects of adsorption on the shape of cyclic voltammograms, Wopschall and Shain (80) showed that weak adsorption may result in enhancement of the peak currents. With strong adsorption of product or reactant a separate adsorption peak may occur prior to or after the normal peak.

Summary.

In this introduction, electrochemically initiated polymerizations have been reviewed. An outline of electrochemical theory relevant to potential methods for studying the initiation and polymerization processes was presented. It should be noted, however, that most of the theory of stationary electrode voltammetry has been developed in the last three years, and has not been subject to vigorous experimental verification even under conventional conditions. The application of such methods to electrochemical studies in aprotic solvents therefore requires caution; it is hoped, however, that the results to be presented now will indicate that the usefulness of the methods outweighs any limitations.

EXPERIMENTAL METHODS

Materials.

SOLVENTS. Tetrahydrofuran (Fisher Certified grade) was dried by passing through an alumina column and stirring over calcium hydride. After fractional distillation, it was stored in vacuo over calcium hydride on a high vacuum line. Dimethylformamide (Fisher Certified grade) was dried in a similar manner. This solvent was then fractionally distilled under reduced pressure and stored over calcium hydride and anhydrous copper sulphate. Immediately before use it was distilled into the reaction cell under reduced pressure of purified nitrogen. Hexamethylphosphoramide (Fisher Scientific) was stirred over Linde 4A molecular sieve and then fractionated under reduced pressure of nitrogen.

NITROGEN. Nitrogen was passed through silica gel and bubbled into a solution of benzophenone ketyl anion, prepared by stirring benzophenone in xylene over sodium-potassium alloy. This removed any traces of water, oxygen or carbon dioxide. A liquid nitrogen trap removed xylene vapour from the nitrogen stream.

SALTS. Tetra-n-butylammonium perchlorate (Southwestern Analytical, Polarographic grade) was dried by gentle warming under high vacuum conditions for over twelve hours. Tetra-n-butylammonium bromide (Eastman Organic) was used as received. Sodium tetraphenylboride (Fisher Certified reagent) was purified by dissolving in tetrahydrofuran, filtering and cooling the solution. The resultant precipitate was filtered off and dried under high vacuum. Tetramethylammonium

tetraphenylboride was prepared by adding an aqueous solution of sodium tetraphenylboride to an aqueous solution containing an equivalent amount of tetramethylammonium chloride. The bulky white precipitate of tetramethylammonium tetraphenylboride was filtered off, washed repeatedly with water, dried and recrystallized from methyl ethyl ketone.

ELECTROACTIVE MATERIALS. Methyl methacrylate, styrene and α -methylstyrene (Matheson, Coleman and Bell) were purified by passing through an alumina column, fractionating under reduced pressure, and stored over calcium hydride under vacuum conditions. Each was twice distilled in vacuo immediately before use. Acenaphthylene (Aldrich Chemical) was recrystallized from ethanol and sublimed under high vacuum. Acenaphthene (Practical grade) was eluted from a column of alumina and recrystallized from toluene. 1,1-Biacenaphthylidene, mp 277°C was synthesized by the method described by Dolinski and Dziewonski (81). 1,1-Diacenaphthenyldiene, mp \sim 270°C (K & K Laboratories) and 2,2-diphenyl-1-picrylhydrazyl (Eastman Organic) were used as received. 1,1-Diphenylethylene (Fisher Scientific) was stirred over calcium hydride and distilled under reduced pressure. Trans-stilbene, triphenylethylene and tetraphenylethylene (Aldrich Chemical) were purified by repeated crystallizations from toluene. All melting points were close to the literature values.

Apparatus.

ELECTRONIC EQUIPMENT. The most important feature of the electrochemical methods used in this report was that the potential of the working electrode was controlled relative to that of a reference electrode. The control

was achieved using a Wenking 61 RH electronic potentiostat (Figure 1). This model was capable of fast response to changes in electrode potential. Although its current output was limited (< 1 Amp.), the maximum voltage output of 90 V between the working and counter electrodes was sufficient for work in high resistance non-aqueous solvents. The potentiostat was equipped with an internal voltage source which enabled potentials of from 0 to 2 volts to be applied to the working electrode. To obtain higher potentials or to vary the potential with time as required for cyclic voltammetry, an external voltage source was necessary. Initially, the triangular voltage input was produced by using a precision Helipot potentiometer driven by a reversible electric clock motor as a voltage divider. The voltage output derived from mercury cells increased linearly with time at a rate depending on the motor speed. The motor was then reversed manually to obtain a voltage sweep in the reverse direction. This method was time-consuming and lacked accuracy, so a transistorized triangular waveform generator was constructed which provided a symmetrical waveform of suitable amplitude with a frequency range from 0.01 Hz to 10 kHz (82). This generator was later replaced by a Hewlett-Packard 3300A function generator with 3304A sweep/offset plug-in unit, providing square, triangular, sine and sawtooth signals over a similar frequency range.

The current flowing through the electrolytic cell was indicated by a panel meter on the potentiostat. For higher accuracy the voltage drop across a small resistance R_e (Figure 1) was measured on Hewlett-

Packard 419A dc null voltmeter. This instrument also served to amplify the voltage drop so that a signal proportional to the current could be recorded automatically on a Heathkit Servo-recorder during controlled potential electrolyses.

A Houston Instruments X-Y recorder was initially used to record the current potential curves (voltammograms). The potential of the working electrode relative to the reference electrode was applied to the X axis, while a voltage proportional to the current flowing was applied to the Y axis using the Hewlett-Packard voltmeter. However, the response time of this X-Y recorder and of the voltmeter were rather high, and the two axes of the recorder shared a common ground, so that the voltammetric curves were liable to distortion. The use of the more sensitive Moseley Autograf 7030A X-Y recorder completely eliminated these problems. All voltammograms reproduced in this thesis were obtained on the latter recorder. Some experiments were performed at higher scan rates; the voltammograms were obtained using a Hewlett-Packard 130C X-Y oscilloscope and a Polaroid camera. The arrangement of apparatus used to obtain cyclic voltammograms is summarized in Figure 5.

GAS CHROMATOGRAPHY. The depletion of monomers during controlled potential electrolysis was followed using a Microtek ^{DSS-161} gas chromatograph with thermal conductivity detectors. Peak areas were determined using a Microcord model 44 chart recorder and an Integraph model 49 electronic integrator. On regular columns 'tailing' of the polar dimethyl-formamide solvent interfered with the determination of styrene. Two column packings were prepared which eliminated this problem.

FIGURE 5(a).

ARRANGEMENT OF APPARATUS FOR CYCLIC VOLTAMMETRY.

FIGURE 5(b)

SCHEMATIC CIRCUIT CONFIGURATION FOR CYCLIC VOLTAMMETRY.

- I. TRIANGULAR WAVE GENERATOR.
- II. POTENTIOSTAT.
- III. X-Y RECORDER OR OSCILLOSCOPE.
- IV. ELECTROLYSIS CELL.

The potentiostat terminals are labelled as in Figure 1.

- A. Working electrode.
- B. Reference electrode.
- C. Counter electrode.
- D,E. Current recorded, across resistance R_e .
- F,G. Triangular wave input.

FIGURE 5a.

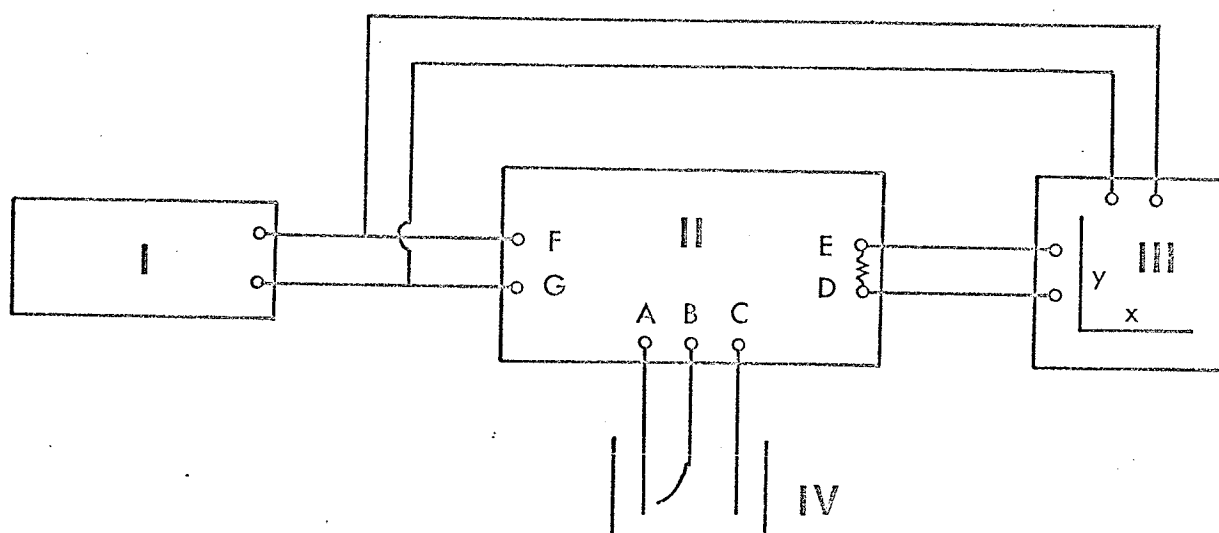
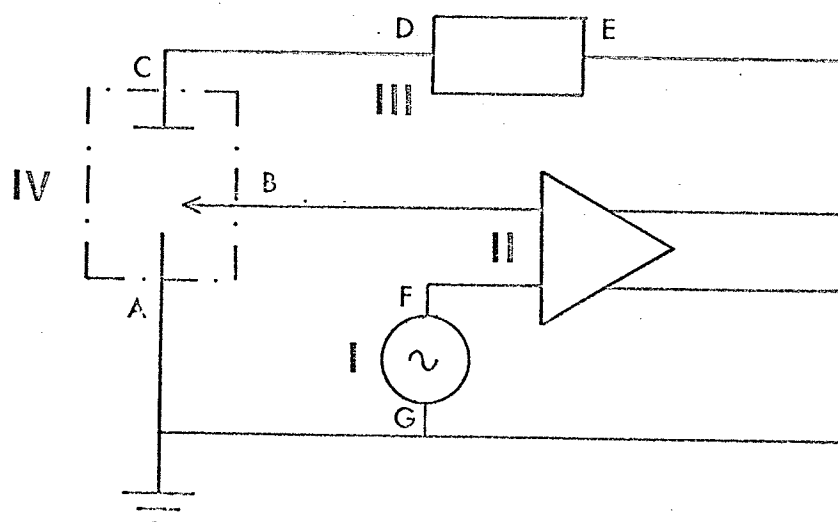


FIGURE 5b.



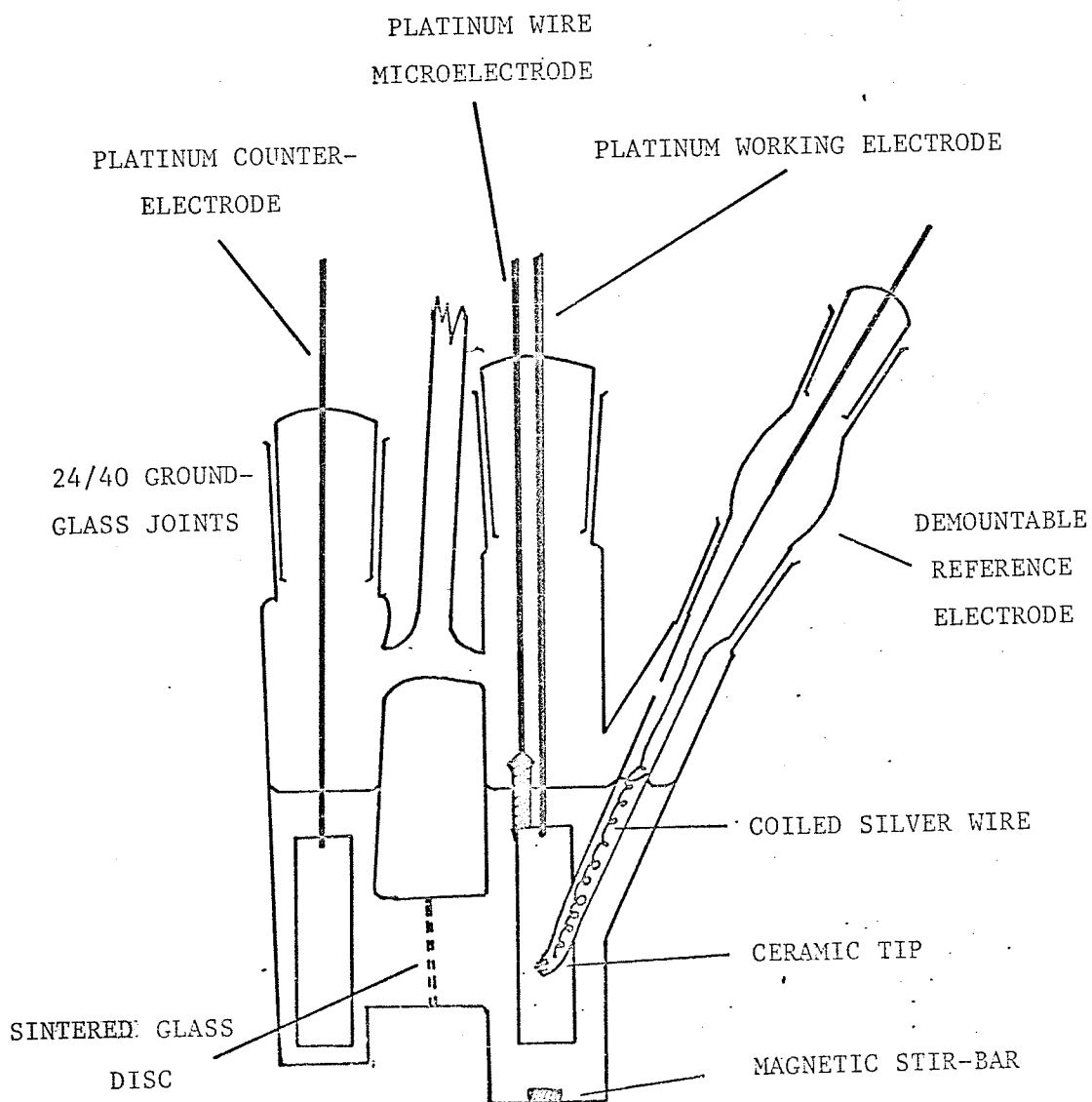
Chromosorb W (Wilkens Instrument) was treated with 5% methanolic KOH solution, dried and treated with a 20% Apiezon L (James G. Biddle Co.) in petroleum ether. Dimethylformamide was eluted in a well-formed peak with this column packing. A second column, from which styrene was eluted before dimethylformamide, was prepared with a support of Fluoropak 80 (Fluorcarbon Co.) and a coating of Carbowax 1540 (Wilkens Instruments).

OTHER INSTRUMENTS. Infra-red spectra were obtained on Perkin-Elmer Model 21 or Model 337 spectrometers. A Varian E3 esr spectrometer was employed to detect radical-anion species.

ELECTROLYSIS CELLS. A typical cell used for controlled potential electrolyses is shown in Figure 6. The cell geometry facilitated the transfer of known amounts of solvent from the graduated receiver to the anode or cathode compartments under high vacuum conditions. The electrode assembly in the cathode compartment could be rotated so that a platinum wire microelectrode was brought close to the reference electrode. Cyclic voltammograms were obtained in the course of controlled potential electrolysis by using the microelectrode. The demountable vacuum-tight reference electrode was separated from the catholyte by a ceramic tip sealed in glass donated by Proton Laboratories Inc. The ceramic tip proved superior to asbestos fibres sealed in glass which were employed in the first few experiments. A serum-capped orifice was used for sample withdrawal in some cells. Figure 7 shows the cell used for cyclic voltammetry. The working electrode consisted of the cross-section of a 1/16 inch diameter platinum wire

FIGURE 6.

CELL FOR CONTROLLED-POTENTIAL ELECTROLYSIS.



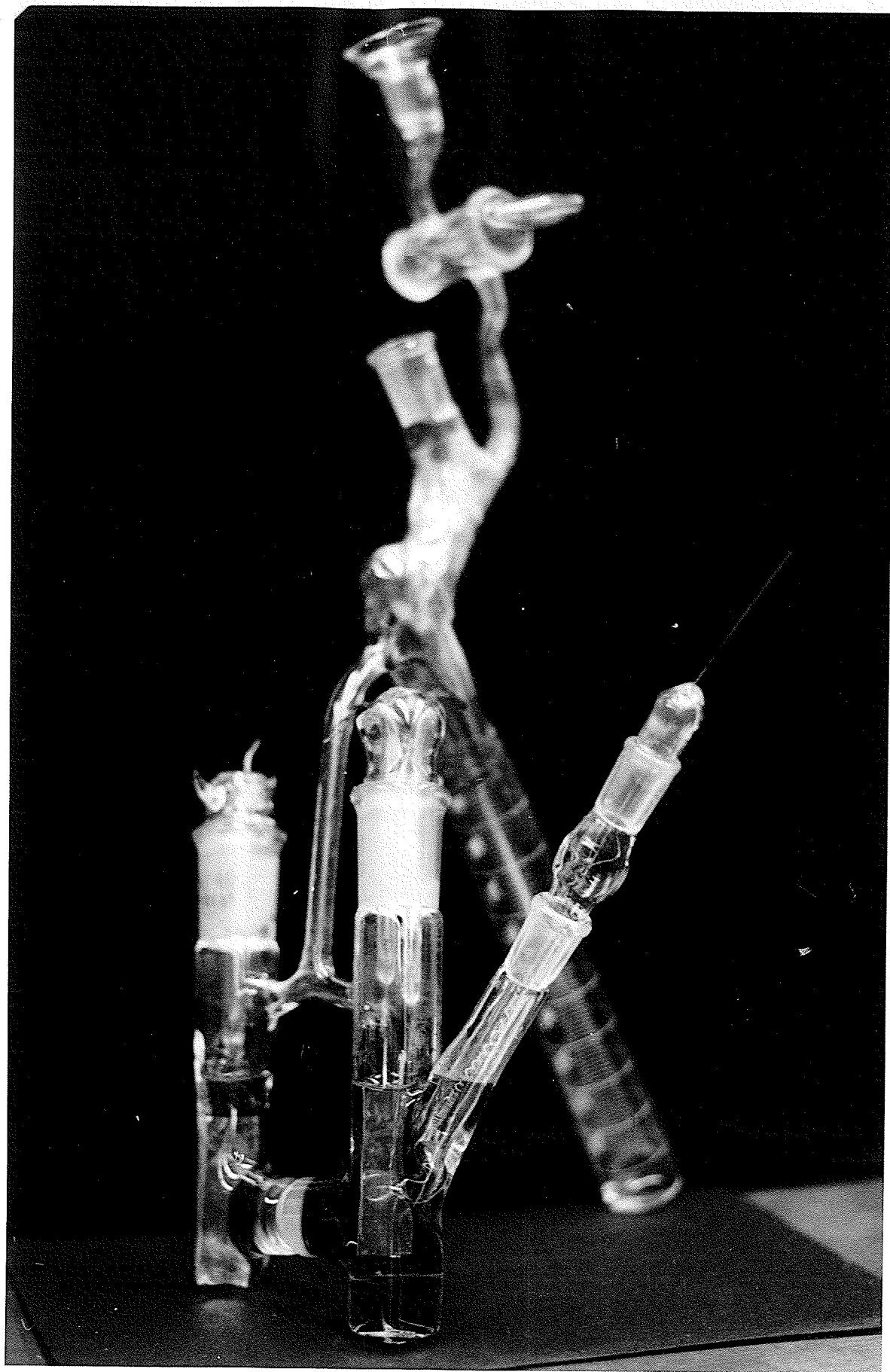
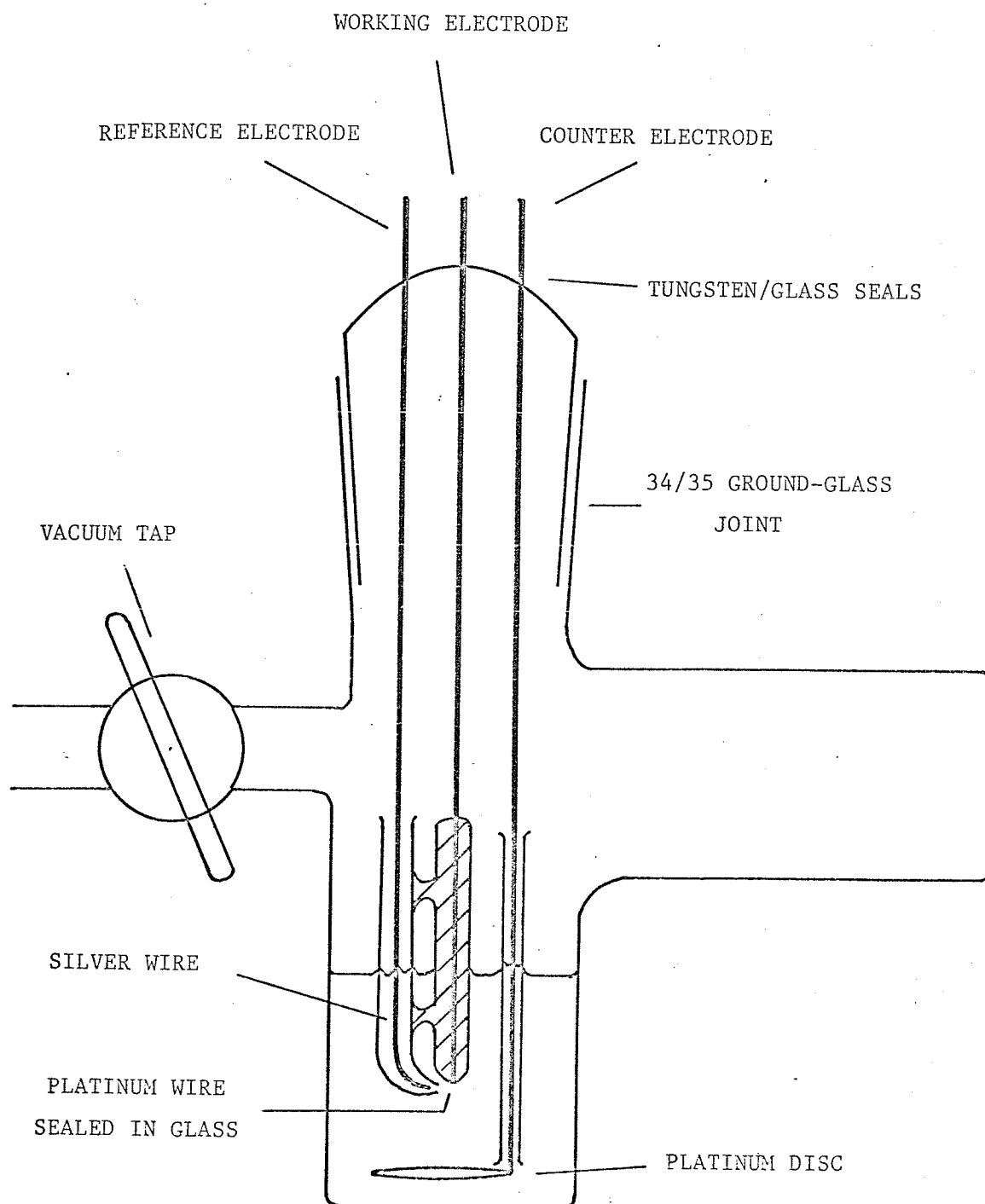
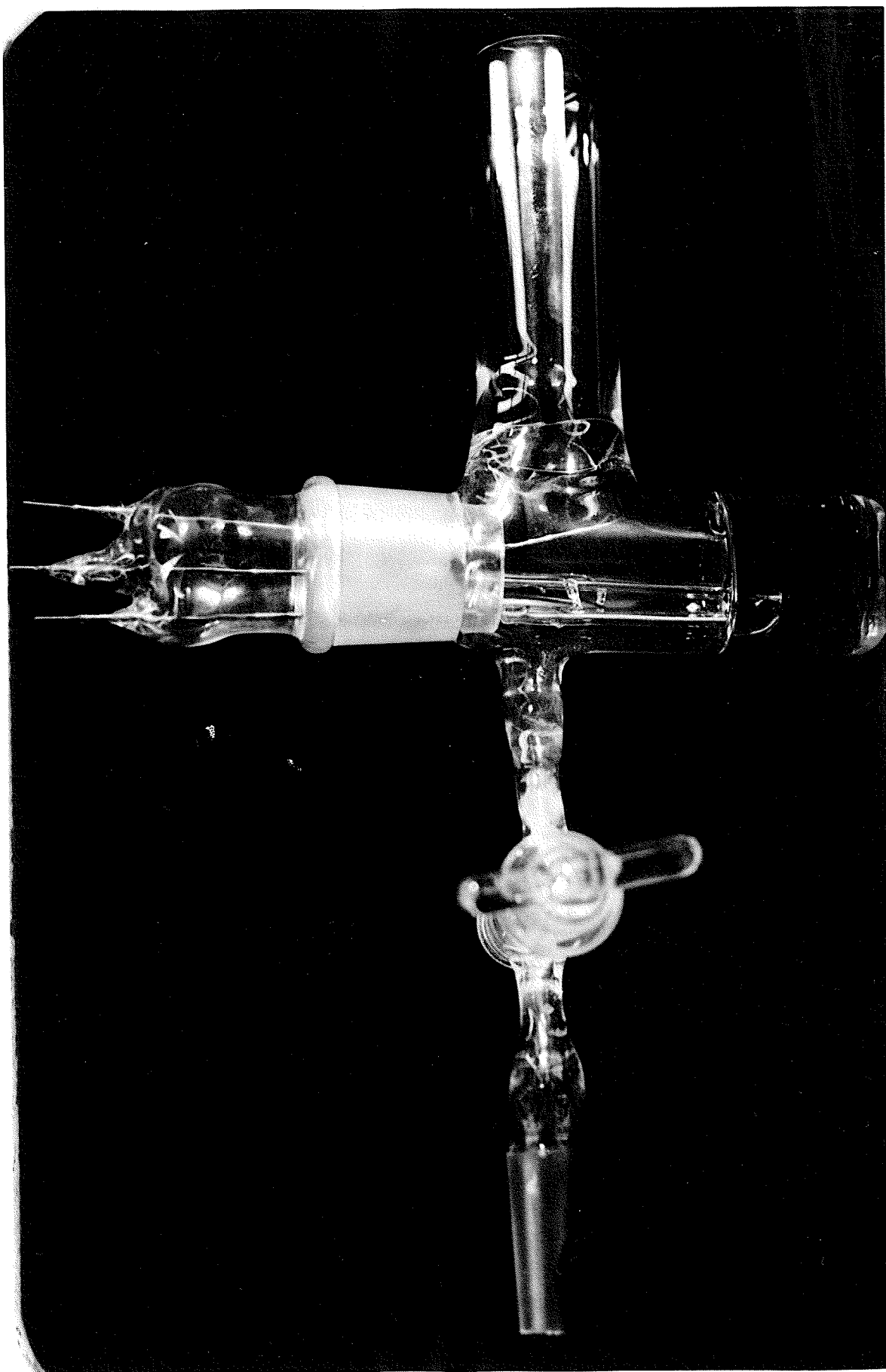


FIGURE 7.

VACUUM CELL USED FOR CYCLIC VOLTAMMETRY.





sealed in glass. A simple silver wire sheathed in a glass capillary proved adequate as a reference electrode, and avoided the risk of contamination from conventional reference electrodes. Figure 8 illustrates the cell used to generate radical anions for electron spin resonance studies. The flat portion of the cell, made from collapsed quartz tubing, was inserted directly in the cavity of an esr spectrometer.

METHOD

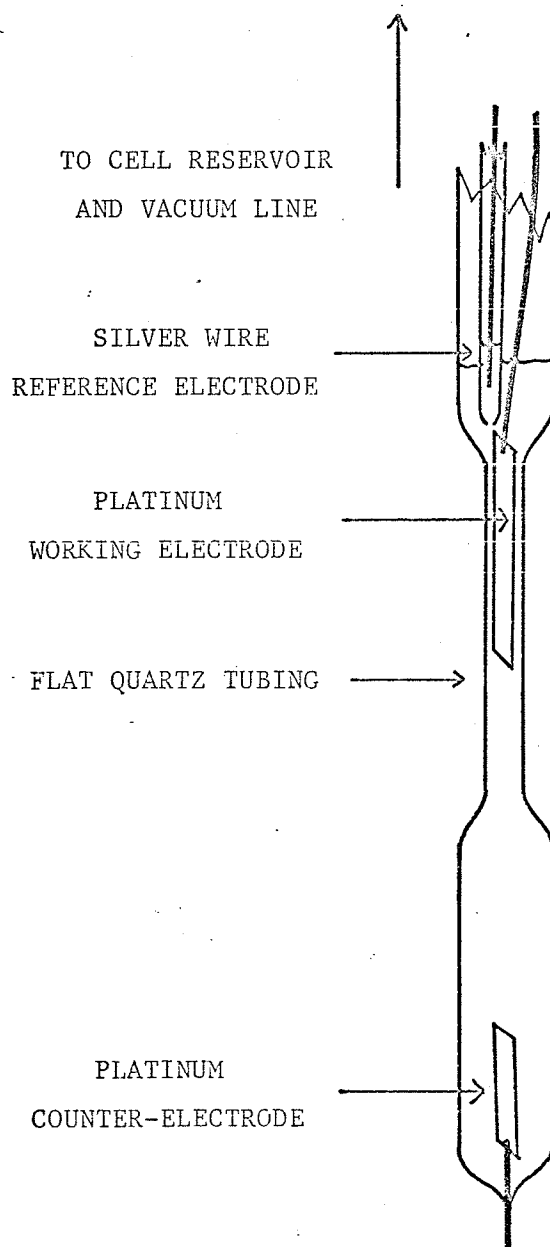
The experimental methods used in this investigation will be illustrated by two examples.

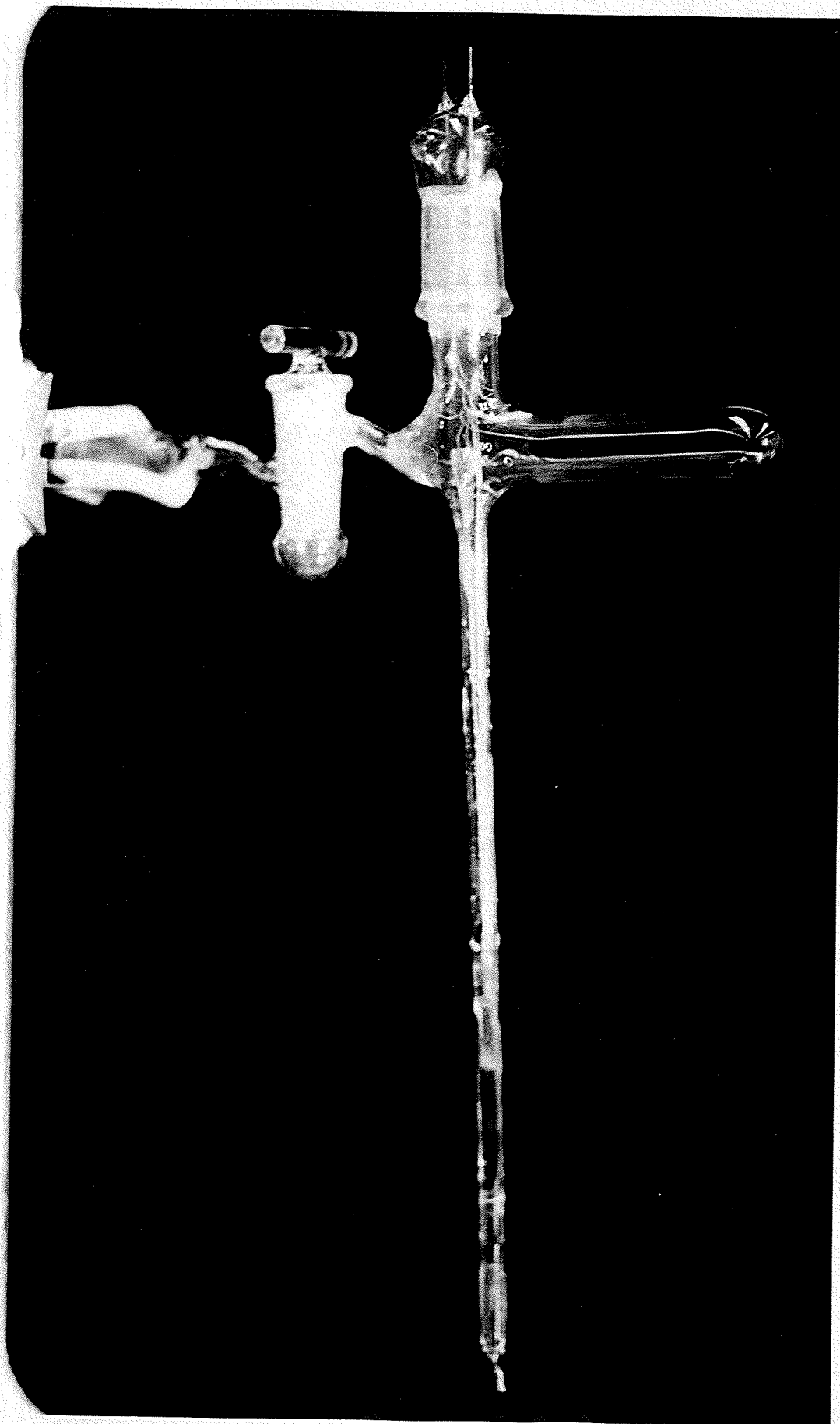
The Controlled Potential Electrolysis of Styrene.

Tetrabutylammonium perchlorate, 4.5g, was placed in each of the electrode compartments of an electrolysis cell similar to that shown in Figure 6. After evacuation under high vacuum overnight, dimethylformamide was distilled into the cell under reduced pressure of purified nitrogen. By careful tilting of the cell, 55 ml was transferred from the graduated receiver to the cathode compartment. The reference electrode was prepared by adding a solution of silver perchlorate in dimethylformamide (0.1 M) to the assembly shown in Figure 6. The cell was filled with nitrogen and the reference electrode introduced. The electrical connections were made (Figure 5) with the platinum wire as the working electrode. Previously distilled styrene, stored under nitrogen in a serum-capped flask was injected into the cathode compartment, and the voltammetric peak height for each injection was determined. When a total of 1200 μ l of styrene

FIGURE 8.

CELL USED FOR ESR EXPERIMENTS.





had been added, the planar platinum electrode was connected and controlled potential electrolysis performed at -2.9 V vs Ag/Ag^+ reference electrode. The electrolysis current was recorded; the area under the curve gave the amount of current passed. The depletion of monomer was also followed by gas chromatography. After electrolysis, a sample of the catholyte was diluted with water and extracted with ether. The organic portion was then extracted with 5N HCl to remove any amine. After dilution and treatment with picric acid, a picrate, m.p. $104-5^\circ\text{C}$ was isolated. This corresponded to the literature value for the melting point of tri-*n*-butylamine picrate (83). A gas chromatographic analysis of the catholyte also indicated a peak with the same retention time as an authentic sample of tri-*n*-butylamine. The residue of the ether extract on evaporation gave a waxy residue which on recrystallization from methanol melted sharply at 51°C , and gave an infrared spectrum corresponding closely to that for 1,4-di-phenylbutane (84).

Cyclic Voltammetry of Stilbene.

The cell illustrated in Figure 7 was carefully cleaned. The silver wire electrode was washed with dilute nitric acid with water and with high purity ether. Tetrabutylammonium perchlorate (1.0g) and 0.0063 g trans-stilbene were added, and the cell was attached to a high-vacuum line and pumped down overnight. Thirty ml tetrahydrofuran was distilled into the cell under vacuum. The cell was thermostatted at 25°C in a waterbath. (An electrical heating tape was wrapped around the part of the cell that was not immersed to prevent solvent

condensation.) The electrodes were connected to the circuit shown schematically in Figure 5, and the potential of the working electrode scanned, initially in a cathodic direction, over a suitable voltage range. All voltammograms shown in this thesis were for single cycle (non-repetitive) scans. Sufficient time was allowed between scans for the concentration of electroactive material around the electrode to reach the concentration in the bulk of the solution. Each voltammetric peak was examined at a variety of rates of voltage scan. Peak heights were measured from the base line obtained in the absence of the electroactive material under study, or from the estimated extension of the previous peak where appropriate (72). The peak potentials were extrapolated linearly to the line for zero current to give $(E_p)_{i=0}$ for each peak. A similar extrapolation for the potential at half peak height gave the half peak potential at zero current $(E_{p/2})_{i=0}$. The difference between these two quantities was used as a semi-quantitative measure of the spread of the peak along the potential axis. Other variables determined from voltammetric curves were important in determining the reduction mechanism. These included the amount of potential variation with peak current. This was readily determined from the slope of the line joining the voltammetric peaks at different scan rates. The rate of increase of peak heights with the square root of the scan rate was determined by plotting these quantities graphically.

For asymmetric voltage scans, the frequency of the triangular waveform was increased manually at the end of the cathodic scan. As the peak height on reverse scan is a function of switching potential, the reverse voltammograms are less reproducible than those obtained

with symmetrical triangular voltage scan.

ACCURACY OF VOLTAMMOGRAMS

The errors introduced into the recorded voltammograms due to inaccuracy of the electronic equipment were negligible. The X-Y recorder had a specified accuracy on each axis of better than $\pm 0.2\%$ full scale. Thus, the potential axis gave the potential between reference and working electrode to this precision. The current was determined by measuring the potential drop across a standard 1% resistor, thus, the current flowing through the cell was correct to about 1%. The recorder pen slewing speed of 20 in/sec. and the fast response time of the potentiostat assured high dynamic accuracy. Similarly, the Hewlett-Packard function generator provided a triangular waveform with linearity error less than 1%, and a frequency dial accuracy of $\pm 1\%$ full scale (1 decade range of frequency).

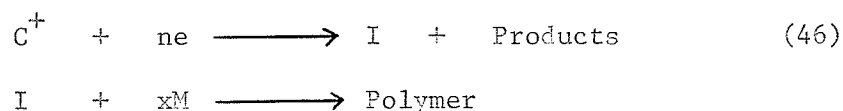
The reproducibility of voltammograms for a given solution was excellent if sufficient time (about thirty seconds) was allowed between scans. However, several sources of systematic errors interfered with the shape of the voltammograms. For example, polarization of the reference electrode, uncompensated resistance between reference and working electrode, or adsorption of material at the working electrode, would each cause distortion. Possible effects of these phenomena will be discussed in the following section of the thesis.

RESULTS AND DISCUSSION

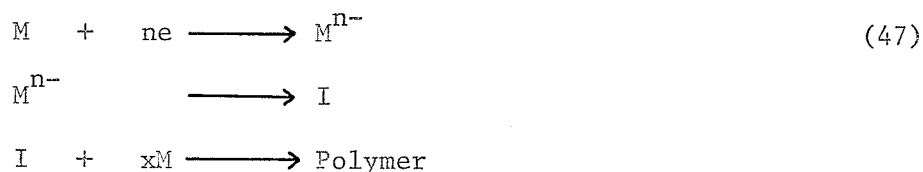
The work reported in this chapter of the thesis may be divided into three main sections. The introductory section demonstrates the possibility of producing polymer anionically at a controlled electrode potential. Secondly, the use of cyclic voltammetry as an adjunct to controlled potential electrolysis in the study of polymerization reactions is described. The third section consists of a more detailed study of electron transfer reactions at the cathode in highly aprotic solvents.

CONTROLLED POTENTIAL ELECTROLYSES

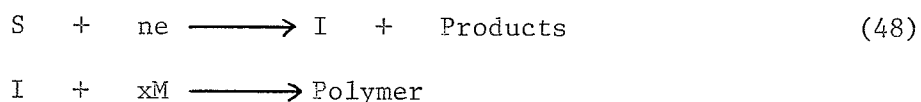
The central purpose of the thesis is the investigation of anionic chain electropolymerizations. Such polymerizations require in general, a monomer M, an electrolyte $C^+ A^-$, and a solvent, S. Three possible electrolytic initiation processes may be envisaged. In the first, the initiating species, I, is formed by the discharge of the cation of the supporting electrolyte.



where n is the number of electrons e involved in the electrolytic reduction of C^+ . Secondly, direct electron transfer to the monomer may occur at an electrode potential less cathodic than that at which salt discharge occurs. The monomer reduction product then initiates polymerization, either directly or after further chemical reaction.



A third possible initiation mechanism involves as a first stage reduction of the solvent:-



Preliminary electrochemical evidence was required as to which of these processes occurred in electrolytic polymerizations. Such polymerizations have, in general, been performed at platinum electrodes in highly aprotic media, and usually require relatively high monomer concentrations. On the other hand, polarography (the most widely used electrochemical method of investigation) is performed at a mercury electrode usually in a proton donating medium and at relatively low concentrations of electroactive material.

Rather than attempt to draw conclusions from polarographic measurements, preliminary experiments were performed under conditions very similar to those employed in electrolytically initiated polymerizations, but with provision for measurement and control of the electrode potential. The electrolytic cell used is shown in Figure 6. A silver/silver bromide couple was used as a reference electrode, and the potential of the platinum working electrode was adjusted using an electronic potentiostat. In order to determine which of the above initiation mechanisms was operative, current-potential curves were obtained for a variety of monomers, solvents and salts known to

produce polymer on electrolysis. With only salt and solvent in the electrolysis cell, the potential of the working electrode was increased in a cathodic direction. The current flowing through the cell was negligible until the potential at which the salt cation discharged; then the current increased very rapidly with increasing potential. Monomer was then vacuum-distilled into the cell, and again a current/potential curve was obtained. If an electrolysis current flowed at a potential less cathodic than that necessary to electrolyse the salt, then this indicated that the added monomer was being reduced directly, and so direct electron transfer to monomer was a possible initiating mechanism (equation 47).

Current/potential plots for methyl methacrylate, and styrene with dimethyl formamide (DMF) and tetrahydrofuran (THF) as solvents and tetrabutylammonium ($\text{N}(\text{Bu})_4^+$) salts as electrolytes are shown in Figure 9. The results clearly indicated that direct electron transfer to these monomers occurred at platinum electrodes in aprotic solutions of tetra-alkylammonium salts. The current voltage curves were very similar in both THF and DMF; however, the low solubility of tetra-alkylammonium halides in tetrahydrofuran, coupled with a low dielectric constant produced solution resistances of such magnitude (up to 300 kilohms) that at its maximum voltage output the potentiostat only passed a very limited current. By using the more soluble perchlorate or tetraphenylboride salts in place of the halides, the effect of the solution resistance was lessened. Another electrode reaction of interest in electrolytically initiated polymerization studies is the

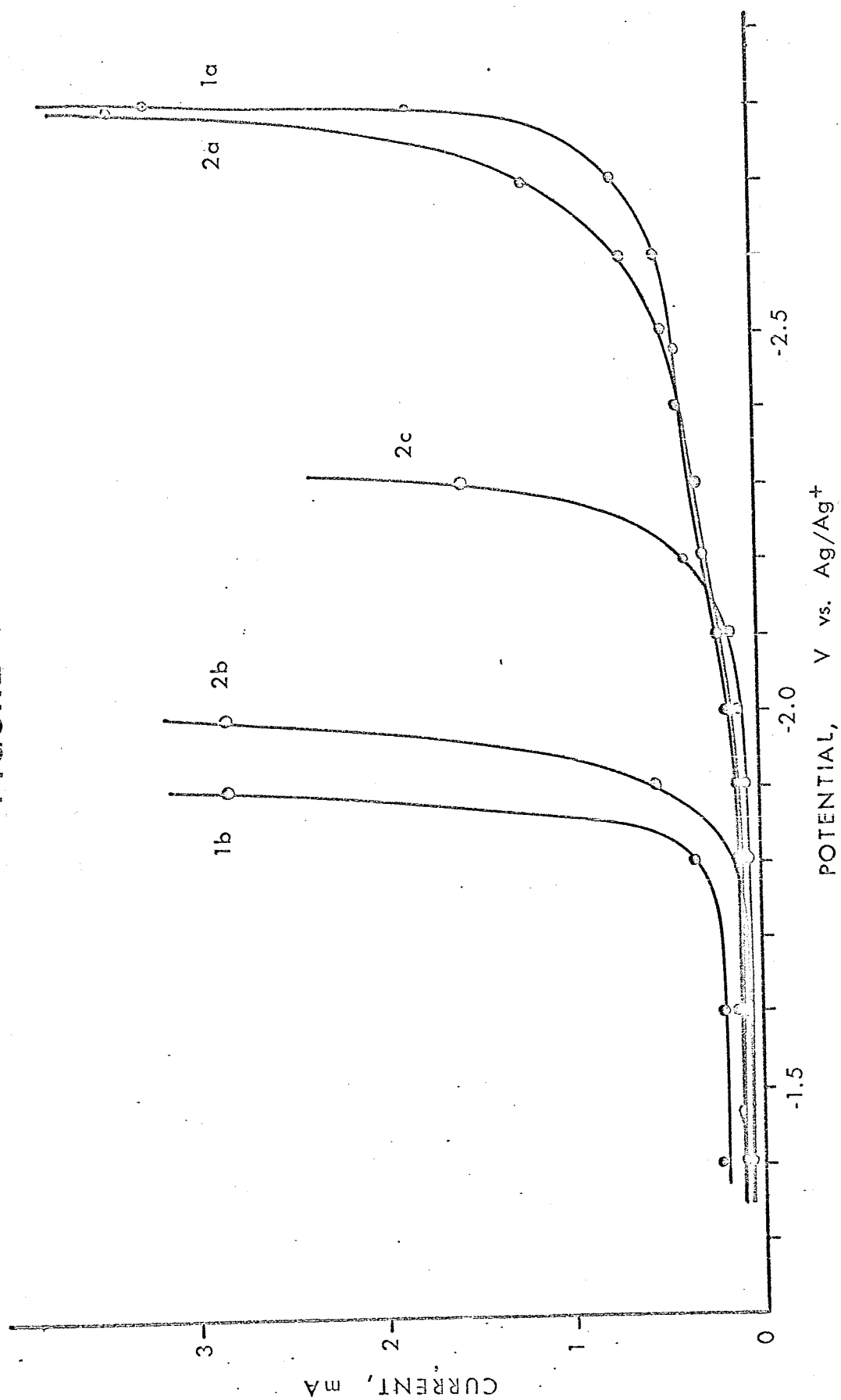
FIGURE 9.

CURRENT/POTENTIAL PLOTS FOR THE REDUCTION OF METHYL METHACRYLATE
AND STYRENE AT A PLATINUM ELECTRODE.

- 1a. Tetrabutylammonium bromide, 1 g, in 60 ml dimethylformamide.
- 1b. Solution 1a with 3.0 ml methyl methacrylate.
- 2a. Tetrabutylammonium tetraphenylboride, 0.75 g, in 75 ml
tetrahydrofuran.
- 2b. Solution 2a with 2.0 ml methyl methacrylate.
- 2c. Solution 2a with 2.0 ml styrene.

The working electrode was a 1 sq inch platinum sheet.

FIGURE 9.



generation of living α -methylstyrene anions using sodium tetraphenylboride in tetrahydrofuran. However, current/potential curves for this system showed that both sodium ions and α -methylstyrene were reduced at approximately the same potential (Figure 10). In this case it is not possible to differentiate between direct electron transfer or sodium atom initiation. With this electrolyte, the reference electrode clogged at cathodic potentials, causing problems due to high resistance between the working and reference electrodes.

The electrode reactions suggested on the basis of current/potential curves may be further investigated by performing electrolyses at controlled potentials. Although Figure 9 showed that direct electron transfer occurred, it remained to determine whether or not this process initiated polymerization. The solutions were electrolysed above the monomer reduction potential, but below the salt discharge potential. However, on electrolysing the ~ 0.5 molar solutions that had been used to obtain the current/potential curves, no polymer was isolated on precipitation with methanol although the colours characteristic of the monomer anions had been evident at the cathode surface. A reconsideration of the previous data on similar anionic polymerizations initiated electrolytically (85) showed that fairly high monomer concentrations and current densities were required for polymer formation. Accordingly, the effect of increasing the monomer concentration was considered. The current/potential curves for methyl methacrylate in tetrahydrofuran (Figure 11) indicated that at higher monomer concentrations some factor was limiting the increase of current with

FIGURE 10.

CURRENT/POTENTIAL PLOTS FOR α -METHYLSTYRENE IN SODIUM TETRAPHENYL-
BORIDE-TETRAHYDROFURAN SOLUTION.

- 1a. Sodium tetraphenylboride, 0.75 g, in 80 ml tetrahydrofuran.
- 1b. Solution 1a with 1.0 ml α -methylstyrene.

FIGURE 11.

THE EFFECT OF MONOMER CONCENTRATION ON CURRENT/POTENTIAL PLOTS.

- 1a. $N(Bu)_4$ tetraphenylboride, 0.75 g, in 75 ml tetrahydrofuran.
- 1b. Solution 1a with 2.0 ml methyl methacrylate.
- 1c. Solution 1a with 5.0 ml methyl methacrylate.
- 1d. Solution 1a with 10.0 ml methyl methacrylate.

FIGURE 10.

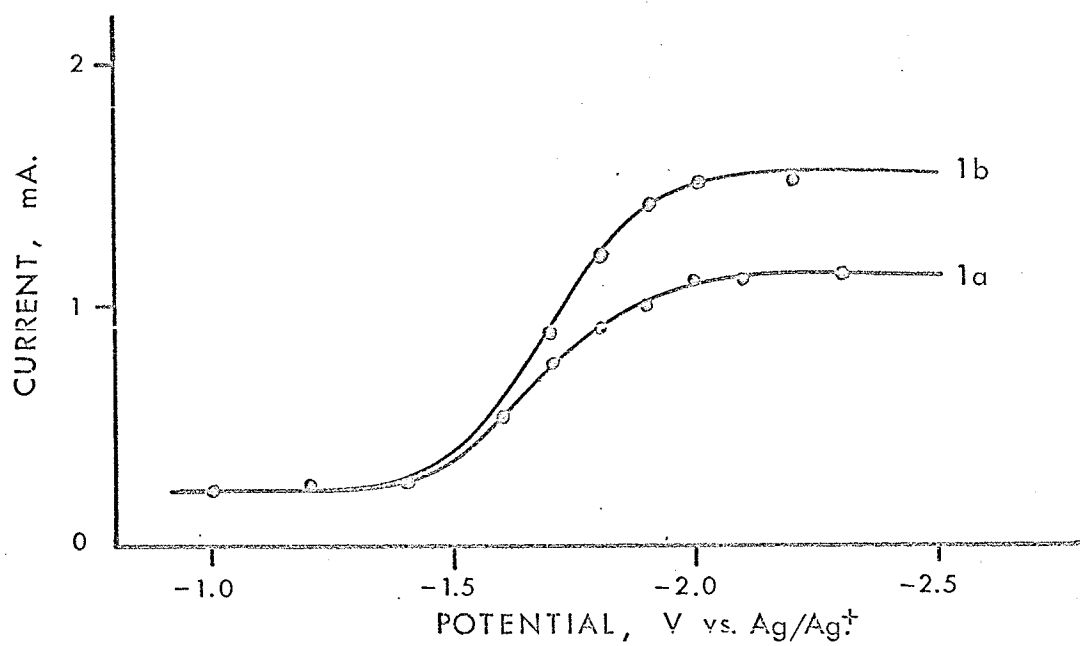
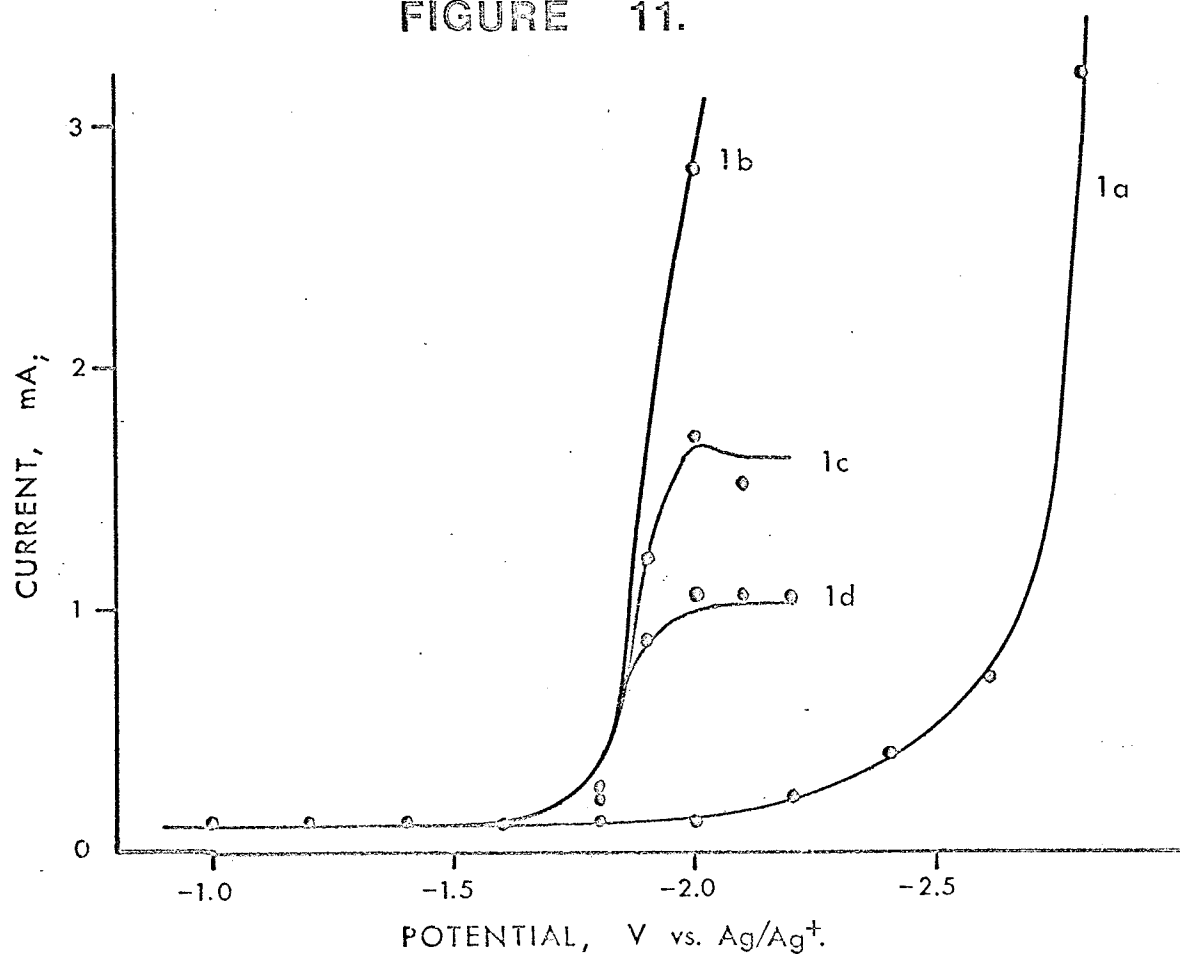


FIGURE 11.



potential; the higher the monomer concentration, the lower was the current. This interesting phenomenon will be discussed later in the light of the fact that controlled potential electrolysis of this monomer-rich solution did in fact produce a yield of 0.8 g polymer for the passage of 3.7×10^{-5} Faradays of electricity. If polymer were the only electrolysis product, then these figures would allow the estimation of the number of monomer units consumed per electron passed and hence, under ideal conditions, the molecular weight might be estimated. However, the low yield of polymer formed relative to the monomer consumed indicated the presence of side reactions. To determine the reason for this, an independent analytical method for following the consumption of monomer was necessary. Accordingly, a series of controlled potential electrolyses were performed under relatively rigorous conditions of purity. A gas chromatographic method was developed to follow the depletion of monomer, and current vs time curves were also recorded to follow the progress of the reaction. By integrating the current/time curve, the relationship between the amount of monomer electrolysed and the number of Faradays passed was determined. Figure 12 indicates the results for the electrolyses of styrene and methyl methacrylate in dimethyl formamide with tetra-n-butylammonium perchlorate as supporting electrolyte. The electrolysis currents were in the range from 10 to 1 mA, and the solutions were electrolysed at controlled potential for about eight hours. In this time, the electrolysis current and the monomer concentration for methyl methacrylate had dropped almost to zero

FIGURE 12.

GRAPH OF THE DECREASE IN MONOMER CONCENTRATION WITH AMOUNT OF
ELECTRICITY PASSED DURING THE CONTROLLED-POTENTIAL POLYMERIZATION
OF STYRENE AND METHYL METHACRYLATE.

LINE A. STYRENE.

LINE B. METHYL METHACRYLATE.

ELECTROLYSED AT 25°C IN 0.07 M $\text{N}(\text{Bu})_4\text{ClO}_4$ -DMF SOLUTION.

FIGURE 12.

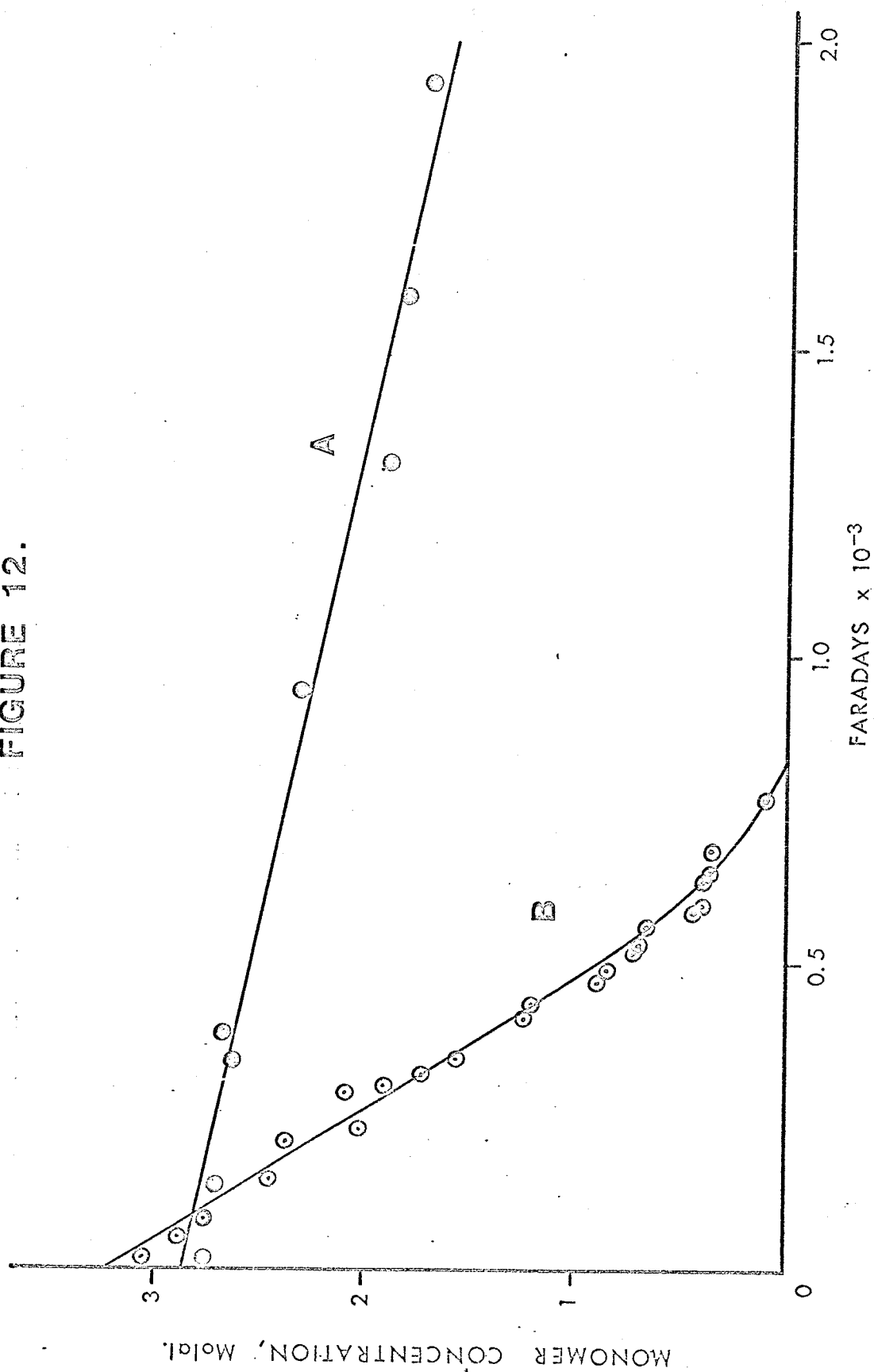


(Figure 12, Line B). Initially, 0.07 mole methyl methacrylate was present in the cathode compartment, and this was electrolysed by 0.84×10^{-3} Faradays of electricity, corresponding to 83 monomer units per electron. An approximately linear relationship was apparent between the amount of current passed and the quantity of monomer consumed. Similar results were obtained in the case of styrene (Figure 12, Line B); however, the electrolysis of a styrene proceeded at a much lower rate, so the reaction was not carried out to completion. About 14 moles of styrene reacted per Faraday of electricity passed through the cell.

Despite the fact that only small quantities (1 to 2 gms) of polymer were isolated by precipitation in methanol, these results showed conclusively that the polymerization of styrene and methyl methacrylate in aprotic solutions of tetra-alkylammonium salts may be initiated by a direct electron transfer process.

As these electron transfer processes occur at different electrode potentials for different monomers, the possibility existed of selectively initiating polymerization with one of a number of monomers present in solution. The monomer pair styrene and methyl methacrylate were of particular interest in view of the results of recent electro-initiated copolymerization experiments (85,86,87). Gas chromatography was used to measure the rate of depletion of this pair of monomers in several controlled potential electrolyses. In conventional anionic polymerization, the initially formed copolymer consisted of methyl methacrylate units (88). This was also found with electroinitiated copolymerizations in tetrahydrofuran (87).

It was shown in Figure 9 that methyl methacrylate was reduced at a lower electrode potential than styrene. As expected on this basis, the methyl methacrylate but not the styrene was consumed when a mixture of these monomers in tetrahydrofuran was electrolysed below the styrene reduction potential. After the methyl methacrylate had been electrolysed, the styrene was then reduced by raising the potential. However, no polymer precipitated in methanol, indicating the formation of low molecular weight products. In DMF, electrolytic copolymerization results were anomalous in that styrene was incorporated in the copolymer (87). However, controlled potential electrolysis of the monomer pair below the styrene reduction potential again indicated that only methyl methacrylate was consumed; no reaction of anions derived from methyl methacrylate with styrene monomer was detected. Such a cross-polymerization would be expected if styrene entered the copolymer. Again, no solid copolymer was isolated. Therefore, extrapolations from these controlled-potential experiments performed at low current densities to the previous copolymerizations must be made cautiously.

The discrepancy between the amounts of high molecular weight polymer isolated and the quantities of monomers consumed in the controlled-potential electrolyses suggested that much of the monomer formed oligomeric products. The yield and nature of these polymers formed by constant-current electrolyses have already been studied (39,40,41,85) so rather than attempt to improve the yields of high molecular weight polymer under controlled-potential conditions, the initiation process and the fate of the ionic species were investigated

using potentiostatic methods.

It has been noted already that high monomer concentrations favour polymer formation. Therefore, low monomer concentrations were used to investigate the products of the initiation and termination reactions. Conditions of rigorous purity and careful experimental techniques were necessary, as less than 1 g. of starting material was used. Styrene was electrolysed in dimethylformamide below the discharge potential of the tetrabutylammonium perchlorate supporting electrolyte. The styrene content of the catholyte was determined by gas chromatography. The current decreased with time in the manner expected for controlled-potential electrolysis in a stirred solution (Figure 13a). Although the electrolysis was not carried quite to completion, it is apparent from Figure 13b that 6.5×10^{-3} Faradays of current were required to electrolyse the styrene. Initially 6.56×10^{-3} moles of styrene were present, so within experimental error, one styrene molecule was consumed for each electron passed. This result indicated that no polymerization occurred under the conditions employed.

The transfer of one electron to a styrene molecule initially would produce a reactive radical ion. In order to determine the subsequent reaction of this species it was necessary to try to isolate the small amount of reaction product and to identify it. By means of retention time data on two gas chromatograph columns of different character, it was possible to detect the residual styrene and a little ($< 5\%$) ethyl benzene, which is the expected two-electron reduction

FIGURE 13.

CONTROLLED POTENTIAL ELECTROLYSIS OF STYRENE AT LOW CONCENTRATION
IN ANHYDROUS DIMETHYLFORMAMIDE.

The catholyte contained 0.75 ml styrene in 62 ml of 0.06 M
 $\text{N}(\text{Bu})_4\text{ClO}_4$ -DMF solution, which was electrolysed below the salt
discharge potential at 25°C.

FIGURE 13a. GRAPH OF ELECTROLYSIS CURRENT VERSUS ELECTROLYSIS
TIME.

FIGURE 13b. GRAPH OF AMOUNT OF STYRENE IN THE CATHOLYTE VERSUS
QUANTITY OF ELECTRICITY CONSUMED.

FIGURE 13a.

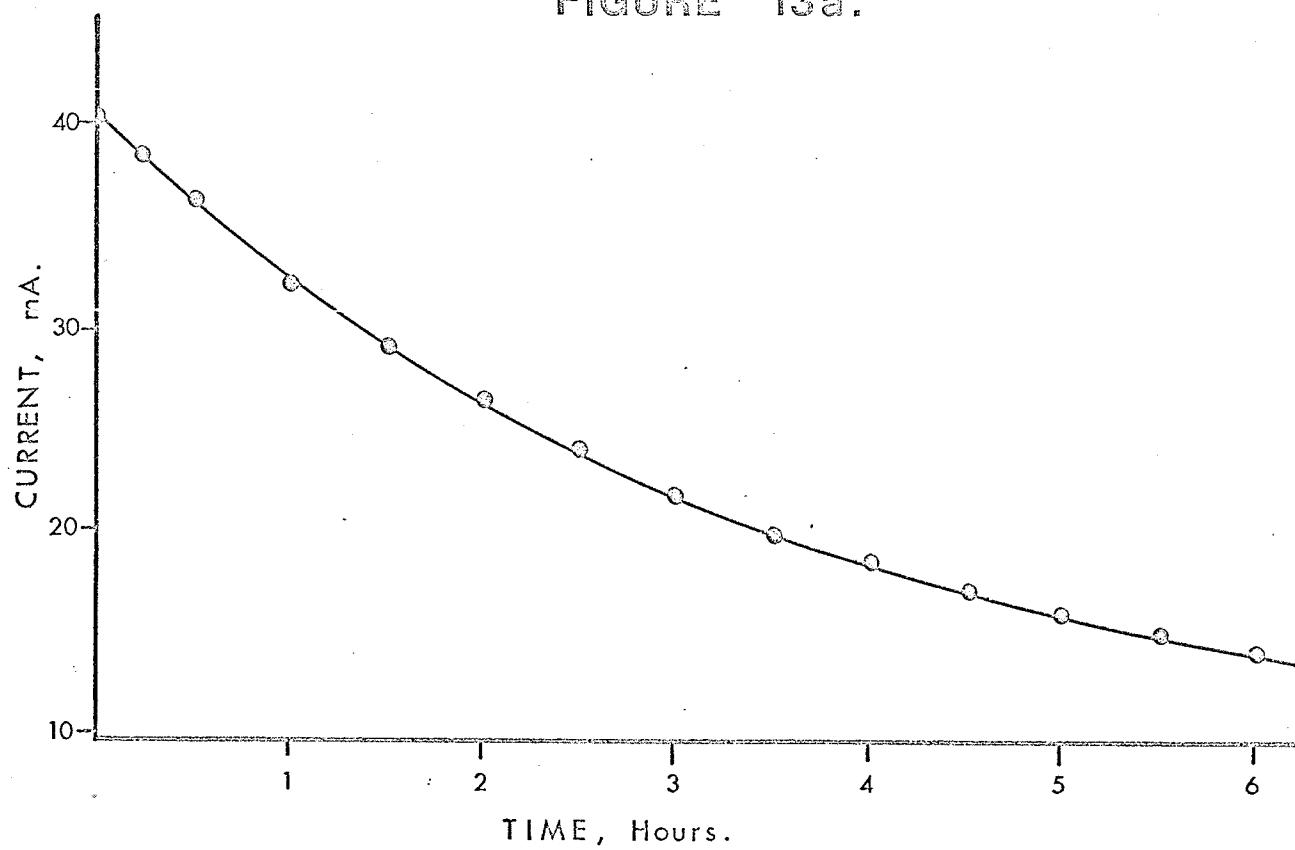
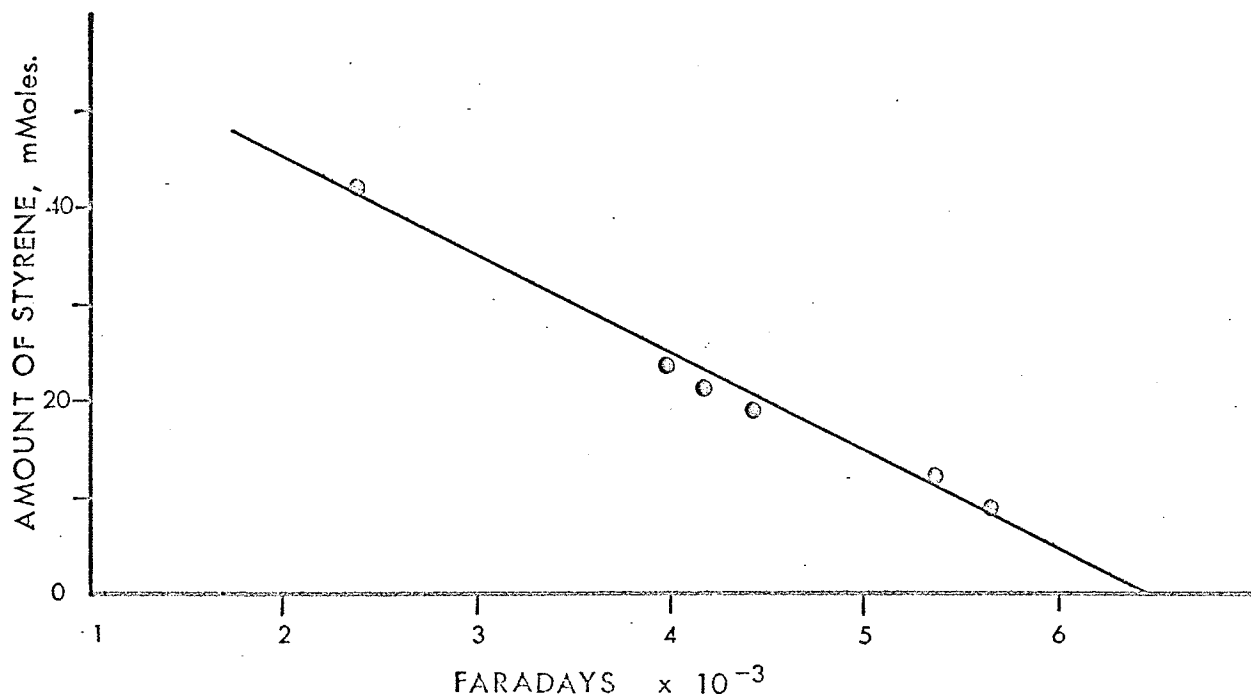
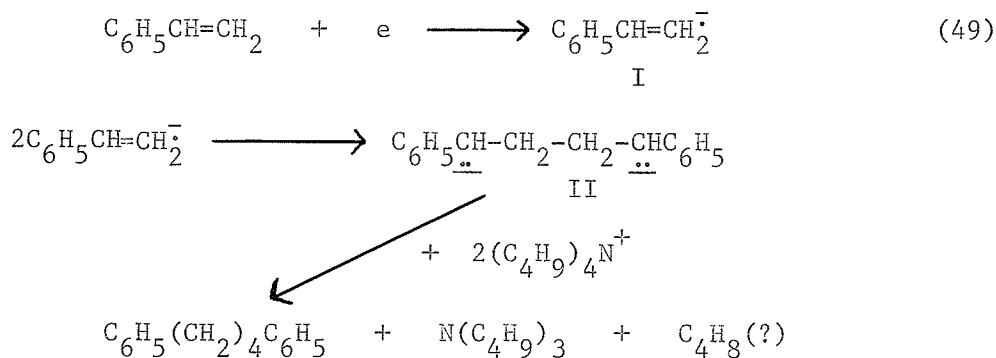


FIGURE 13b.



product. Further treatment of the reaction mixture resulted in the isolation of the major reaction product, 1,4-diphenylbutane. This tail-to-tail dimer of styrene was identified by melting-point and infrared data.

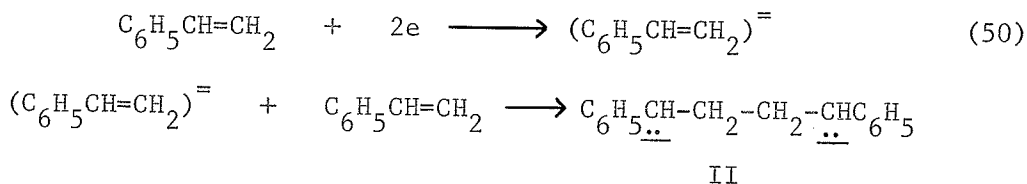
The dimerization of two styrene radical ions would be expected to produce a di-anionic species, which then protonated to give the observed reaction product. In order to investigate the source of the protons, a further controlled-potential electrolysis of styrene was performed, this time at higher salt concentrations. Again one electron was consumed per styrene molecule, and 1,4-diphenylbutane was isolated. In addition, tri-n-butylamine was detected by gas chromatography and isolated as its picrate. The electrolysis was carried out below the salt discharge potential so the tri-n-butylamine must have resulted indirectly from proton abstraction from the tetra-n-butylammonium cation. Because of the very small quantities involved, the isolation of these reaction products was not quantitative, but the evidence nevertheless suggests the following reaction sequence.



No C_4 hydrocarbons were detected because of their volatility.

This mechanism is consistent with the reaction schemes proposed

for electroinitiated polymerizations in dimethylformamide solutions of tetra-alkylammonium salts. At higher monomer and lower salt concentrations the dianion II may react with further styrene molecules by an anionic chain mechanism; termination of the chain may similarly involve attack on the counter-cation. It should be noted that these results do not eliminate the possibility of a two-electron transfer to a styrene molecule followed by attack on a second molecule to give species II.



However, simultaneous two electron reduction of aromatic hydrocarbons is very rare. Unless protonation occurs after the first electron transfer, a more cathodic potential is generally necessary for a second electron transfer (89).

These results showed that controlled potential electrolysis was a useful tool for investigating electrolytic polymerizations. However, the possibility of introducing air and other impurities when withdrawing samples for gas chromatography led to a search for methods of following the consumption of monomers in a sealed system.

VOLTAMMETRY AND MONOMER CONCENTRATION

Voltammetry at a solid micro-electrode was chosen over more conventional spectrophotometric methods because it was hoped that electrochemical information could be obtained in addition to measurements of the concentration of electroactive components in the solution.

The diffusion conditions are well defined for voltammetry at a solid stationary electrode (see thesis introduction), so this method is superior to determining the concentration of electroactive substance by measuring the current in a stirred solution during controlled-potential electrolysis. Although a satisfactory agreement between current and monomer concentration as determined by gas chromatography was found in several of the reported electrolyses, any variation in the rate of stirring altered the thickness of the diffusion layer, and, therefore, the current changed according to equation (17).

An electrolysis cell was constructed containing both a large platinum electrode for controlled-potential electrolysis, and a platinum wire micro-electrode for voltammetry. A series of cyclic voltammograms were obtained at different monomer concentrations in order to test the dependence of peak height on the concentration of electroactive material given in equations 35 and 41. The results for styrene with three different concentrations of supporting electrolyte are shown in Figure 14. The relationship between concentration and peak height was found to deviate from linearity quite markedly. The height of the voltammetric peaks reached a limit despite further increases in monomer concentration. In examining this phenomenon more closely, it was found that both the value of the limiting peak current and the concentration of monomer at which it was attained were very dependent on the concentration of $\text{N}(\text{Bu})_4\text{ClO}_4$ used as supporting electrolyte. At low concentrations of electrolyte, the peak heights reached a relatively low limiting value at low styrene concentration (curve A; Figure 14) while the converse was true at high electrolyte concentrations (curve C; Figure 14).

FIGURE 14.

VARIATION OF VOLTAMMETRIC PEAK CURRENT DENSITY WITH MONOMER
CONCENTRATION; EFFECT OF SALT CONCENTRATION.

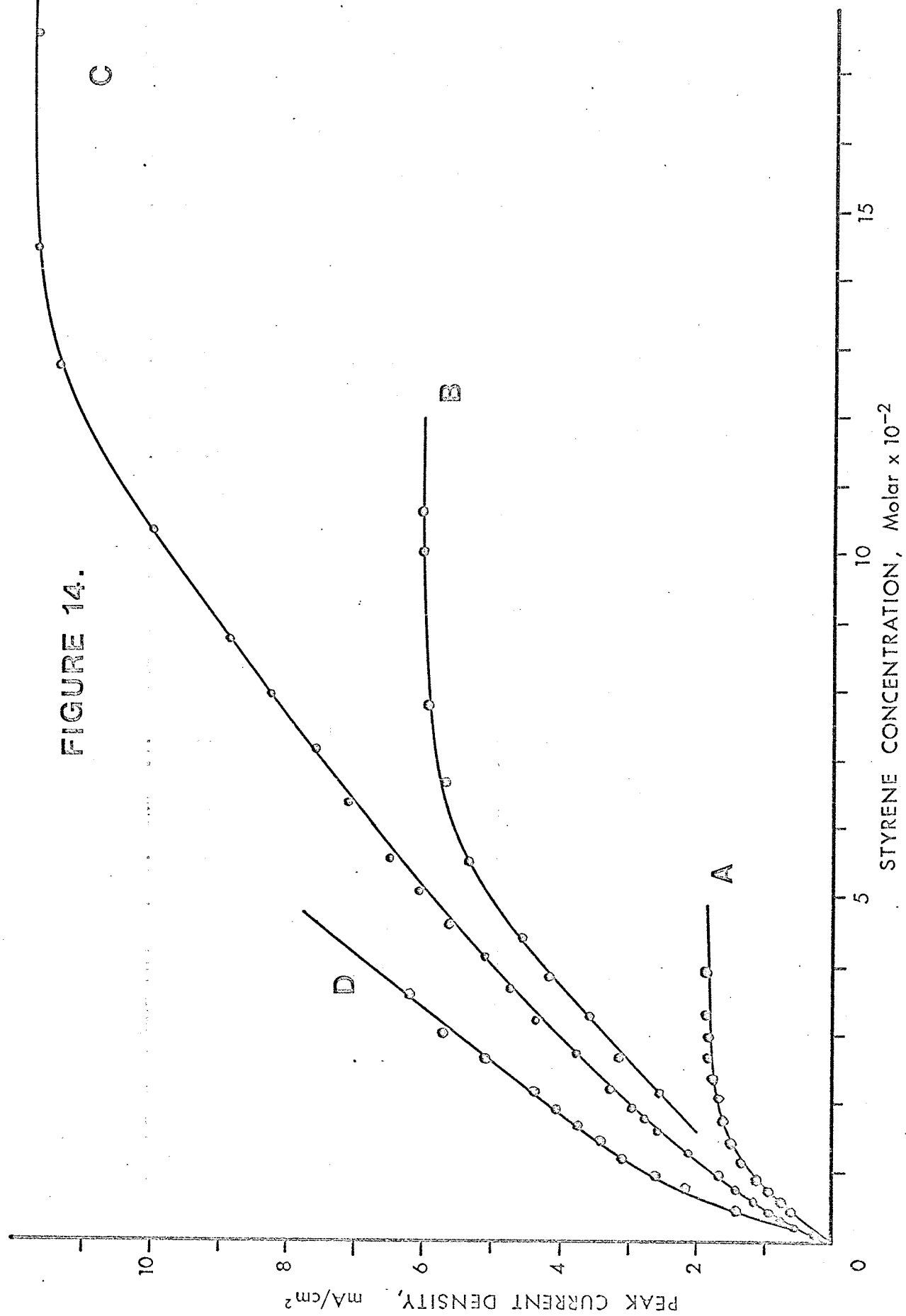
Curve A. Styrene in 0.62×10^{-2} M $\text{N}(\text{Bu})_4\text{ClO}_4$ -DMF solution.

Curve B. Styrene in 5.6×10^{-2} M $\text{N}(\text{Bu})_4\text{ClO}_4$ -DMF solution.

Curve C. Styrene in 0.24 M $\text{N}(\text{Bu})_4\text{ClO}_4$ -DMF solution.

Curve D. α -Methylstyrene in 5.6×10^{-2} M $\text{N}(\text{Bu})_4\text{ClO}_4$ -DMF solution.

FIGURE 14.



There are two possible effects of changing the electrolyte concentration which might explain the variation in peak potential with monomer concentration. Firstly, the electrical resistance of the solution will decrease with increasing electrolyte concentration. The effect of solution resistance will be fully considered later in the thesis. Secondly, the controlled potential electrolyses have shown that the electrolyte cation reacts with the anionic species formed by monomer electrolysis, thus preventing polymerization. Low concentrations of electrolyte will reduce the rate of reaction of the postulated dianionic species $\text{C}_6\text{H}_5\text{CHCH}_2\text{CH}_2\text{CHC}_6\text{H}_5$ with the salt cation; this dianion can therefore react with further neutral monomer molecules in solution. Effectively, this will reduce the number of monomer molecules diffusing towards the electrode, in turn reducing the peak current. As the tendency to polymerize will increase with increasing monomer concentration, this effect will counterbalance the increase in peak current expected on adding monomer. The variation of peak currents with concentration may be explained qualitatively in this manner. As the tetrabutylammonium cation concentration was increased, polymerization became less likely, and larger concentrations of monomer were required to produce the effect ascribed to polymerization. A series of voltammograms for α -methylstyrene provided evidence to support this postulate. This monomer is known to polymerize much less readily than styrene. Curve D; Figure 14, showed that the peak height increased linearly with concentration of α -methylstyrene without

reaching a limit such as styrene reached at similar concentrations of electrolyte (Curve B). This reasoning presupposes that both monomers are of similar reactivities towards tetrabutylammonium cations.

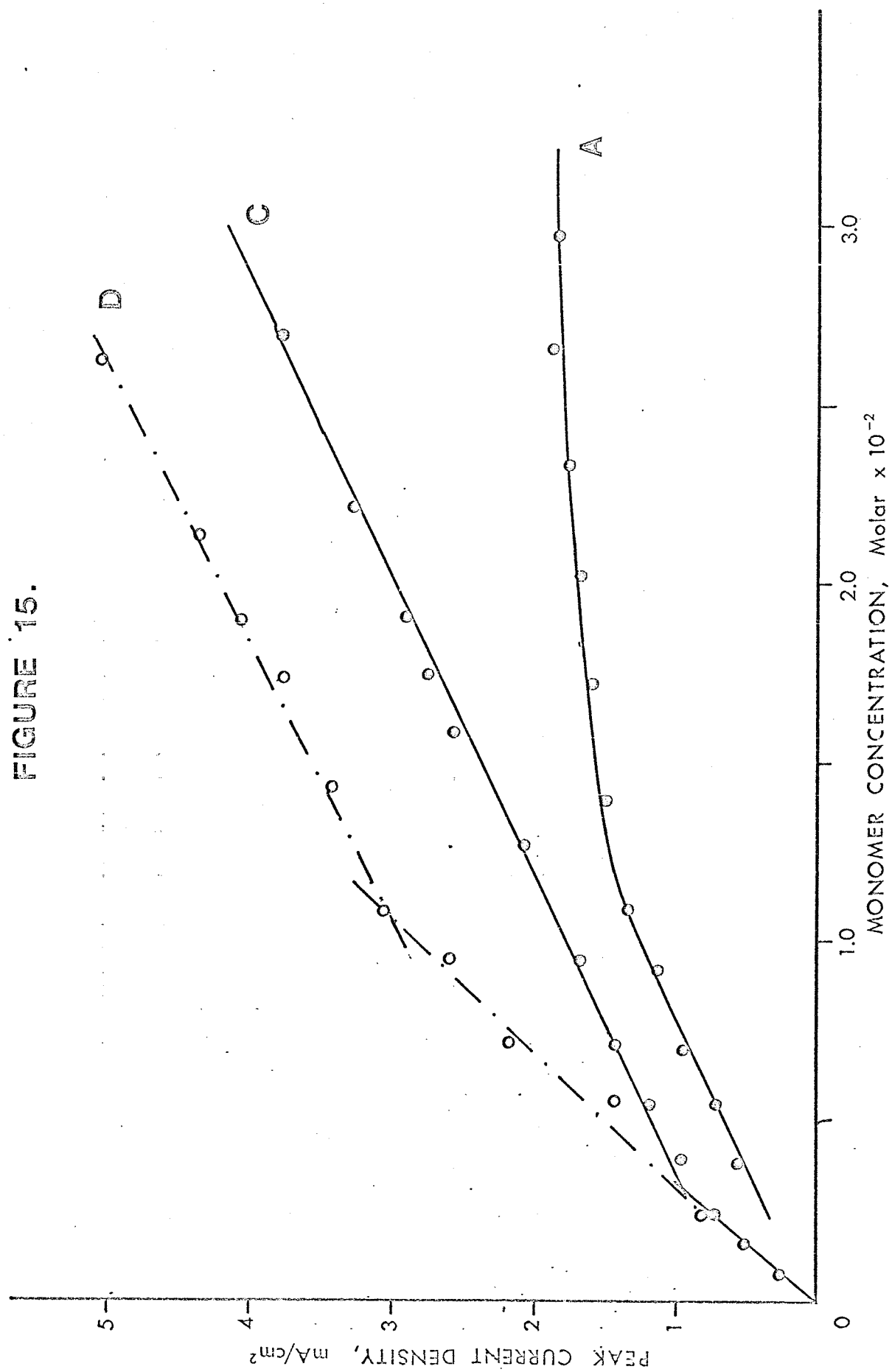
The curves of voltammetric peak height versus concentration also deviated from linearity at low concentrations. This was illustrated by replotting the low concentration data from Figure 14 on a larger scale in Figure 15. Both curves C and D increased in gradient at low concentrations. Equation (35) predicted that peak heights would vary as $(n)^{3/2}$, where n was the number of electrons transferred. The gradient of curve C increased from 125 to 300 $\mu\text{A cm}^{-2} \text{ mM}^{-1}$, while curve D for α -methylstyrene increased from 125 to 275 $\mu\text{A cm}^{-2} \text{ mM}^{-1}$. In each case, the ratios of the gradients were within experimental error of $(2)^{3/2}$, predicted for a change from a one electron to a two electron transfer. This suggested that at the lower concentrations of monomer, the electrolytically-formed radical anions did not dimerize but rather reacted with the electrolyte, abstracting a proton and undergoing a further one electron reduction according to the mechanism proposed by Hoijsink (90). Normally, aromatic hydrocarbons only undergo such a process in the presence of an active proton donor such as water, but it appears from this and other evidence to be presented later in the thesis that radical anion species derived from vinyl compounds are more active proton abstractors than cyclic aromatic hydrocarbons. Further evidence that the electrolyte acted as the proton donor was that at low electrolyte concentrations (Curve A) no change in slope occurred; the two electron process had diminished in importance.

FIGURE 15.

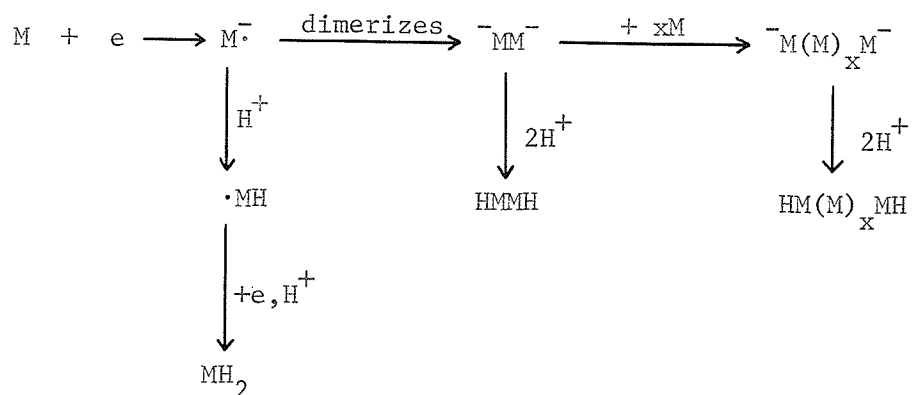
THE VARIATION OF VOLTAMMETRIC PEAK CURRENT WITH MONOMER CONCENTRATION;
LOW CONCENTRATION DATA FROM FIGURE 14 REPLOTTED ON A LARGER SCALE.

Data as for Figure 14.

FIGURE 15.



For this curve, the inflexion above 1.5×10^{-2} M styrene was ascribed to the onset of polymerization reactions. Thus, in summary, the reaction scheme may be written:-



Here, as the ratio of tetrabutylammonium salt to the monomer was decreased, the products for styrene reduction changed from the two electron product, ethyl benzene, to the dimer, and then to polymeric species.

If the model proposed for the effects of polymerization is correct, then under similar conditions monomers which polymerize readily would be expected to give smaller peak currents than less active compounds. It was found that the peak heights per unit concentration for the following compounds were in the order; acrylonitrile < methyl methacrylate < styrene < α -methylstyrene < 1,1-diphenylethylene. This order is the same as that for the compounds' reactivity in anionic polymerization. This suggested that the relative rates of propagation to termination might be determined from such data. However, the difficulty of obtaining reproducible voltammograms with monomers which polymerize readily permitted only qualitative interpretation.

The results demonstrated that the application of cyclic

voltammetry to anionic polymerizations provided a useful additional method of investigation. The interpretation of the voltammetric peak current data at varying monomer concentration was in complete accord with the results obtained using controlled-potential electrolyses.

A DETAILED STUDY OF SELECTED ELECTROLYTIC REACTIONS USING CYCLIC VOLTAMMETRY

The Redox Behaviour of Diphenylpicrylhydrazyl

The only voltammetric parameter used in the discussion above was the peak current. However, this was only one of several possible sources of information. The peak potential, the change of peak potential and peak current with scan rate, and the detailed shape of the forward and reverse voltammograms all provide information about the reactions taking place at the electrode. No detailed studies to test the applicability of the theory to organic reactions have been reported. Accordingly, some experiments on model organic compounds were planned. Tetrahydrofuran was chosen as solvent because of its widespread use in conventional living and electro-initiated polymerizations (44,45). It has seldom been used as a solvent for electrolytic studies (91,92) but the unfavourable solution resistance was outweighed by the relative ease of purification and transfer under high vacuum conditions. As a model electroactive compound for organic solvent systems, Solon and Bard (93) suggested the use of diphenylpicrylhydrazyl (DPPH) as they found that this free radical undergoes a one-electron reduction to form a stable anion and a one-electron oxidation

to form a stable cation in acetonitrile, methanol, ethanol, acetone and dimethylsulfoxide. DPPH is also a compound of interest in polymer chemistry and has been widely employed as an inhibitor and free radical trap. An elucidation of its redox behaviour appeared of intrinsic merit. A single compartment vacuum-tight cell (Figure 7) was used to ensure that no water or air were present; as only very low currents were to be passed, no attempt was made to separate the anode and cathode compartments. The effect of very small amounts of products formed at the anode which might interfere with the cathodic reactions was considered to be less important than the increase in cell resistance resulting from a sintered glass barrier between anolyte and catholyte. A simple silver wire sheathed in a glass capillary was tried as a reference electrode in view of the extremely low current drain between reference and working electrode. This simple arrangement eliminated the handling difficulties and the risk of introducing impurities associated with more conventional reference electrodes used with high-vacuum systems. A similar reference electrode had been employed in chronopotentiometric studies (94).

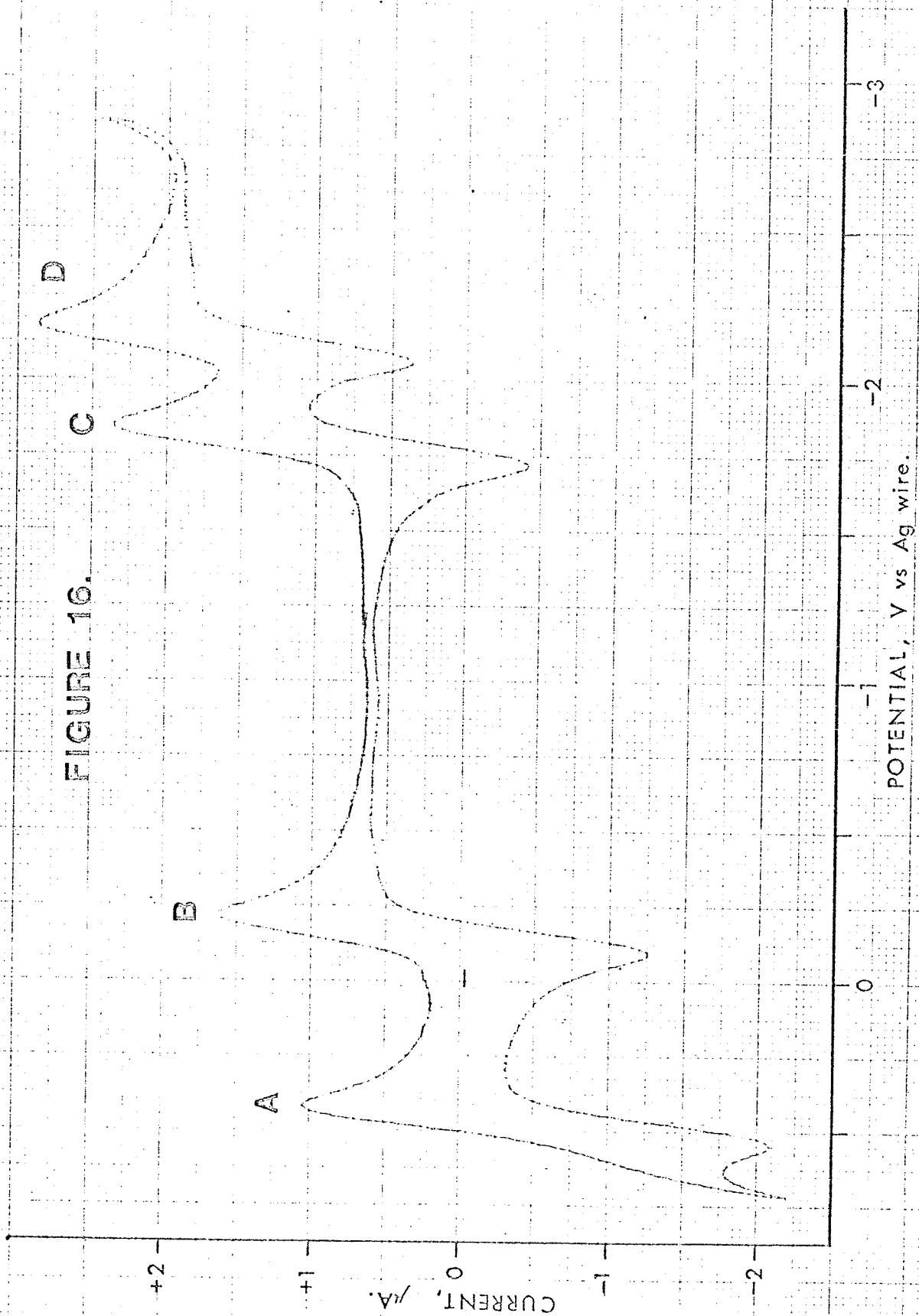
Figure 16 shows a single cyclic voltammetric curve covering the potential range available in the solvent. In addition to the expected formation of a stable cation (A) and anion(B) at the left (anodic) side of the voltammogram, two further single electron transfers (C), (D) occur at more cathodic potentials. It has been shown (95) that in aprotic solvents, aromatic nitro-compounds undergo reversible one-electron reductions to give stable radical ions. At more negative

FIGURE 16.

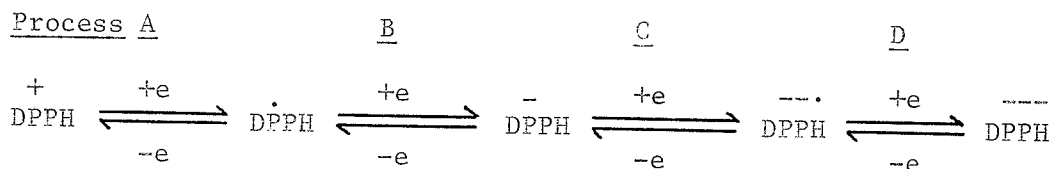
CYCLIC VOLTAMMOGRAM FOR DIPHENYLPICRYLHYDRAZYL (1.0 mM) IN 0.1 M
 $\text{N}(\text{Bu})_4\text{ClO}_4$ -THF.

Scan rate; 0.07 V/sec.

FIGURE 16.



potentials, dianions, unstable in a dimethyl formamide medium, are formed. The voltammetric evidence here suggests that DPPH undergoes a similar reduction of a nitro-substituent. The four electron transfer processes indicated in Figure 16 may be written thus:-



The species represented as ions will presumably exist as ion aggregates with tetra-alkyl-ammonium counter-ions in this solvent.

Each of the electron transfer steps may be examined individually by cyclic voltammetry. For example, Figure 17 indicates the effect obtained by varying the scan rate for process B. The theoretically predicted linear relationship between the peak current and the half power of the scan rate was found (65,71).

Figure 17 also indicates that the values for peak potentials move linearly with increasing peak currents. The cathodic peaks become more cathodic, and the anodic peaks become more anodic as the scan rate is increased. Consequently, the peak potentials were determined by extrapolating, for a range of scan rates, the line through the peak maxima to zero current. The values thus obtained for all four electron processes, together with the corresponding anodic and cathodic peak currents are presented in Table I. The difference between the anodic and cathodic peak potentials ΔE_p is close to 60mV as predicted for a reversible one electron process. From the similarity of all the peak currents, and the nature of the substrate,

FIGURE 17.

THE EFFECT OF SCAN RATE INCREASE ON THE VOLTAMMETRIC PEAK FOR
PROCESS B, $\text{DPPH}^\bullet + e = \text{DPPH}^-$.

DIPHENYLPICRYLHYDRAZYL, 1.0 mM, in 0.1 M $\text{N}(\text{Bu})_4\text{ClO}_4$ -THF.

Scan rates; 0.02, 0.04, 0.07, 0.10, 0.14, 0.20, 0.30, 0.40 V/sec.

FIGURE 17.

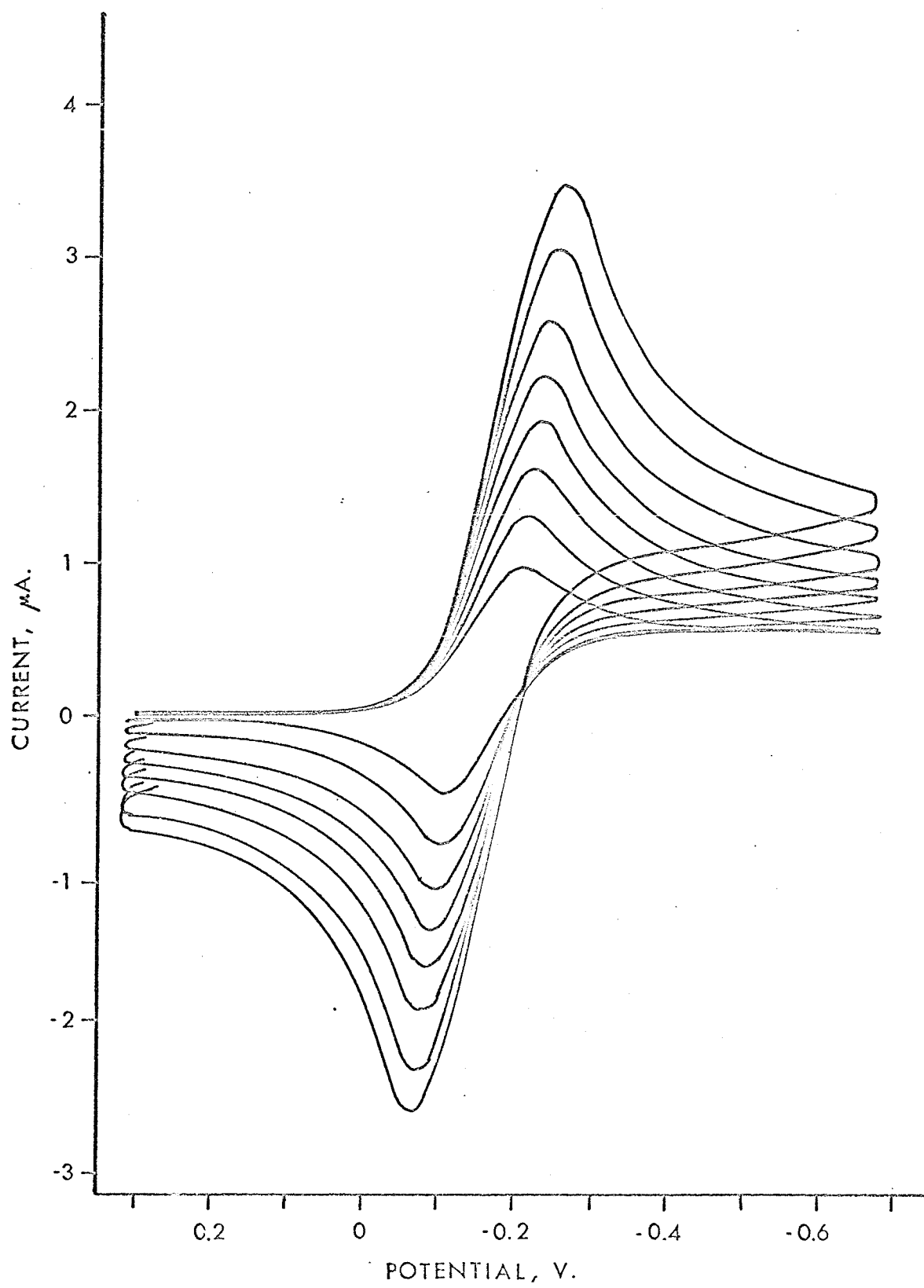


TABLE I

VOLTAMMETRIC DATA FOR DIPHENYLPICRYLHYDRAZYL

PROCESS (i)	<u>A</u>	<u>B</u>	<u>C</u>	<u>D</u>
Peak Potential (ii)				
<u>Volts</u>				
$E_{p,a}$ (anodic)	+0.500	-0.122	-1.714	-2.030
$E_{p,c}$ (cathodic)	+0.436	-0.183	-1.788	-2.110
$E_{p,a} - E_{p,c} = \Delta E_p$	0.064	0.066	0.074	0.080
<hr/>				
Peak Current (iii)				
$i_{p,a}$ (anodic)	1.8 μ A	1.9 μ A	1.6 μ A	1.8 μ A
$i_{p,c}$ (cathodic)	2.2 μ A*	1.9 μ A	1.8 μ A	1.6 μ A*
<hr/>				

(i) See page 69 . Data for 1.0 mM DPPH in 0.10 M THF-NBu₄ClO₄ solution.

(ii) The peak potentials, extrapolated to zero current, are measured versus a silver wire electrode, and hence only the relative values are significant.

(iii) Measured from estimated extension of voltammogram for the preceeding peak (72). Scan rate 0.10 volt/sec.

*Approximate values, due to interference from neighbouring peak.

it thus appears that each of the four electron transfer steps involves a single electron process. Furthermore, it should be noted that the cathodic and anodic peaks are of similar heights, so chemical reactions of any of the species subsequent to electron transfer are seen to be unimportant in the scan time.

There was a pronounced drift of peak potential with current. For reversible electron transfer reactions at a planar electrode, the peak potential should be independent of the peak current.

It has been shown (74) that a potential drift with changing scan rate may be due to:

1. subsequent chemical reaction.
2. uncompensated ohmic resistance between the working and reference electrodes.
3. irreversibility of the electron transfer process.

The first and third possibilities have been eliminated because of the similarity of the anodic and cathodic peaks. A high solution resistance however, would be expected to be important in tetrahydrofuran even at the relatively slow scan rates used here. The effects of uncompensated ohmic resistance on the shape of cyclic voltammograms has been discussed in the introductory chapter of this thesis.

Experimentally, it was found that variation of the scan rate resulted in displacement of all eight peaks along the potential axis, in an anodic direction for anodic peaks and in a cathodic direction for cathodic peaks. The peak potential displacements for every process were linear with peak current, and in all cases corresponded to a

shift of $22 \pm 2 \text{ mV}/\mu\text{A}$ peak height. This data can be obtained from Figure 17. The constancy of this shift is believed due solely to uncompensated ohmic resistance.

A confirmatory experiment was performed with the supporting electrolyte concentration reduced to .034 M from .101 M, but under otherwise identical conditions. In this solution of higher resistance, the peaks were again displaced along the potential axis with increasing peak current, but by $74 \pm 6 \text{ mV}/\mu\text{A}$, peak current. This increase in displacement at lower electrolyte concentration is of the magnitude expected for the uncompensated resistance.

A further criterion for the reversibility of the process B is available. Several voltammograms were obtained at different scan rates, and $\log i$ was plotted against E for the lower portion of the cathodic sweep, and $\log \frac{(i_p - i)^{1/2}}{i}$ vs. E for almost the complete cathodic sweep (96) where i = current for a corrected potential E , and i_p = peak current. In all cases, straight lines of gradient $1/66 \text{ mV}$ resulted. This is in good agreement and within experimental error of the value expected for a reversible reaction.

Thus, there is every indication that the potential drift is due to uncompensated resistance, and that for the low scan rates employed, all the electron transfer reactions are reversible. This is a very useful result; by comparing the voltammograms for DPPH with those for other systems under the same conditions, the effects due to the high solution resistance may be allowed for, and hence the effects due to differing electrode processes may be considered.

The stability and reproducibility of these voltammograms obtained under vacuum conditions in tetrahydrofuran were very satisfactory. The results with DPPH as a model compound encouraged the extension of the method to polymerizable systems. However, a more direct application of these results to electrolytic polymerizations should not be overlooked. Inhibitor studies with DPPH, anthraquinone and other free radical traps have been used to determine chain mechanisms; such results should be appraised critically for the following reason. If DPPH \cdot is added to a cathodically initiated polymerization, and no marked reduction in rate is noted, this does not, per se, eliminate the possibility of a free radical mechanism because the free radical DPPH \cdot will be reduced very readily to an anion which will not inhibit a free radical chain mechanism. Quinones are also easily reduced electrolytically, and thus are open to the same objection.

Although of little relevance to polymerization reactions, the discovery of the further reversible reduction steps of DPPH giving a dianion-radical and a trianion is of interest. As far as is known, no other organic system undergoes four reversible electron transfers; it appears that five separate stable oxidation states of DPPH may be produced electrolytically in tetrahydrofuran.

Cyclic Voltammetry of a Model Polymerizable Compound.

The electrolytic reduction of cyclic aromatic hydrocarbons and some of their derivatives in aprotic media to give stable ionic species

is well known (89). However, only a few examples of electrochemical studies on vinyl or ethylenic compounds under similar conditions have been reported (34,97). It was hoped that cyclic voltammetry under the conditions used above with DPPH would provide information on electron transfer to such molecules. Acenaphthylene was chosen as a model polymerizable compound because its properties are intermediate between those of a polycyclic aromatic compound and those of a vinyl compound. Furthermore, it has a relatively low reduction potential, and although it forms polymer by an anionic propagation mechanism, the activation energy is relatively high so that at room temperature polymerization will have little effect on the electrochemical reduction.

The experimental voltammogram for acenaphthylene, obtained when the cathodic potential scan was limited to -2.2 volts, is shown in Figure 18. The anodic and cathodic peak currents were equal for scan rates from 0.4 volts/sec. to 0.02 volts/sec. The separation of anodic and cathodic peak potentials, when extrapolated to zero current was found to be 62 ± 5 mV. The linear shift of peak potential with peak current was of the magnitude expected for uncompensated resistance between the working and counter electrode; this was ascertained by comparison with cyclic voltammograms for DPPH under identical conditions. From this evidence, it was clear that acenaphthylene undergoes an uncomplicated reversible one electron transfer to form a stable radical ion under the experimental conditions employed.

When the cathodic scan was extended to -3.0 V, the voltammogram

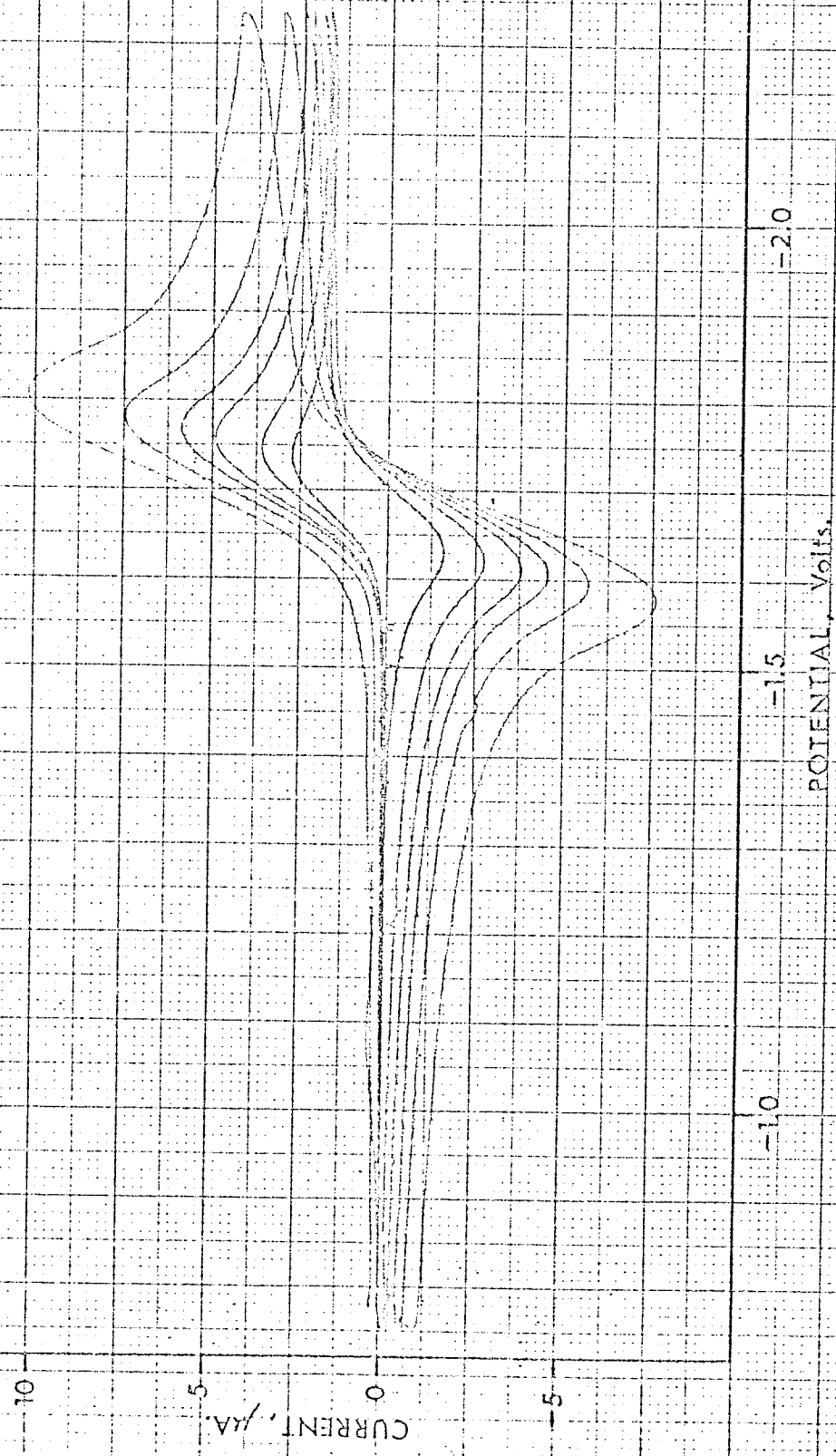
FIGURE 18.

CYCLIC VOLTAMMOGRAM FOR THE FIRST REDUCTION STEP OF ACENAPHTHYLENE.

Acenaphthylene, 1.7 mM, in 0.2 M $\text{N}(\text{Bu})_4\text{ClO}_4$ -THF solution.

Scan rates; 0.05, 0.10, 0.20, 0.30, 0.50, 1.0 V/sec.

FIGURE 18.



became more complex. A further single electron reduction occurred (Figure 19, peak B_c). This electron transfer was irreversible, as indicated by the complete absence of any anodic peak on reverse scan and by the larger shift in peak potential with scan rate. In addition, the anodic peak current for the first electron transfer process (A_a) became smaller than that expected for a reversible process, and a new anodic peak (C_a) appeared at the anodic end of the voltage scan. These two effects were very dependent on the scan rate. At scan rates less than 0.05 volts/sec, the anodic peak for process A was equal to the cathodic peak, and there was no peak for process C. As the scan rate was increased, peak C grew anodically at the expense of peak A_a . The quantitative effects on the four peaks of changing the scan rate are shown in Figure 20.

The second irreversible reduction peak (B_c) indicated that the radical-anion of acenaphthylene, produced in the first reduction step was further reduced to give a dianion which underwent subsequent reactions; these prevented the dianion being reoxidized on reverse scan. The interaction of the dianion with the solution produced a further electro-active species, as at scan rates higher than 0.06 volts/sec., the new oxidation peak (C_a) appeared on the reverse scan at potentials more anodic than -1.0 volts. It is unlikely that this peak resulted from the discharge of a radical anion; the redox potential for common aromatic hydrocarbons is much more cathodic than -1.0 volts. However, the peak was in the region expected for the reduction of hydrocarbon free radical species, where the reduction

FIGURE 19.

CYCLIC VOLTAMMOGRAM FOR ACENAPHTHYLENE REDUCTION SHOWING THE FOUR
ELECTRON TRANSFER STEPS INVOLVED.

Acenaphthylene, 1.7 mM, in 0.2M $N(Bu)_4ClO_4$ -THF solution.

Scan rates; 0.06, 0.12, 0.20, 0.29, 0.44, 0.58, 1.16 V/sec.

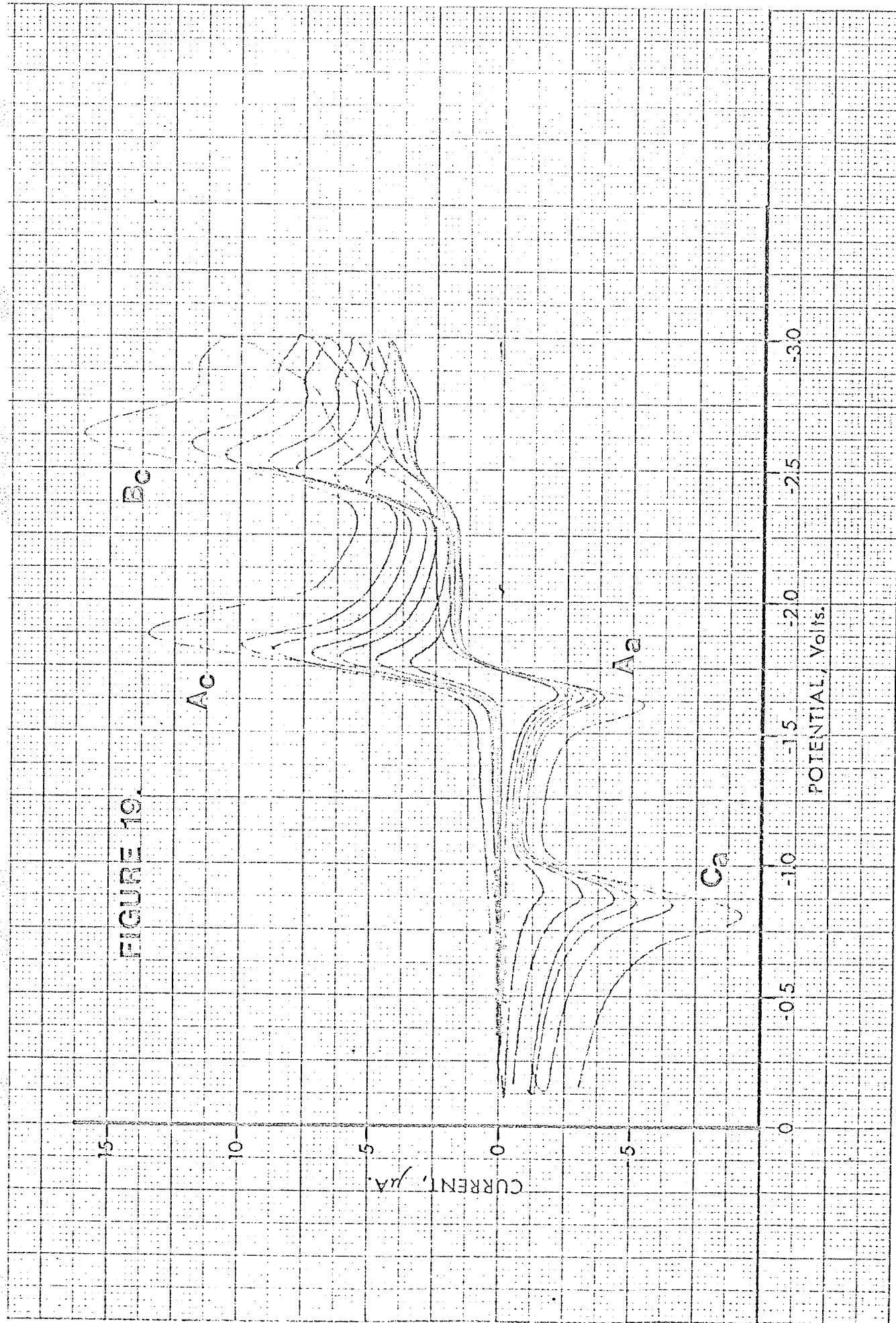
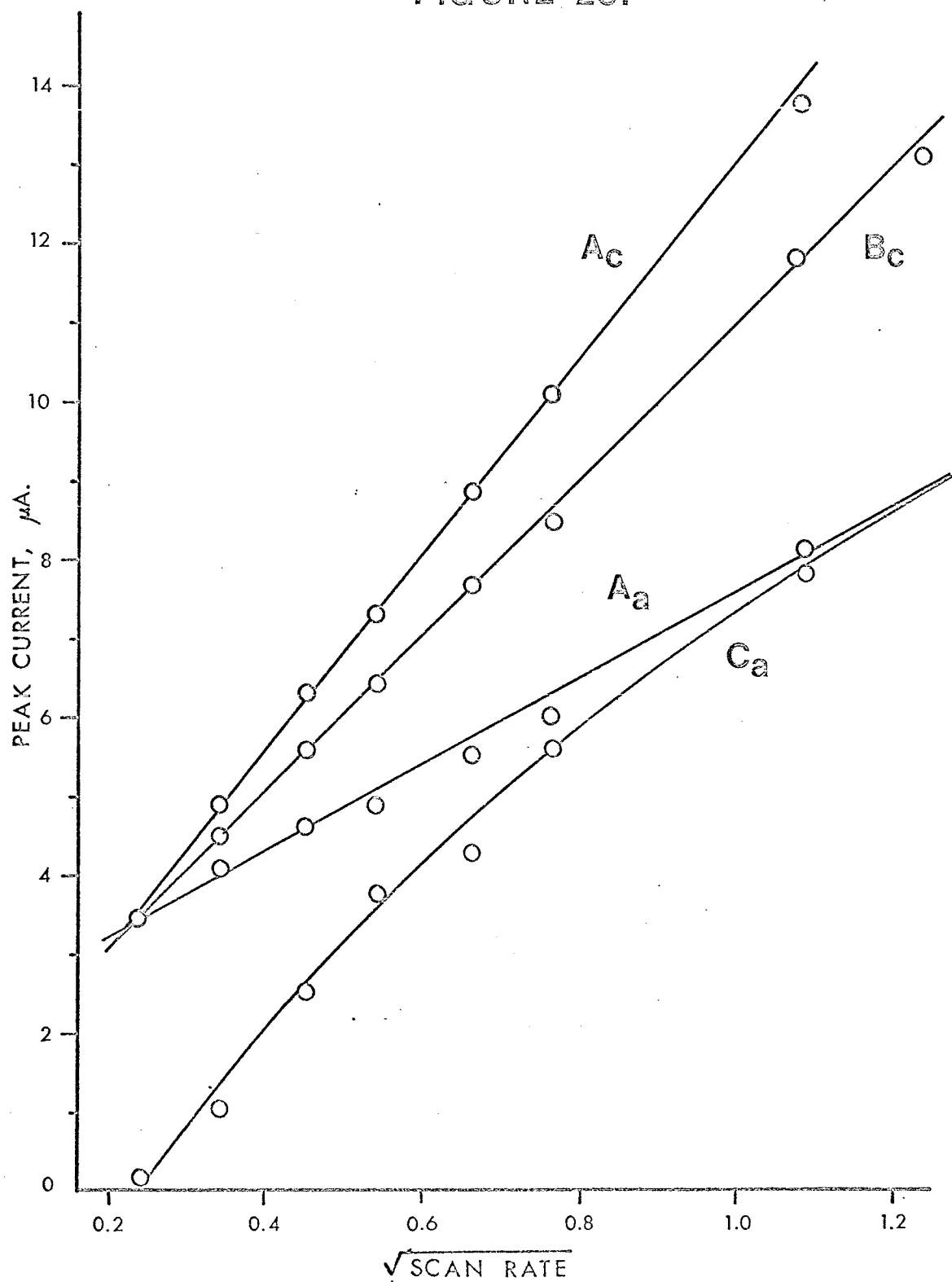


FIGURE 20.

THE VARIATION OF ACENAPHTHYLENE PEAK CURRENTS WITH THE SQUARE ROOT
OF THE SCAN RATE.

Data as for Figure 19.

FIGURE 20.



product is a carbanion. For a carbanion the electronic charge is localized predominantly on a single carbon atom whereas in a radical anion the charge is spread over the π electron system. The simple Huckel Molecular Orbital Theory assumes that no energy barrier need be overcome to place a second electron in a molecular orbital containing one unpaired electron; the triphenylmethyl radical, with the energy of its lowest unfilled orbital equal to zero gives the lowest reduction potential on a correlation of polarographic half-wave potentials with H.M.O. data (98). Thus, it is plausible that the oxidation peak C_a corresponds to electron loss from a carbanion to produce a free radical. During this investigation, the first report of the detection of carbanions produced from polycyclic aromatic compounds by similar electrolytic means was published by Dietz and Peover (99).

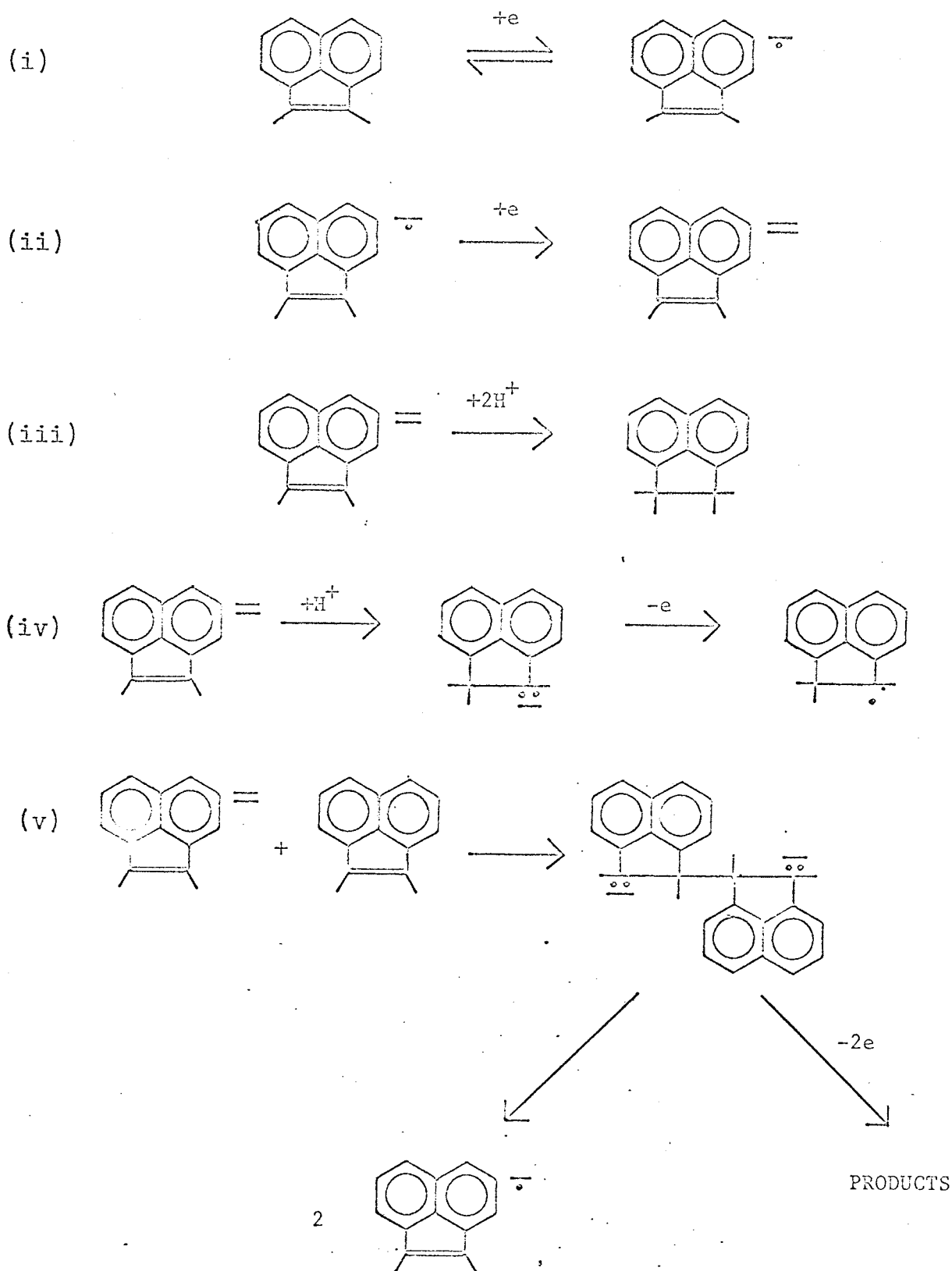
There are several possible reaction mechanisms resulting in carbanion formation from the initial di-anionic reduction product (Figure 21). However, the data shown in Figure 20 indicates that as peak C_a increases with increasing scan rate, peak A_a becomes smaller than A_c . This implies that the dianion reacted either directly with the radical anion, or alternatively with acenaphthylene itself, thus reducing the rate of radical anion formation and hence the anodic peak height A_c . On this basis, reaction sequence (iv) (Figure 21) seems improbable as it does not involve removal of acenaphthylene or its radical anion and thus should not affect the reversibility of process A.

FIGURE 21.

POSSIBLE MECHANISMS FOR THE ELECTROLYTIC REDUCTION OF ACENAPHTHYLENE
IN $\text{N}(\text{Bu})_4\text{ClO}_4$ -THF SOLUTION.

Protonation of the dianion is indicated as giving acenaphthene,
the usual reduction product. However, an alternative reaction path is
predicted by molecular orbital theory (100).

FIGURE 21.



The interpretation of conventional voltammograms involving chemical reactions is difficult, as the amount of electrochemical product formed on the cathodic scan depends on the scan rate. However, it appeared that by using a fixed slow forward scan rate to produce a definite concentration of the reduced species, and then employing several faster reverse scan rates, a clearer indication of the processes might be obtained. Accordingly, a further series of voltammograms was performed (Figure 22) using asymmetric voltage scans (75). The results showed that despite the increasing reverse scan rates, peak A_a for radical anion reoxidation increased only slightly, whereas the oxidation peak C_a increased linearly with the square root of the scan rate about twice as fast as expected for a one-electron transfer process (Figure 23). The rather broad shape of the peak, and the distinct shoulder evident at lower scan rates are compatible with two consecutive single electron oxidations at closely spaced potentials. There exists a possibility that peak C_a might involve electro-active species produced by attack of the initial dianion on solvent or salt. The most likely reaction is proton abstraction from the tetrabutylammonium cation to give a carbanion (Figure 21, iv), tri-n-butylamine and butene. Only the carbanion would be electro-active in the potential range under consideration giving a single electron oxidation. The two electron oxidation found experimentally is incompatible with this reaction sequence.

The reaction mechanism must also explain the fact that at scan rates below 0.06 volts/sec., the voltammogram is precisely that expected for a single reversible electron transfer followed by a further single

FIGURE 22.

CYCLIC VOLTAMMOGRAMS WITH ASYMMETRIC POTENTIAL SCAN FOR 1.7 mM
ACENAPHTHYLENE IN 0.2M $\text{N}(\text{Bu})_4\text{ClO}_4$ -THF SOLUTION.

Forward scan rate; 0.06 V/sec. Reverse scan rates: (1) 0.06 V/sec.
(2) 0.29 V/sec.
(3) 0.58 V/sec.
(4) 1.16 V/sec.

FIGURE 22.

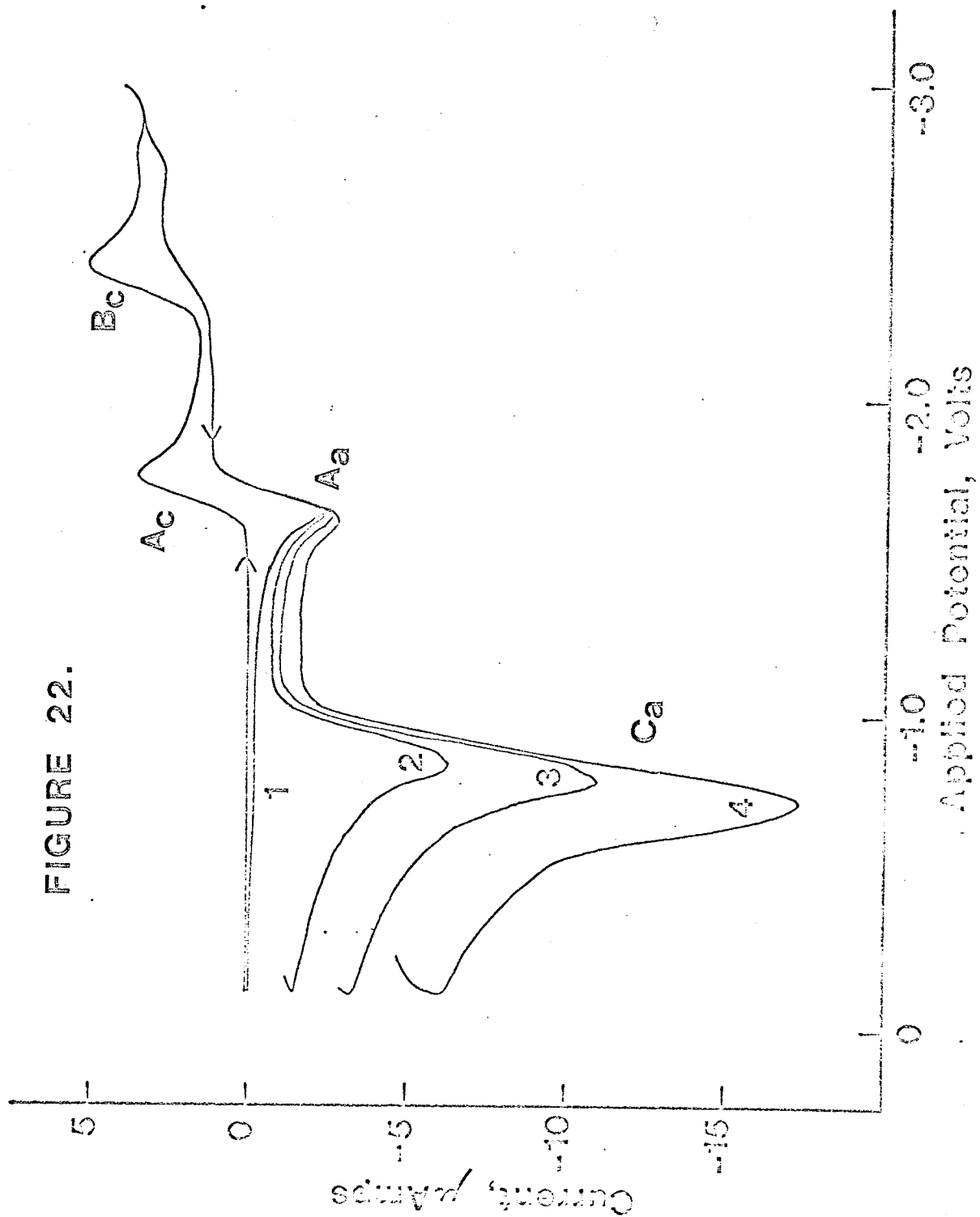
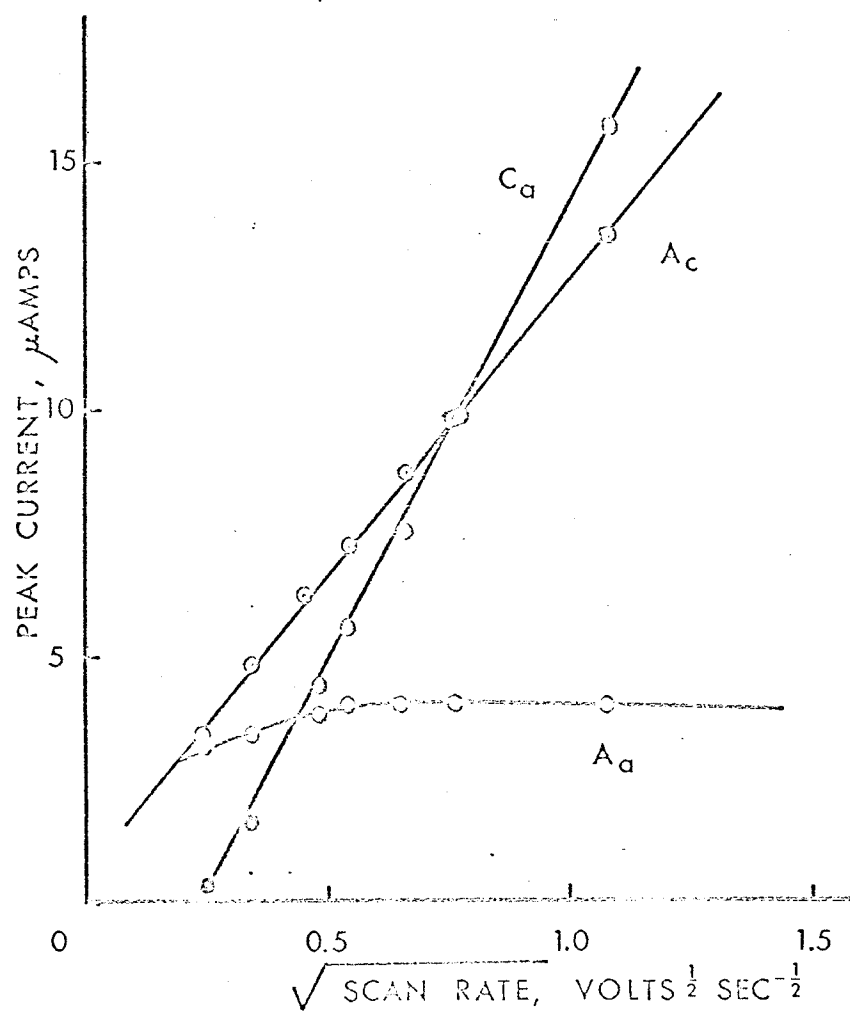


FIGURE 23.

THE VARIATION OF PEAK CURRENT WITH THE SQUARE ROOT OF THE REVERSE
SCAN RATE.

In each case, a constant forward scan rate of 0.06 V/sec was
employed. Other data as for Figure 22.

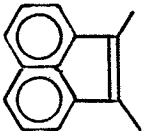
FIGURE 23.



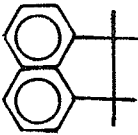
irreversible transfer, (Figure 19). It has been assumed in the past that those aromatic dianions that could be formed electrolytically reacted irreversibly with two protons to form a dihydro-derivative (Figure 21, iii). While this would explain the shape of the voltammograms at low scan rates, it appears that dianion protonation must be discounted for two reasons. Firstly, if protonation occurs rather than attack on an acenaphthylene molecule at low scan rates, then the same product should form at high scan rates. (The bulk concentrations of both acenaphthylene and the proton donor remain constant.) Such a process would remove all electro-oxidizable species at all scan rates, and thus fails to account for peak C_a . Secondly, the expected reduction product from acenaphthylene formed by diprotonation is acenaphthene, which is itself an electro-active compound. The cyclic voltammetry of acenaphthene was performed under conditions similar to those used for acenaphthylene and the results are included in Table II. Acenaphthene was found to undergo one electron reduction at a potential more negative than both peaks for acenaphthylene, so if it was formed in the reduction of acenaphthylene a further voltammetric peak at the appropriate potential should be evident. Figure 19 indicates only a trace of such a peak, thus suggesting that diprotonation of the dianion to give acenaphthene (Figure 21, (iii)) does not occur. The possibility of monoprotonation followed by oxidation (Figure 21, (iv)) has been discounted because the rate of change of peak height C_a with scan rate is greater than expected for a one electron process.

TABLE II.
CYCLIC VOLTAMETRIC DATA FOR ACENAPHTHYLENE AND RELATED COMPOUNDS.

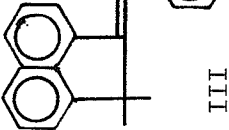
	Peak Potential, Volts(i).					
	A _c	A _a	B _c	C _a	D _a	E _a
Acenaphthylene, I.	-1.74	-1.67	-2.60	-1.10	-	-
Acenaphthene, II.	-2.91	-2.75	-	-	-	-
1,1-Biacenaphthylidene, III.	-2.10	-2.04	-2.42	-1.44	-1.17	-1.08
1,1-Diacenaphthenylidene, IV.	-2.20	-2.14	-2.47	-1.48	-1.21	-1.10



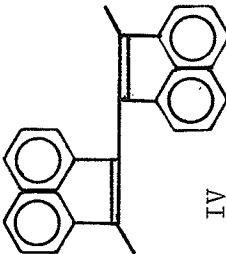
I



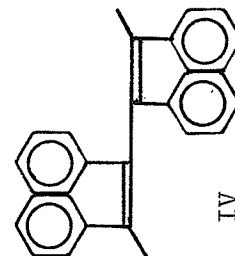
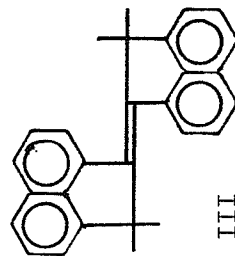
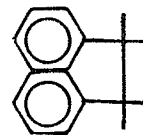
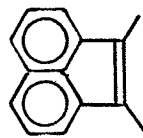
II



III



IV



(i) Peak potentials at zero current vs. Ag wire in 0.1 M N(Bu)₄ClO₄-THF solution.
The peaks are labelled as in Figures 19 and 24.

On this basis, a mechanism (Figure 21, (v)) may be proposed to explain the effect of scan rate change on the voltammograms from acenaphthylene. The di-anion formed by two consecutive one electron transfers to acenaphthylene attacks a further acenaphthylene molecule to give a dimeric dicarbanion. At high scan rates, the dimer is reduced (peak C_a) to give a diradical as initial product, while the depletion of the acenaphthylene causes a reduction in the rate of formation of the radical anion, and hence in the size of the anodic peak A_a . At lower scan rates the dimeric dianion decomposes to give two radical anions, and peak C_a disappears. This suggestion may be justified as the monomer \rightleftharpoons dimer equilibrium for acenaphthylene radical anions would be expected to be to the left; the cyclic voltammograms (Figure 18) indicate that dimerization did not occur under the conditions employed. The regeneration of the radical ions is reflected in the oxidation peak A_a which attains its full reversible height at low scan rates.

While this interpretation of the change in shape of the voltammograms is qualitative, it appears to be compatible with the relative reactivities of the species involved.

Since a dimeric species is postulated as an intermediate in the reaction sequence, the cyclic voltammetry of dimers of acenaphthylene was investigated. Results for 1,1-biacenaphthylidene and 1,1-di-acenaphthenylidene are summarized in Table II. The shapes of the voltammograms were very similar to those for acenaphthylene. The formation of stable radical anions for these compounds occurred at

more negative potentials than that for acenaphthylene (Figure 24). However, the peaks for dianion formation were closer to the first peaks in the dimeric compounds than was the case for acenaphthylene. This is probably due to the greater degree of charge separation possible in the extended π -electron systems of the dimers. On the reverse scan three ill-defined peaks were obtained at all scan rates employed. The asymmetric scan technique indicated that for 1,1-diacenaphthenylidene peak C_A (Figure 24) resulted from a one electron oxidation, and that the closely spaced peaks D_A and E_A together resulted from the second electron oxidation. Thus, protonation of the dianions in these cases again does not occur. One of the oxidation peaks E_A is at the same potential (within experimental error) as that found for peak C_A in the acenaphthylene voltammograms; this is an indication that the same species is involved. However, the information available from the cyclic voltammograms above allows only speculation as to the nature of the reduction products from the dimeric species.

Confirmation of the reaction mechanism for acenaphthylene reduction is not possible using the standard controlled potential techniques because of the transient nature of the intermediates. However, the radical ion nature of the species formed in the first reduction step was confirmed by esr techniques. The species were generated by controlled potential electrolysis in $\text{THF-NBu}_4\text{ClO}_4$ solution at a platinum electrode in the cavity of an esr spectrometer. Hyperfine coupling constants in agreement to the literature values for the unassociated acenaphthylene radical ion were obtained (101).

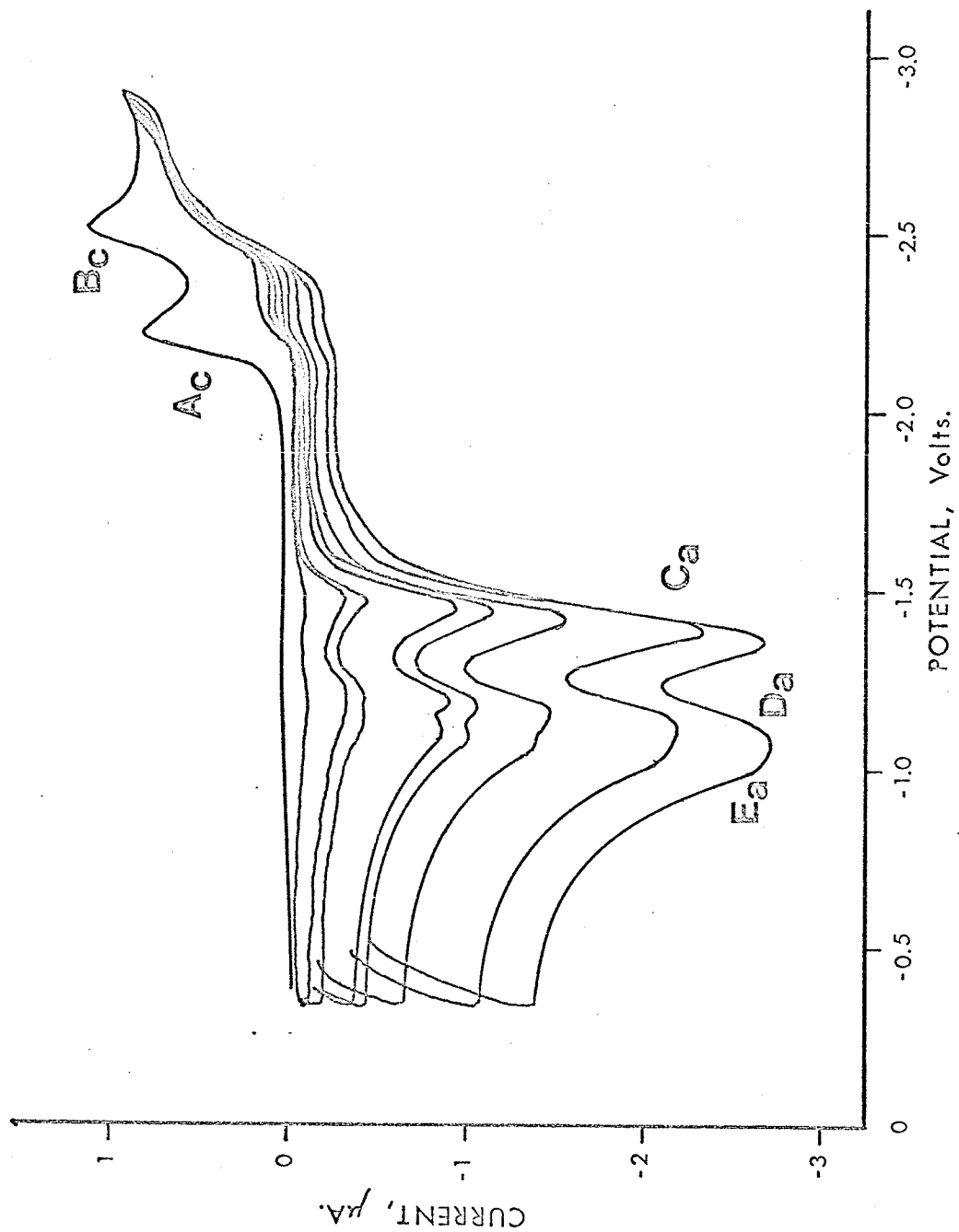
FIGURE 24.

ASYMMETRIC SCAN VOLTAMMOGRAM FOR 0.5 mM 1,1-DIACENAPHTHENYLIDIENE IN
0.1M $\text{N}(\text{Bu})_4\text{ClO}_4$ -THF SOLUTION.

Forward scan rate; 0.05 V/sec.

Reverse scan rates; 0.05, 0.10, 0.15, 0.25, 0.35, 0.50, 0.75, 1.0 V/sec.

FIGURE 24.



The possibility of detecting the radical species postulated as resulting from acenaphthylene oxidation peak C_a using a potentiodynamic method was investigated. By applying a square-wave potential pulse of $-0.5V \rightarrow -3.0V$ at a frequency of 2 cycles per second, it was hoped that dianion formation and reaction would be followed by oxidation of the carbanion to a free radical species. As the amplitude of the potential pulse was increased to the values listed, the esr spectrum characteristic of the radical ion diminished in strength by about two orders of magnitude and superimposed on it appeared a further spectrum, the most prominent feature of which was a doublet of splitting 8 gauss. This was attributed tentatively to a radical of structure $Ar\dot{C}HR$, where extensive delocalization of spin density into the aromatic system has occurred.

It is clear from this cyclic voltammetric investigation of electron transfer to acenaphthylene that the technique provides a most useful method for investigating the interactions of the relatively unstable radical, radical ion and ionic intermediates produced in aromatic hydrocarbon reductions. Information on these processes is not only applicable to anionic polymerization studies and to carbanion chemistry generally, but is also of intrinsic interest in Molecular Orbital Theory. Dietz and Peover (99) studied this aspect in the first report of the electro-oxidation of polycyclic aromatic carbanions. However, these authors proposed that the dianions formed by two-electron reduction are monoprotonated, giving a monomeric carbanion. This corresponds to the reaction scheme (iv) (Figure 21) rather than

scheme (v) independently proposed to explain the experimental results reported in this thesis. The difference is reasonable in view of the different conditions employed. Dietz and Peover used DMF as solvent; proton abstraction is more likely from DMF than from THF. Furthermore, the anhydrous conditions attainable with THF that are essential for living anionic polymerization have not been achieved in DMF. The greater stability of the reduction products in THF enables slower scan rates to be employed. Thus, current-potential curves can be recorded more accurately with pen-and-ink recorder rather than with oscilloscope and camera.

Some conclusions of more direct application to polymerization studies may be drawn from the results for acenaphthylene. The reversibility of the first electron transfer to the uncharged molecule suggests that polymerization initiated by the stable radical anion is unlikely. However, the dimeric dicarbanion formed after the second electron transfer does not protonate rapidly. By analogy with conventional anionic polymerization mechanisms, anionic polymerization is then possible if the electrode potential is sufficiently cathodic to allow the formation of the dianion, and conditions in the bulk of the solution are compatible with chain propagation.

APPLICATION OF CYCLIC VOLTAMMETRY TO THE REDUCTION OF PHENYL-SUBSTITUTED ETHYLENES

The voltammetric results for acenaphthylene and related compounds indicated that extension of the method to more usual monomers

was desirable. The reduction of styrene was of particular interest because of the results reported earlier in this thesis. In view of recent unreported work from these laboratories on the behavior of the stilbenes and 1,1-diphenylethylene as co-monomers with styrene in electrolytically initiated systems, these other phenyl-substituted ethylenes were also examined. Previous investigations (91,102) of the electrochemical reduction of the phenyl-substituted ethylenes in DMF and acetonitrile by conventional polarography and electrolysis (not at controlled potential), have elucidated the general features of the reductions; however, the polarographic criteria for reversibility gave ambiguous results which were not readily interpreted in terms of the proposed mechanisms. A comparison with results in THF at a platinum electrode was thus also interesting from an electrochemical viewpoint.

Each of the phenyl substituted ethylenes will be considered in turn. The general factors influencing the reduction behavior will then be examined briefly.

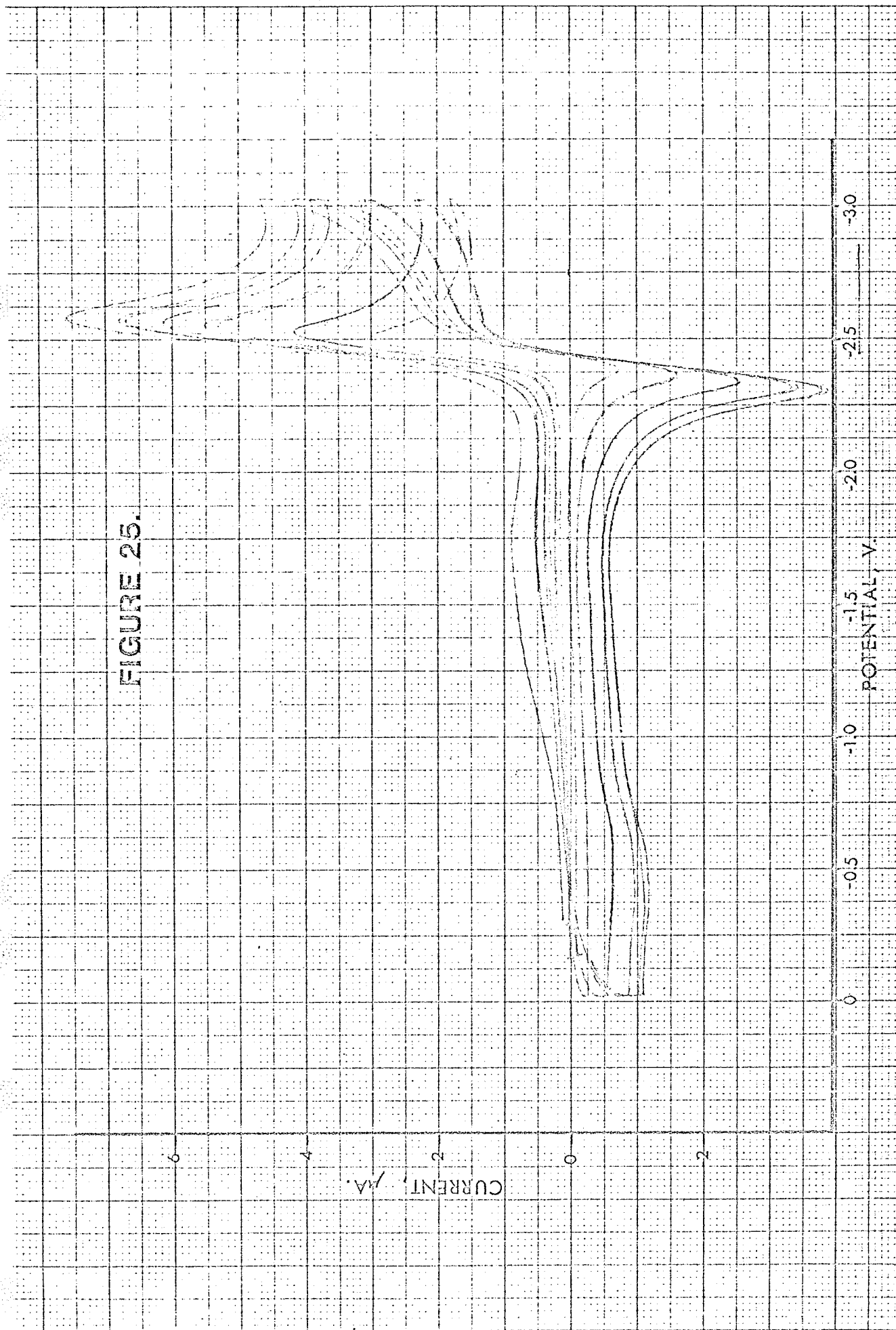
TETRAPHENYLETHYLENE. Cyclic voltammograms for tetraphenylethylene at a variety of scan rates were obtained (Figure 25). The most striking feature was the large anodic peak, indicating that the reduction product was relatively stable in solution. This was consistent with the linear shift of peak potential with increasing current; the value was that expected for uncompensated ohmic resistance alone. The cathodic peak height was about twice that obtained under identical conditions for known one electron transfer processes and the peak shape was sharper. The separation of cathodic and anodic peak potentials extrapolated to

FIGURE 25.

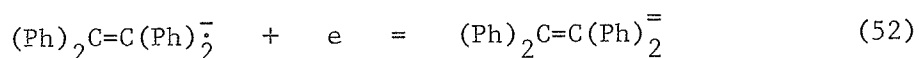
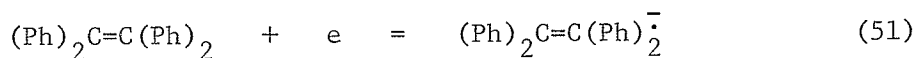
CYCLIC VOLTAMMOGRAM FOR THE REDUCTION OF TETRAPHENYLETHYLENE, 0.9 mM,
IN 0.1M $\text{N}(\text{Bu})_4\text{ClO}_4$ -THF SOLUTION.

Scan rates; 0.06, 0.15, 0.30, 0.48, 0.60 V/sec.

FIGURE 25.



zero current was found to be 60 ± 4 mV. Now from equation 35, the peak height for a reversible two electron transfer should be $(2)^{3/2}$ times that for a single electron transfer, and from equation 36, the peak separation should be 30 mV. These discrepancies may be resolved by considering a recent theoretical treatment of multistep charge transfers by Polcyn and Shain (72). The experimental results obtained for tetraphenylethylene coincided with those predicted for a substance undergoing two successive reversible electron transfer steps at potentials separated by less than 0.1 volts. Thus, the reduction process may be written:-



Neither the radical-anion nor the dianion appears to be protonated to any appreciable extent in the time interval involved. Thus this reaction differs from most two electron reductions of aromatic hydrocarbons. The appearance of the reverse peak on the cyclic voltammogram enables this unusual mechanism to be assigned with a high degree of confidence; polarographic results are much more ambiguous (97).

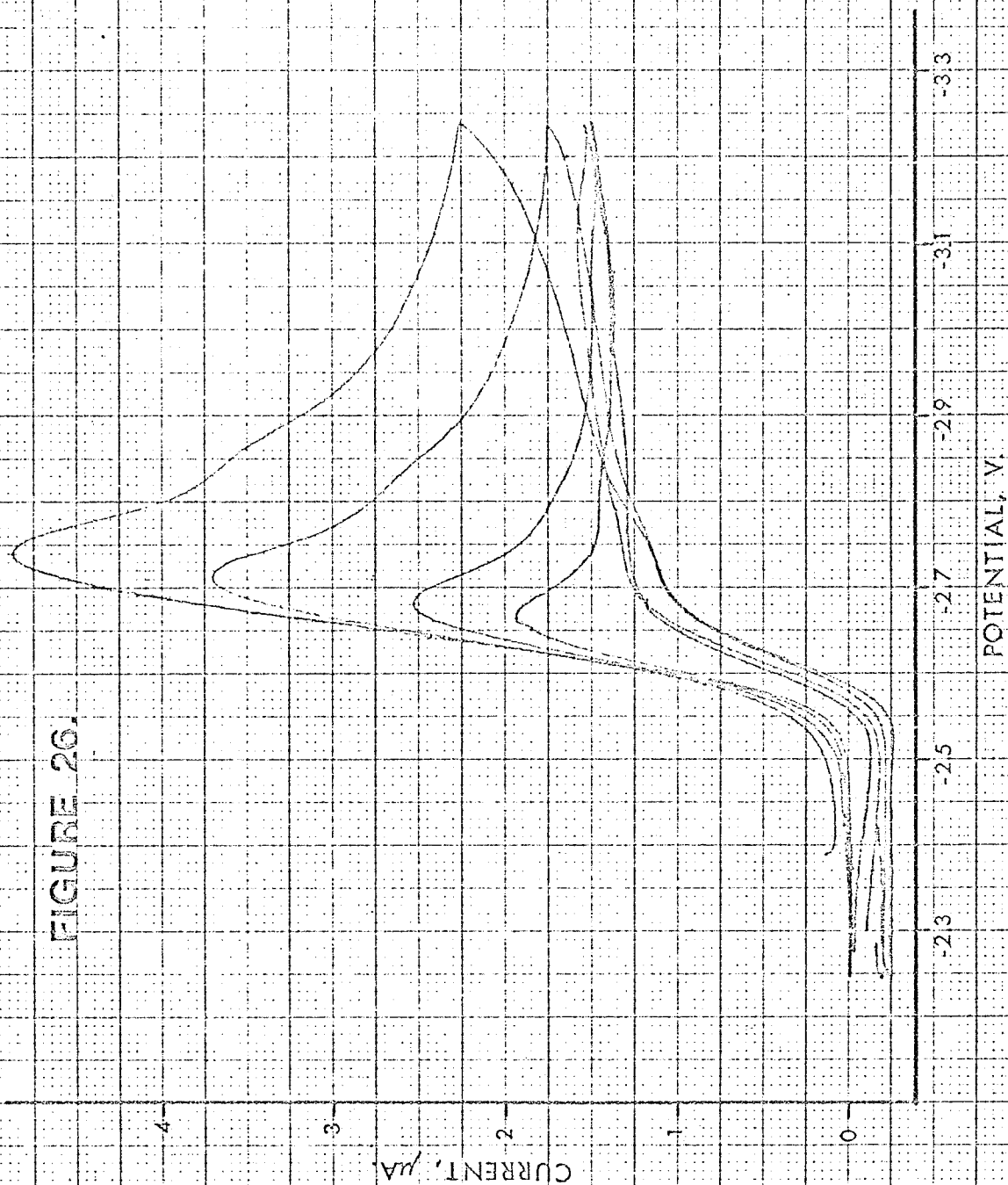
TRIPHENYLETHYLENE. The voltammetric peak height for triphenylethylene was also found to be about twice that expected for a one electron transfer. However, no anodic peak was evident on reverse scan, and the peak was narrower and sharper than that expected for a reversible transfer (Figure 26). The rate of potential shift with increasing current was greater than could be attributed to uncompensated resistance, indicating either an irreversible electrode process or some subsequent

FIGURE 26.

CYCLIC VOLTAMMOGRAM FOR THE REDUCTION OF TRIPHENYLETHYLENE, 0.87 mM,
IN 1.0M $\text{N}(\text{Bu})_4\text{ClO}_4$ -THF SOLUTION.

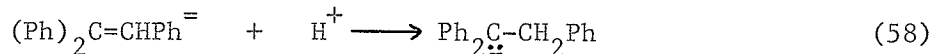
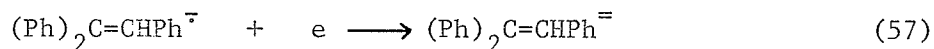
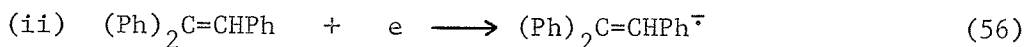
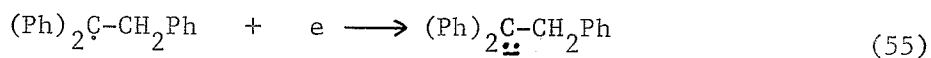
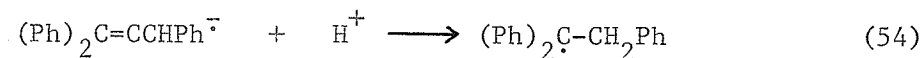
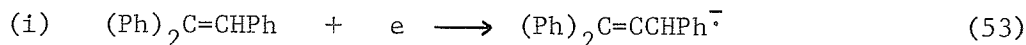
Scan rates; 0.02, 0.04, 0.10, 0.20 V/sec.

FIGURE 26.



chemical reaction of the initial electrochemical product.

There are two plausible mechanisms that are compatible with these results:-

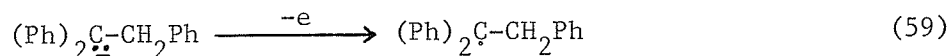


The first mechanism was proposed by Hoiijtink et al. (90) to explain the reduction of aromatic hydrocarbons in the presence of proton donors. They showed from molecular orbital theory that the radical formed by protonation of the radical-anion (equation 54) was reduced (equation 55) at lower potentials than that for initial electron transfer (equation 53). However, this mechanism would require fast protonation of the triphenylethylene radical-anion where the only proton source in solution was the tetrabutylammonium salt. It seems unlikely in view of the stability of the stilbene radical-anion under identical conditions (see below) that such reaction occurred.

The second reaction mechanism is more likely. A second electron is transferred to the radical anion (equation 57) at a potential close to that for the first transfer. The dianion formed is sufficiently basic to abstract a proton from the salt cation and produce a carbanion

(equation 58). The narrowness of the peak, measured by the difference between the peak and the half-peak potential (Table III) also supports the mechanism involving two electron reduction prior to protonation.

In view of the detection of the dicarbanion of acenaphthylene by asymmetric scan techniques, an attempt was made to detect the carbanion which both mechanisms predict as product (equations 55 and 58). The anodic peaks formed on varying the reverse potential scan rate were rather misshapen and indicated an irreversible reaction. By comparing the change of peak height the square root of scan rate for both the forward and reverse reactions (Figure 27) the rate of peak increase for the reverse reaction was found to be about half that for the forward reaction. This indicates that the peak may be assigned to the oxidation of the carbanion produced by reduction and protonation.



Thus, two electrons were required for the reduction (equations 56, 57 and 58) and only one for the oxidation (equation 59), in agreement with the asymmetric scan data. The irreversibility of the oxidation reaction may be explained by the high reactivity of the free-radical species formed; unlike anion radicals, this species is uncharged and therefore, electrostatic repulsion does not hinder dimerization or disproportionation.

The carbanion oxidation mechanism (equation 59) may be assigned to the anionic peak for triphenylethylene using the molecular orbital considerations that were applied previously. Experimental evidence for the electrolytic oxidation of an ethylenic carbanion has not been

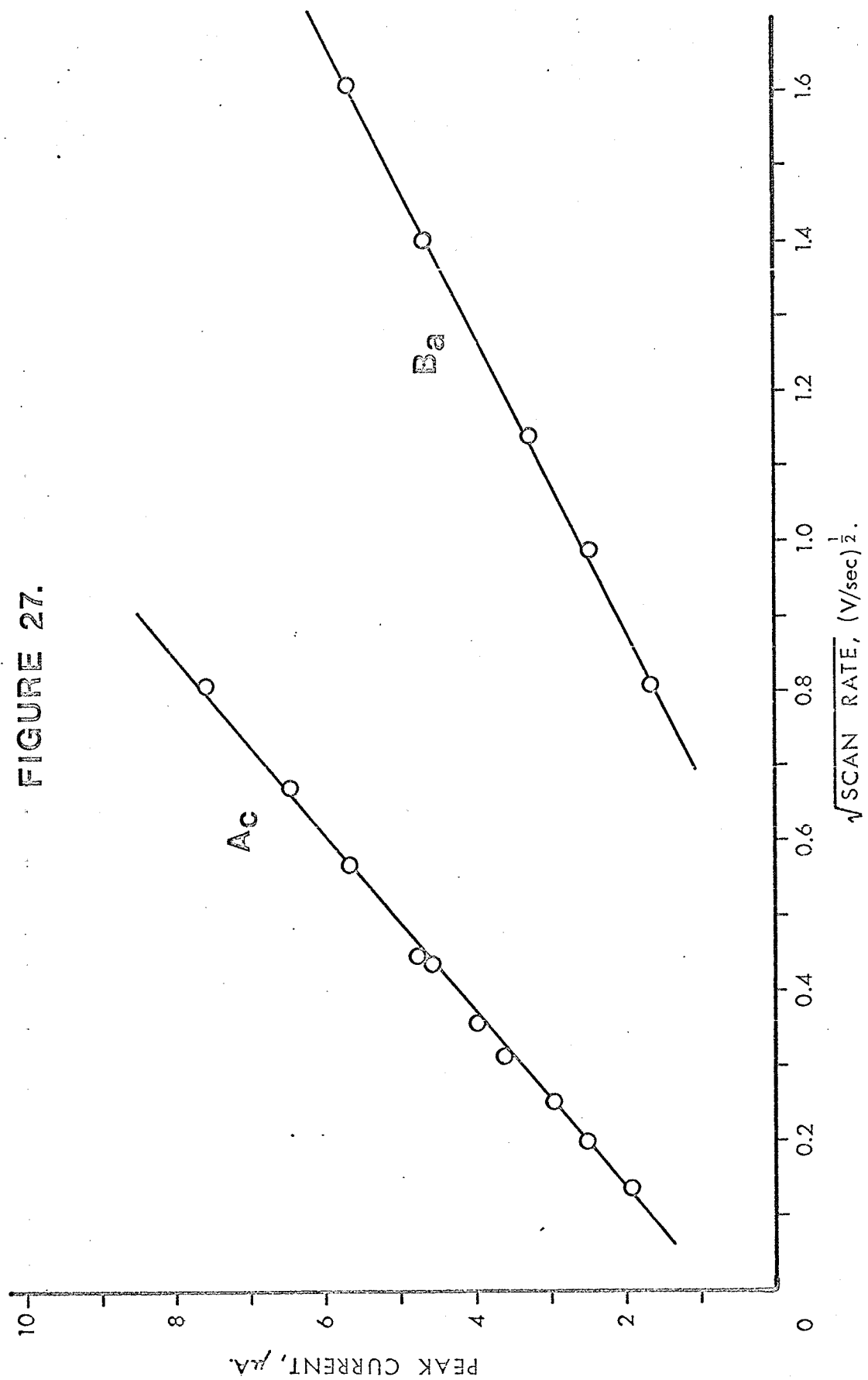
FIGURE 27.

THE RATE OF CHANGE OF CATHODIC AND ANODIC PEAK HEIGHTS WITH THE SQUARE ROOT OF THE SCAN RATE FOR TRIPHENYLETHYLENE.

The points on line A_c represent peak currents for the reduction of triphenylethylene, 0.87 mM, in 1.0M N(Bu)₄ClO₄-THF solution.

The points on line B_a represent peak currents for the reoxidation of carbanion products from triphenylethylene reduction. Asymmetric potential scans with a forward scan rate of 0.12 V/sec were employed.

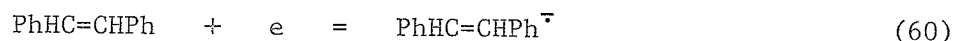
FIGURE 27.



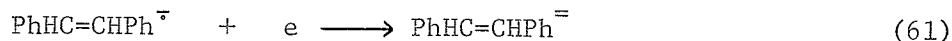
reported previously.

TRANS-STILBENE. Trans-stilbene exhibited typical behavior for polycyclic aromatic compounds. The reduction mechanism has been well-established by conventional polarography in DMF (97,102).

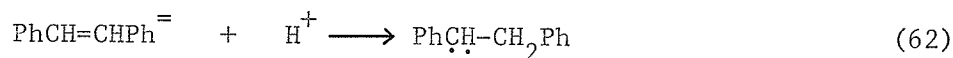
The cyclic voltammogram (Figure 28) showed that the reduction occurred in two stages. If the potential scan was limited to -2.8 V, so that only the first reduction step occurred, then it was found that the cathodic and anodic peaks were of equal height, and all other parameters also clearly indicated a single reversible one electron reduction. The radical ion of trans-stilbene was thus stable under the conditions used:



The subsequent reduction step at more cathodic potentials also involved the transfer of a single electron:



The absence of a corresponding anodic peak on reversing the scan indicated that the dianion had undergone further reaction. In this case, protonation by the salt cation was probable.



Again, the product was a carbanion. However, although an oxidation peak was formed at the expected potential, its rate of growth with scan rate was less than that expected for a one electron transfer. This may indicate that the carbanion was capable of further proton abstraction (equation 63) thus reducing the amount available for

FIGURE 28.

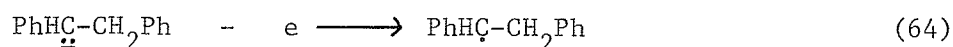
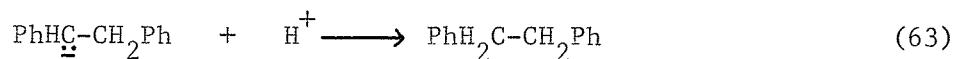
CYCLIC VOLTAMMOGRAM FOR TRANS-STILBENE, 1.16 mM, IN 1.0M
 $\text{N}(\text{Bu})_4\text{ClO}_4$ -THF SOLUTION.

Scan rates; 0.07, 0.14, 0.21, 0.35, 0.49, 0.70 V/sec.

FIGURE 28.

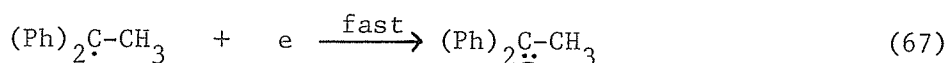
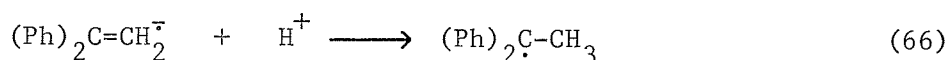
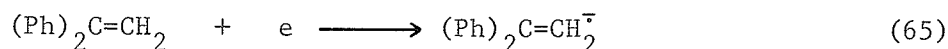


electro-oxidation (equation 64).

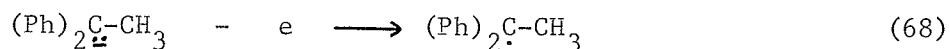


A small unexplained peak at -1.6 V interfered with the accurate interpretation of the asymmetric scan data.

1,1-DIPHENYLETHYLENE. A similar interference occurred when asymmetric potential scans were performed on 1,1-diphenylethylene (Figure 29). For this substance, a two-electron irreversible reduction was found. However, the peak was much broader than that for triphenylethylene, suggesting that a different mechanism was involved. If a radical-ion was formed initially, the absence of a phenyl substituent on one of the olefinic carbon atoms would be expected to decrease the steric hindrance towards proton abstraction from the salt cation. In this case, Hoijsink's mechanism (90) would be expected.



The carbanion formed was oxidized at -0.5 V on reverse scan. The asymmetric scan technique indicated that the anodic peak increased at half the rate of the cathodic peak, indicating a one-electron oxidation (equation 68).



Unlike the corresponding stilbene carbanion, there was thus no evidence

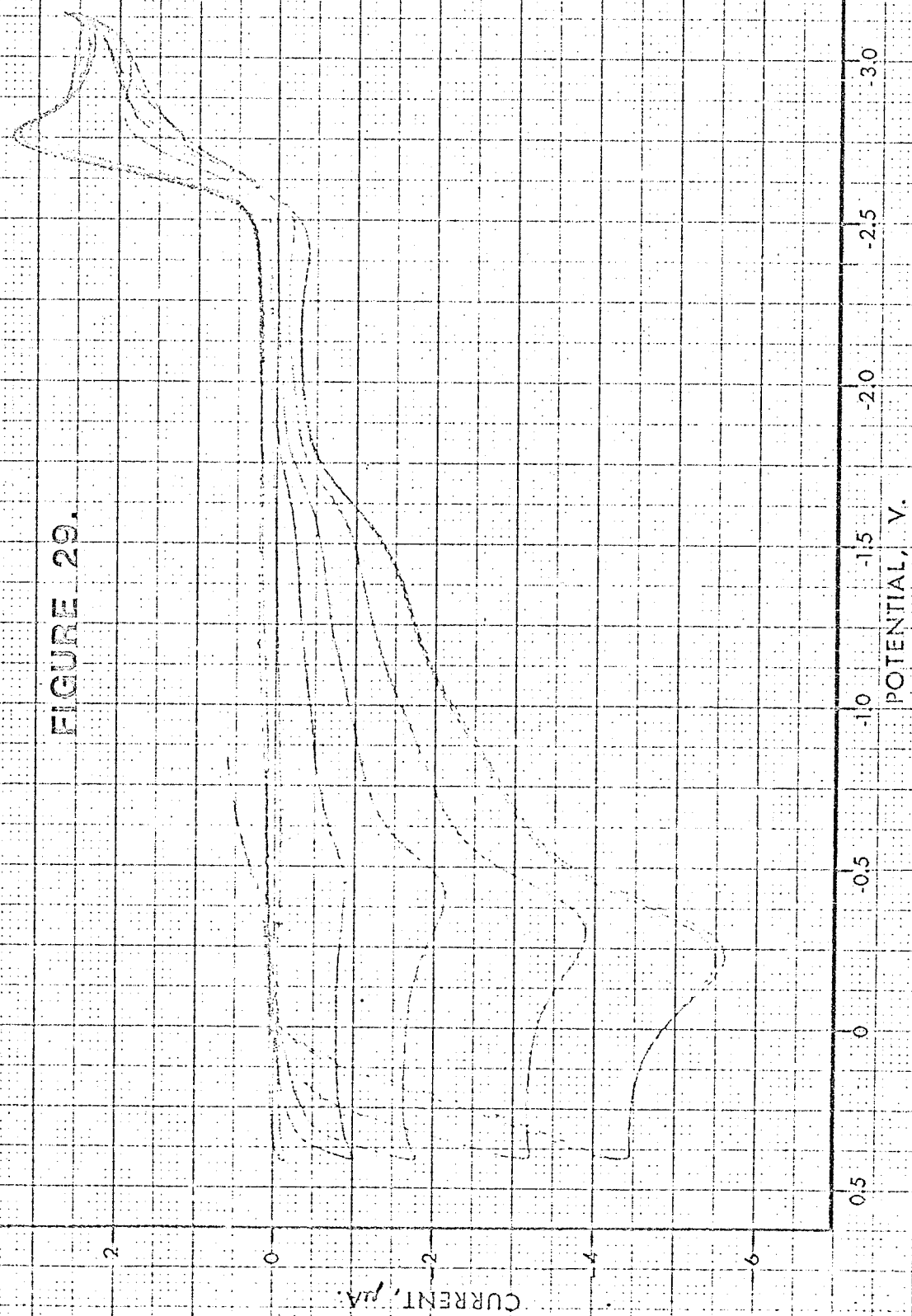
FIGURE 29.

CYCLIC VOLTAMMOGRAM WITH ASYMMETRIC POTENTIAL SCAN FOR 1,1-DIPHENYL-ETHYLENE, 0.87 mM, IN 0.1M $\text{N}(\text{Bu})_4\text{ClO}_4$ -THF SOLUTION.

Forward scan rate; 0.07 V/sec.

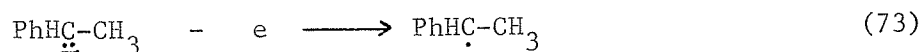
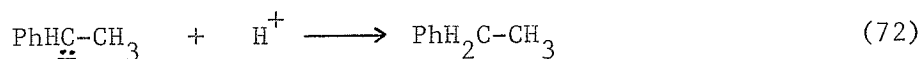
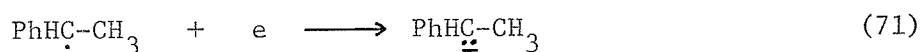
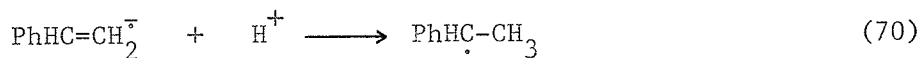
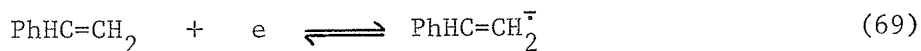
Reverse scan rates; 0.35, 0.70, 1.4, 2.1 V/sec.

FIGURE 29.



of protonation of the 1,1-diphenylethylene carbanion, presumably due to the steric effect of the two phenyl substituents at the nucleophilic site.

STYRENE. Under the experimental conditions used here, the cyclic voltammogram for styrene (Figure 30) resembled that for 1,1-diphenylethylene, except that the peak due to anodic reoxidation of the carbanion was very much smaller than expected for a one electron transfer. This behavior was consistent with the diminished steric hindrance in the styrene carbanion compared with the 1,1-diphenylethylene carbanion. A second protonation step (equation 72) thus takes place before electrolytic reoxidation (Equation 73) can occur:



To aid in comparing the behavior of the phenyl substituted ethylenes, cyclic voltammograms for each, obtained under identical conditions are shown in Figure 31, and some of the numerical data available from the cyclic voltammograms are presented in Table III. Some general features of the results in this Table should be noted. The peak potentials are measured against a silver wire electrode, and therefore comparison between the results for different substances is probably unjustified; however, the relative potentials for different

FIGURE 30.

CYCLIC VOLTAMMOGRAM FOR THE REDUCTION OF STYRENE, 1.44 mM, IN
 $\text{N}(\text{Bu})_4\text{ClO}_4$ -THF SOLUTION.

Scan rates; 0.07, 0.14, 0.24, 0.34, 0.48, 0.68 V/sec.

FIGURE 30.

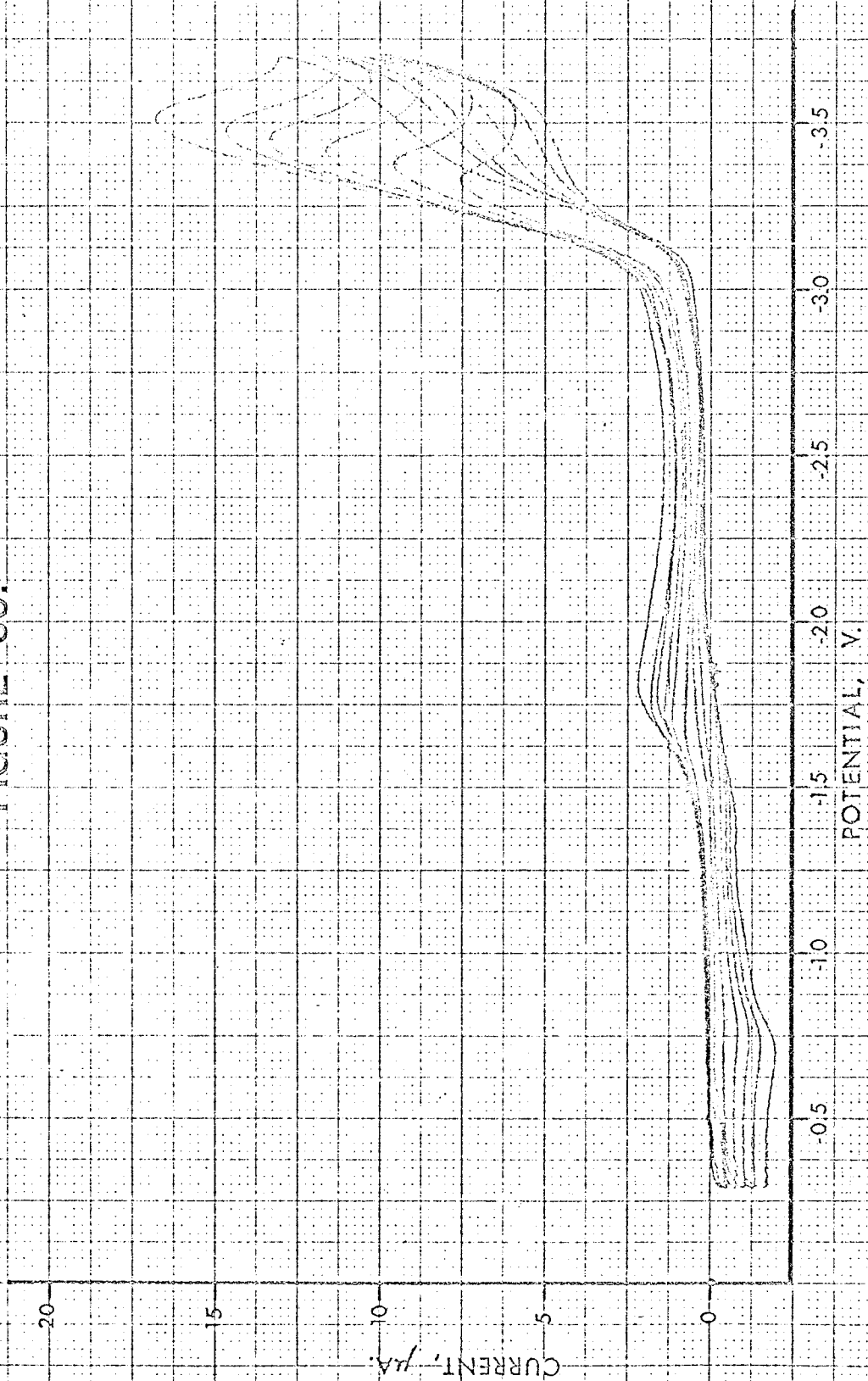


FIGURE 31.

A COMPARISON OF CYCLIC VOLTAMMOGRAMS FOR THE PHENYL-SUBSTITUTED ETHYLENES.

- A. TETRAPHENYLETHYLENE (0.90 mM).
- B. TRIPHENYLETHYLENE (0.87 mM).
- C. TRANS-STILBENE (1.16 mM).
- D. 1,1-DIPHENYLETHYLENE (0.87 mM).
- E. STYRENE (1.44 mM).

All voltammograms were obtained under similar conditions in 0.1M $\text{N}(\text{Bu})_4\text{ClO}_4$ -THF with a scan rate of 0.15 V/sec.

FIGURE 31.

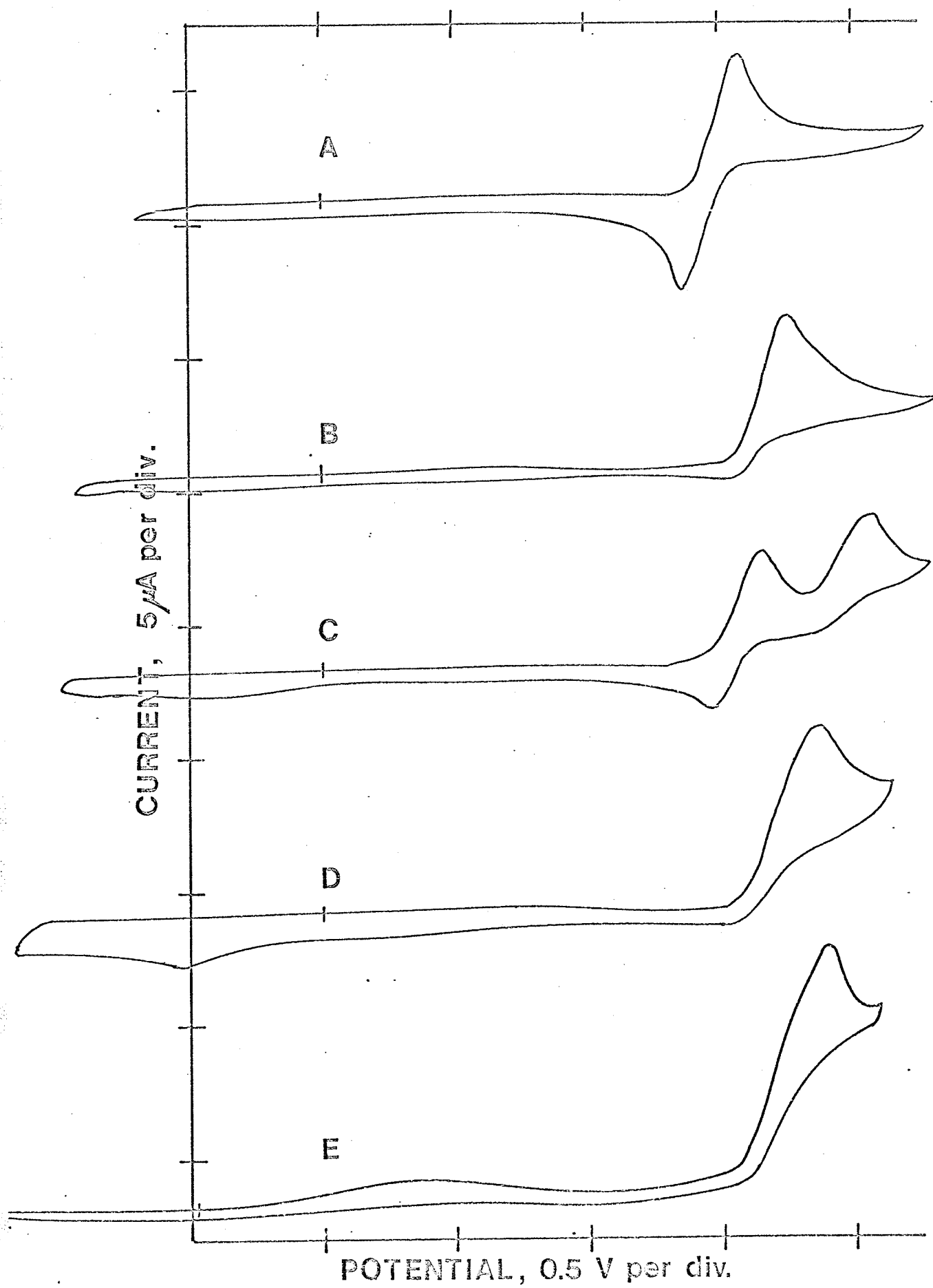


TABLE III.

CYCLIC VOLTAMMETRIC DATA FOR PHENYL-SUBSTITUTED ETHYLENES.

	Tetraphenyl- ethylene	Triphenyl- ethylene	Stilbene	1,1-Diphenyl ethylene	Styrene
$(E_{p,c})_{i=0}$, Volts (i).	-2.47	-2.61	-2.55 -2.90	-2.56	-3.18
Millimolar peak height, $\mu A/mm$.	3.16	3.16	1.85 ~1.8	3.05	3.54
$\Delta E_p / \Delta i_p$, $\mu A/mV$.	18	27	22 23	29	20
$(E_p - E_{p/2})_{i=0}$, mV.	42	36	67 -	100	100
$(E_{p,a})_{i=0}$, Volts (i).	-2.39	-0.82	-2.48 -0.65	-0.52	-0.80
Relative n_{ox} (ii).	2	1	1 0.5	1	0.2
$\Delta E_p / \Delta i_p$, $\mu A/mV$.	25	71	20 40	40	55

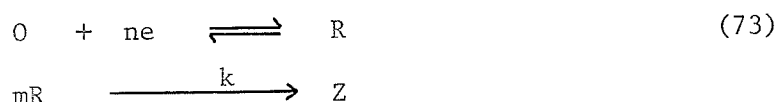
(i) Peak potentials at zero current vs. Ag wire in 0.1 M $N(Bu)_4ClO_4$ -THF solution.

(ii) Apparent number of electrons in reoxidation step. Determined by relative peak height increase with scan rate.

peaks in a given voltammogram are reproducible within the quoted limits.

In order to facilitate comparison, the peak heights for all substances are quoted for a given concentration and scan rate. The variation in peak heights, therefore, depends on the number of electrons transferred and the diffusion coefficient in each case.

The variation in peak potential with scan rate again provides important diagnostic information on the electrode processes. As mentioned previously, for an uncomplicated reversible electron transfer process, the peak potential is independent of the scan rate. For an irreversible electron transfer, the variation in peak potential with scan rate depends on the transfer coefficient (42). A more complicated variation is found in general for electron transfers coupled to homogeneous chemical reactions (71). However, for a reversible electron transfer followed by a fast irreversible chemical reaction, the voltammogram is identical to that for an irreversible electron transfer with the transfer coefficient α equal to one. Thus, a modification of equation (42) is applicable in this case as was indicated first by Saveant and Vianello (103). For the process



the peak potential varies linearly with the logarithm of the scan rate. Thus, at 25°C a ten-fold increase in the scan rate results in a peak variation of $60/n (m + 1)$ mV. The practical effect of these predictions on the shape of experimental voltammograms reported in this thesis is

of interest. Consider the voltammogram for a given concentration of electroactive species where the scan rate is chosen to give an initial peak height of 1 μA at some potential E_p . For a reversible electron transfer, it has been shown previously that under the experimental conditions employed, the uncompensated ohmic resistance introduces a linear variation of peak potential with scan rate of 20 mV per μA peak height. The additional variations of peak potential expected for subsequent chemical reactions and for irreversible charge transfers were calculated for a typical range of scan rates, and the results were presented graphically in Figure 32. It may be seen that deviations from linearity are relatively small for those cases involving subsequent chemical reactions. Experimentally, the cathodic peak potentials for all the substituted ethylenes are found to vary linearly with scan rate; the voltammograms are not sufficiently accurate to enable detection of the small degree of curvature expected for the non-reversible process. However, the rate of cathodic peak shift with current, $\Delta E_p / \Delta i_p$ (Table III) is, in general, larger for processes which were irreversible, with two exceptions. Despite the absence of anodic peaks for the styrene and stilbene (second peak) voltammograms, $\Delta E_p / \Delta i_p$ for the cathodic peaks is almost that expected for the reversible case. A possible explanation is that the rate of chemical reaction is not sufficiently fast relative to the scan rate for the simplifying conditions to apply. In this case, $\Delta E_p / \Delta i_p$ may approach that for a reversible transfer process (71).

In the discussion on the shape of the voltammograms, it has been implicitly assumed that the absence of an anodic peak for a

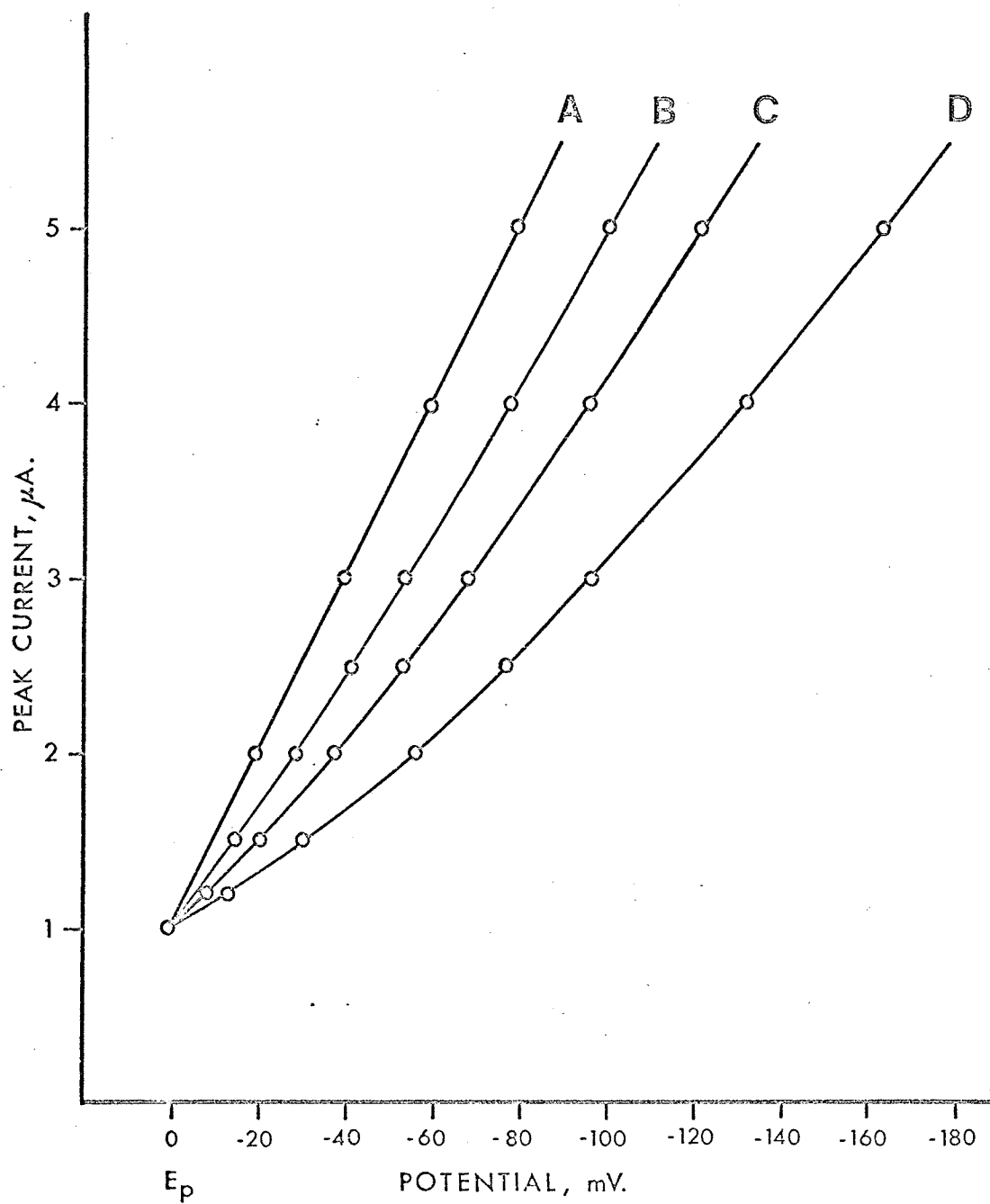
FIGURE 32.

THE VARIATION OF PEAK POTENTIAL WITH PEAK CURRENT AS THE SCAN RATE IS INCREASED.

- A. REVERSIBLE ELECTRON TRANSFER, $O + ne = R$.
- B. REVERSIBLE TWO-ELECTRON TRANSFER, FOLLOWED BY A FAST FIRST ORDER REACTION, $O + 2e = R$, $R \xrightarrow{k} Z$.
- C. REVERSIBLE ONE-ELECTRON TRANSFER FOLLOWED BY A FAST FIRST ORDER REACTION, $O + e = R$, $R \xrightarrow{k} Z$.
- D. IRREVERSIBLE ELECTRON TRANSFER, $O + ne \longrightarrow R$, ($\alpha n_a = 0.5$).

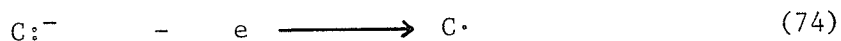
Other details in text.

FIGURE 32.



given process indicates that the product of the cathodic process is depleted by chemical reaction. However, if the electrochemical reaction were totally irreversible, then the anodic process would also be absent. This latter explanation is unlikely because in every case where a cationic process appears irreversible, a new oxidation peak at anodic potentials appears. These oxidation peaks, ascribed to carbanionic species formed from the initial reduction products, would not result from a slow (irreversible) electron transfer.

By consideration of Figure 32, it appears that a fast electron transfer followed by a homogeneous reaction has a lower value of $\Delta E_p / \Delta i_p$ than a slow (irreversible) electron transfer. The values in Table III for the reduction processes are compatible with the former mechanism. However, the values of $\Delta E_p / \Delta i_p$ listed for the oxidation peaks at anodic potentials are much larger, suggesting that the rate of electron transfer is slow for the process



In summary, the results for the phenyl substituted ethylenes show that as expected from chemical considerations, the stability of the anionic species produced by electrolytic reduction increases with the number of phenyl substituents. This is illustrated in Table IV. Cyclic voltammetry thus indicates the nature of the electron transfer reactions with much less ambiguity than classical polarography. In addition, the previously unreported carbanion electro-oxidation may be investigated.

TABLE IV.

A SUMMARY OF THE RELATIVE STABILITIES OF THE ANIONIC SPECIES DERIVED
FROM PHENYL-SUBSTITUTED ETHYLENES UNDER VOLTAMMETRIC CONDITIONS.

Compound	Dianion, R^{2-}	Radical-anion, $R^{\bullet-}$	Carbanion, $RH^{\bullet-}$
Tetraphenylethylene	Stable	—	—
Triphenylethylene	Protonated	—	Stable
Stilbene	Protonated	Stable	Protonated
1,1-Diphenylethylene	—	Protonated	Stable
Styrene	—	Protonated	Protonated

One unexpected result of relevance to electropolymerization studies is that under the experimental conditions for voltammetry, the radical anions of styrene and 1,1-diphenylethylene do not dimerize, but undergo protonation and further reduction. These radical-ions are therefore more basic than those derived from polycyclic hydrocarbons. As the tetrabutylammonium cations are the source of the protons, the use of such salts in vinyl polymerizations will lead to inefficient chain initiation. However, the results reported for controlled potential electrolyses in DMF at higher styrene concentrations and lower electrolyte concentration show that these conditions favour dimerization.

In view of results indicating the importance of protonating reactions in tetrabutylammonium electrolytes, numerous attempts were made to study electron transfer reactions in solutions of alternative electrolytes. These will now be considered.

INVESTIGATION OF ALTERNATIVE ELECTROLYTE SYSTEMS

Acenaphthylene Reduction in THF with Sodium Tetraphenylboride as Electrolyte.

The behavior of carbanions associated with alkali metal counterions is of interest because of the importance of these species in living anionic polymerizations. The use of alkali metal salts as electrolytes would facilitate a study of such processes without interference from protonation reactions. Unfortunately, as mentioned previously, the discharge potential of sodium ions is less cathodic

than that for most monomers. Direct electron transfer to the monomer does not occur, and voltammetric measurements are not informative. However, acenaphthylene reduces at relatively anodic potentials, and is also of interest as it may be polymerized by sodium metal. The reduction of acenaphthylene in tetrahydrofuran with sodium tetraphenylboride as supporting electrolyte was therefore studied by cyclic voltammetry. This particular salt was chosen because it is sufficiently soluble in THF and it has been shown to be inert to attack by very basic carbanions (44,45).

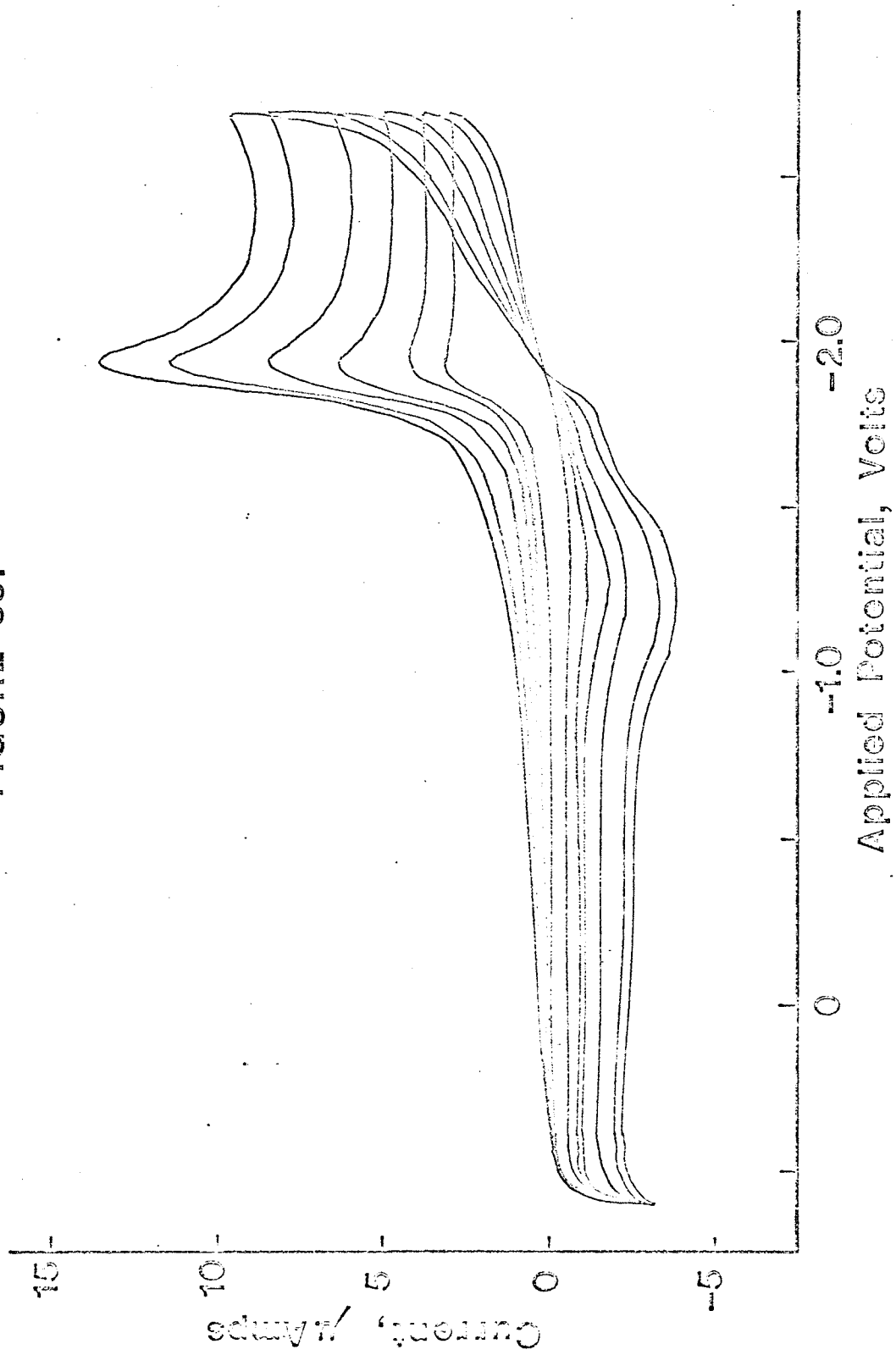
The use of sodium tetraphenylboride in place of tetrabutylammonium perchlorate resulted in a marked change in the shape of voltammograms. Instead of the pattern of four peaks obtained with the tetra-alkylammonium salt (Figure 19), only a single reduction peak was found in the region below sodium ion discharge (Figure 33). With sodium tetraphenylboride it was difficult to obtain reproducible voltammograms. Unless the electrolyte was carefully purified, peak heights indicated that a two electron process took place. In order to obtain reproducible peak heights, it was necessary to scan in an anodic direction to potentials at which decomposition of solvent or electrolyte could occur before commencing the cathodic scan. Otherwise peak heights were erratic, possibly because of film formation on the electrode. The alteration in the shape of the voltammograms on changing the supporting electrolyte emphasized the effect of the positive counterion on the reactivity of the reduced species. With sodium tetraphenylboride, no reverse peak or trace of a second

FIGURE 33.

CYCLIC VOLTAMMOGRAM OF ACENAPHTHYLENE, 2.0 mM, IN 1.0M
 NaBPh_4 -THF SOLUTION.

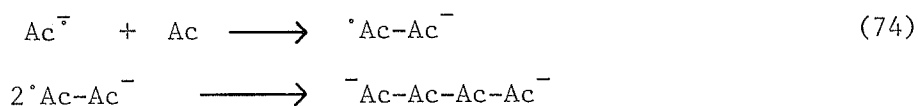
Scan rates; 0.07, 0.14, 0.21, 0.35, 0.56, 0.70 V/sec.

FIGURE 33.



reduction peak was apparent. The peak heights were rather smaller than those with tetrabutylammonium salts, and the current flowing at potentials more cathodic than the peak potential was higher than normal.

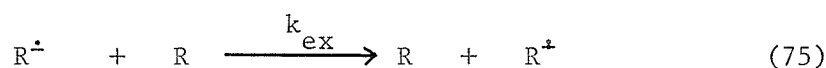
The lack of an anodic peak implies that either the radical anion formed initially reacts with some species in solution, or that the electron transfer process is very slow. If the former explanation is correct, then the acenaphthylene radical anion with sodium counterion is more reactive than the same radical anion associated with a tetrabutylammonium counterion. Some evidence for enhanced radical anion reactivity with alkali metal counterions has been published (104). Dimerization might account for the irreversibility of the voltammogram. Alternatively, attack on a neutral acenaphthylene molecule may be energetically feasible. This latter is consistent with the mechanism proposed by Rembaum for initiation of the anionic polymerization of acenaphthylene (105).



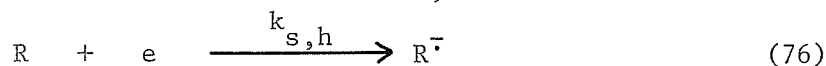
However, the voltammetric shape (Figure 33) is not entirely in accord with either of these mechanisms. Although all the usual precautions were taken, it is conceivable that traces of impurity were reacting with the reduction product.

The possibility that the irreversible character of the reduction of acenaphthylene was due to a slow electron transfer process

must also be considered. In tetrahydrofuran, the ionic species exist as ion aggregates; thus acenaphthylene radical anion is associated with a solvated cationic counterion. The reduction process must therefore involve the simultaneous transfer of a sodium cation from the electrode surface to the acenaphthylene radical anion. Conceivably, this process may be slower for the more tightly adsorbed sodium ions than for the larger tetra-n-butylammonium ions. An interesting, if circuitous, argument may be advanced against this explanation. Marcus (106) in a theoretical treatment of electron transfer reactions derived a relationship between the homogeneous rate constant k_{ex} for the electron exchange reaction



and the heterogeneous rate constant $k_{s,h}$ for the electrode process



The relationship may be simplified to give:

$$(k_{ex}/Z_{solv})^{1/2} \simeq k_{s,h}/Z_{el} \quad (77)$$

where Z_{solv} and Z_{el} are collision frequencies, of about 10^{11} mole⁻¹sec⁻¹ and 10^4 cm sec⁻¹ respectively. If the rate of homogenous electron exchange can be determined, then the order of magnitude of the electron transfer rate at an electrode may be calculated. Electron spin resonance techniques have been used to determined the rate of electron exchange between aromatic radical anions and molecules (108); with alkali metal counterions in tetrahydrofuran the values for k_{ex}

lie between 10^7 and 10^{10} litres mole⁻¹ sec⁻¹. By substitution into equation (77) the electron transfer rate constant, $k_{s,h}$ under similar conditions should be greater than 10^2 cm sec⁻¹. In fact, if the experimental voltammograms are irreversible because of slow electron transfer, then k_s must be less than 10^{-5} cm sec⁻¹. (This value was estimated for the voltammogram under discussion by using Nicholson's criterion for irreversibility (74)). Even allowing for the approximate nature of the calculations, the difference of seven orders of magnitude between the apparent and calculated rate constants appears to rule out a slow electron transfer as explanation for the irreversible nature of the voltammograms with sodium counterions. It should be mentioned that this argument relating esr and voltammetric data already has been applied with reasonable success to the electrolytic reduction of anthracene with tetra-alkylammonium counterions in DMF (89).

The difference in voltammetric behavior on changing the supporting electrolyte is not restricted to acenaphthylene reduction. A variety of other hydrocarbons give similar results. For example, with lithium perchlorate as electrolyte, stilbene gave only one distorted irreversible peak instead of the series of peaks found previously with tetrabutylammonium perchlorate (Figure 28). Again, recent esr data (108) substituted into equation 77 indicates that the electron transfer is fast, and so the irreversibility apparently results from chemical reaction.

α -Methylstyrene Reduction in Hexamethylphosphoramide with
Tetramethylammonium Tetraphenylboride Electrolyte.

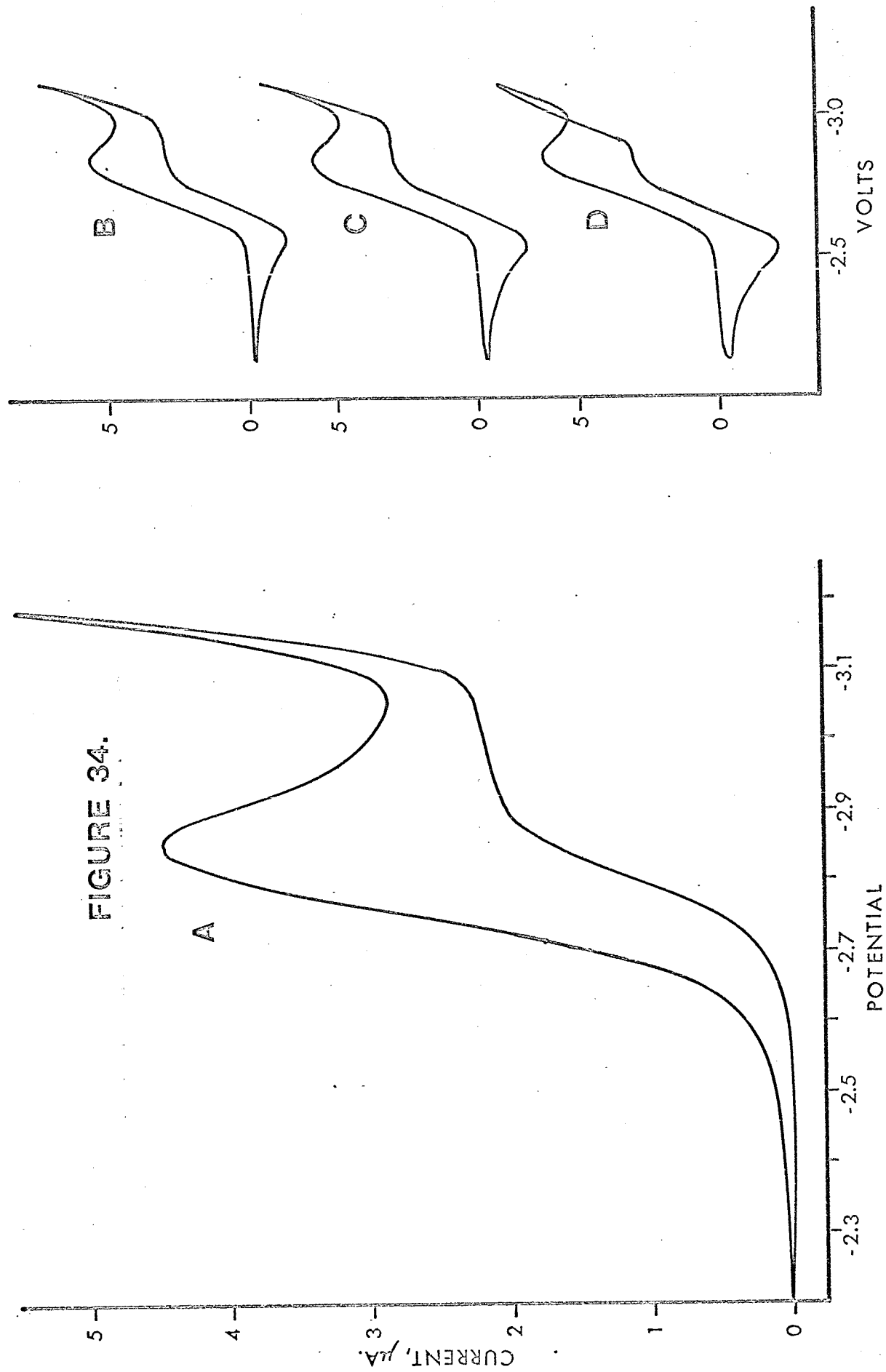
The difficulty in obtaining reproducible voltammograms with alkali metal salts as supporting electrolytes led to further investigations of possible inert cations. It was suggested (109) that tetramethylammonium salts would be more stable than tetra-alkyl-ammonium salts containing β hydrogen atoms. Accordingly, tetramethylammonium tetraphenylboride was synthesized, but this salt was insufficiently soluble in tetrahydrofuran to give useful results. The possibility that hexamethylphosphoramide $(N(CH_3)_2)_3PO$ would be a suitable solvent was investigated. This compound is not attacked by carbanions (110) or alkali metals (111), and has a relatively high dielectric constant (112). Its use as a solvent for electrolytically living initiated anionic polymerization was demonstrated by Bhadani (113) who reported that α -methylstyryl anions were stable in a hexamethylphosphoramide solution of tetramethylammonium tetraphenylboride.

Some exploratory voltammetric experiments were therefore performed with this solvent and salt. A background scan with salt and solvent alone was satisfactory. On adding α -methylstyrene, the voltammogram shown in Figure 34 was obtained. At low scan rates, the peaks were clearly indicative of an irreversible process. The peak height was close to the value expected for a one electron transfer. This correlation was based on the data obtained in tetrahydrofuran solution; the effects of uncompensated resistances in tetrahydrofuran

FIGURE 34.

CYCLIC VOLTAMMOGRAMS FOR α -METHYLSTYRENE, 4.0 mM, IN HEXAMETHYL-
PHOSPHORAMIDE WITH 0.04M $N(CH_3)_4BPh_4$ AS SUPPORTING ELECTROLYTE.

- A. SINGLE SCAN, AT 0.02 V/SEC.
- B. STEADY STATE MULTICYCLE SCAN, AT 0.8 V/SEC.
- C. STEADY STATE MULTICYCLE SCAN, AT 1.2 V/SEC.
- D. STEADY STATE MULTICYCLE SCAN, AT 2.0 V/SEC.



and in hexamethylphosphoramide were similar, as a lower salt concentration was used with the latter. A one electron transfer mechanism implied that in this solvent/salt system, the α -methylstyrene radical anion was not protonated and further reduced, but underwent further chemical reaction.

In this system, the potentialities of cyclic voltammetry were further illustrated by increasing the scan rate over three orders of magnitude. At higher scan rates (Figure 34) an anodic peak became apparent, indicating that the chemical reaction was no longer sufficiently fast to remove all the radical anions formed during the cathodic scan. When the scan rate reached about 20 volts/sec, the voltammograms (obtained using an oscilloscope) were effectively reversible. A rough estimate of the pseudo first order rate constant for the chemical reaction may be made by considering the theoretical data of Nicholson and Shain (71). They showed that for a voltammogram shape to change from reversible to totally irreversible, k_f/a should increase from 0.05 to 10, where k_f is the first order rate constant for the succeeding chemical reaction (equation 43) and $a = nFv/RT$. Substituting the experimental scan rate values, k_f is found to be of the order of 40 sec^{-1} . Thus the method is applicable to the fast reactions of labile radical-anion species. A more detailed examination of the voltammograms was not feasible due to experimental and theoretical difficulties. Thus, at the higher scan rates, the voltammograms were obtained for steady state multicycle potential scans; the repetitive scan theory is more

complex than that for single scan techniques considered in the introduction of this thesis, and has only been calculated for uncomplicated reversible electron transfers (70).

On considering the nature of the reaction system, the assumption that the radical anion disappears in a pseudo first order reaction is probably unjustified. It serves, however, to illustrate the order of magnitude of rates of reaction accessible by the technique. A more likely reaction, considering the relative concentrations of species present near the electrode, is dimerization. This conclusion is suggested by the study by Szwarc of the reactions of α -methylstyrene radical anions associated with sodium counterions (114). However, the experimental results were insufficiently detailed, and the half-life for the dimerization was too large compared to the scan rates for the theoretical correlations (77,78) to be useful.

These results in hexamethylphosphoramide with tetramethylammonium salts are very significant in that the single electron transfer demonstrated that protonation and subsequent further reduction did not occur. This solvent system is, therefore, eminently suitable for the study of the more reactive radical anions and carbanions which were found to suffer protonation in the tetrahydrofuran solutions of tetrabutylammonium salts.

Other Applications of Cyclic Voltammetry to Electropolymerizations.

In the work reported in this thesis, the emphasis has been on the study of electrode processes related to the initiation of anionic

chain polymerization. However, the methods of study are applicable to other problems in electrolytic polymerization. Two examples will be considered briefly.

Mechanism of Salt Discharge.

It was shown (45) that termination in electrolytic living anionic polymerizations was due to chemical species produced by the anodic discharge of tetraphenylboride ions. The voltammetry of the sodium tetraphenylboride alone was uninformative, but with tetrabutylammonium perchlorate as supporting electrolyte, perchlorate anion was discharged at a more anionic potential than tetraphenylboride, and tetrabutylammonium cation was discharged at a more cathodic potential than sodium. In this case, clear peaks for both tetraphenylboride and sodium ion discharge were obtained. The peak heights were in the ratio 5:2, indicating that at least two electrons were involved in the tetraphenylboride reduction. Furthermore, the sodium ion peak was irreversible in this solvent and electrolyte, suggesting that the electrolytically generated sodium atoms reacted with tetrabutylammonium ions. These results, readily obtained, were useful in interpreting the chemical data.

Electrolytic Formation of Highly Reactive Monomer.

As mentioned in the introduction to this thesis, Gilch (49), polymerized α -halogenated p-xylenes to give poly-p-xylylenes by electrolysis at a mercury cathode in aqueous dioxane with HCl as electrolyte. He postulated a mechanism involving the formation of

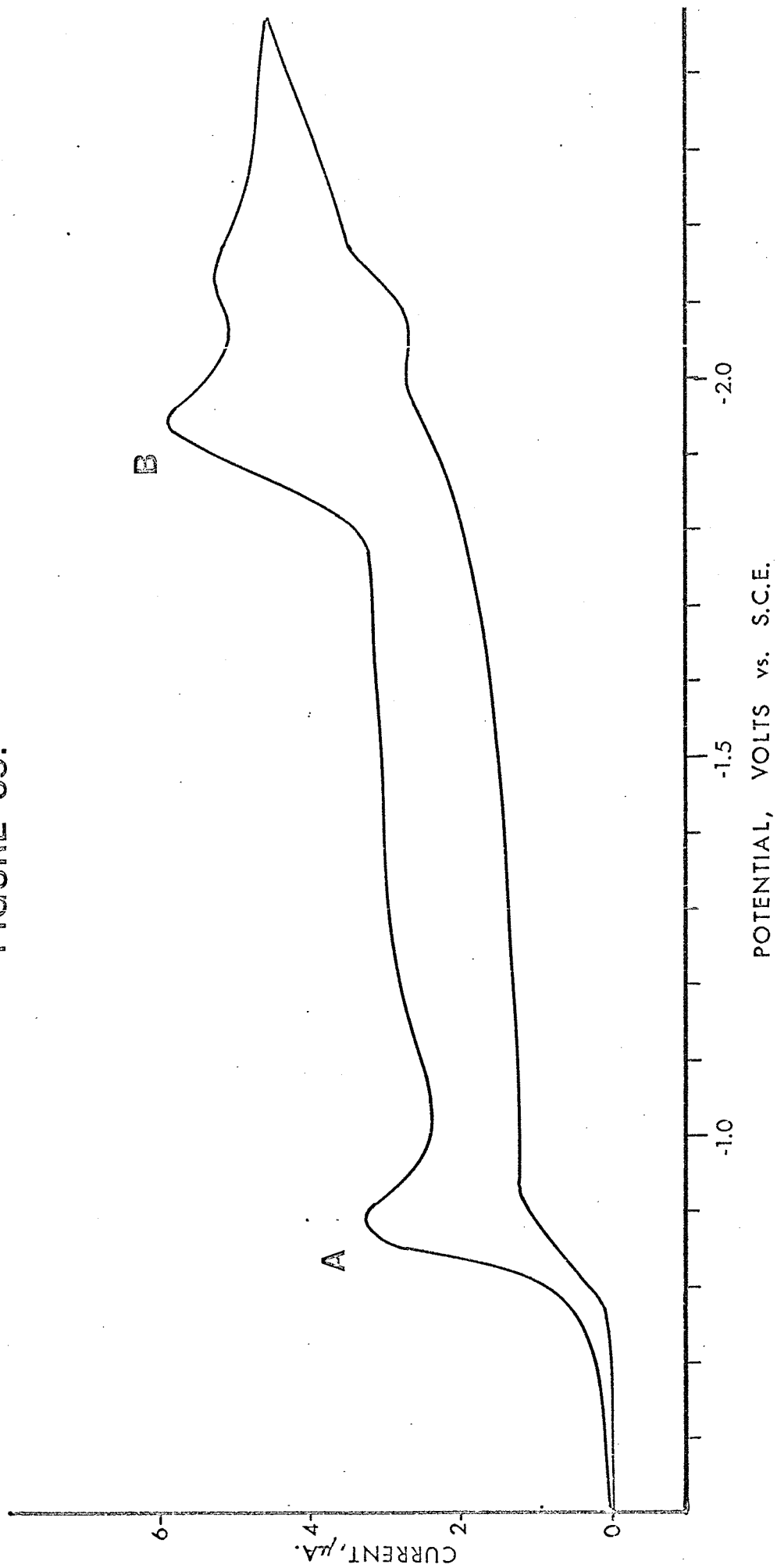
halogenated xylenes via carbanionic intermediates. As carbanions would be extremely unstable in an aqueous acidic medium, it appeared worthwhile, on the basis of this mechanism, to try similar reactions in aprotic solvents. It was found that α,α' -dibromo-p-xylene and $\alpha,\alpha,\alpha',\alpha',\alpha',\alpha'$ -hexachloro-p-xylene in dimethylformamide polymerized readily on controlled potential electrolysis in dimethyl formamide/tetrabutylammonium halide solution. Cyclic voltammetry of the brominated xylene at a hanging drop mercury electrode indicated a second cathodic reduction process in addition to the expected halogen elimination (Figure 35, Peak A). Gilch suggested that the product of the halogen elimination was the reactive species $\text{H}_2\text{C}=\text{C}_6\text{H}_4=\text{CH}_2$. On the basis of Huckel molecular orbital calculations for the lowest unoccupied orbital of this species (115), its electrochemical reduction was expected in the region of the second peak (Peak B, Figure 35). The voltammogram thus provided experimental evidence for the existence of the xylylene intermediates in the electrolytic polymerization. This work was, however, rendered superfluous by a recent paper by Covitz (50) on the electrochemical reduction of α,α' -dibromo-p-xylene. Using polarography, controlled potential electrolysis, coulometry and cyclic voltammetry he reached the same conclusions on the nature of the second reduction step and suggested a reasonable mechanism for the halide elimination. The experiments with α -halogenated xylenes were reported because they were performed before Covitz's results were published, and they illustrate a further application of cyclic voltammetric methods to electropolymerization reactions.

FIGURE 35.

CYCLIC VOLTAMMOGRAM FOR α, α' -DIBROMO-p-XYLENE, 1.0 mM, IN
DIMETHYLFORMAMIDE, WITH 0.03M $N(Bu)_4ClO_4$ AS SUPPORTING ELECTROLYTE.

Scan rate, 0.04 V/sec at a hanging drop mercury electrode. The
potential was measured relative to a saturated calomel reference
electrode.

FIGURE 35.



CONCLUSIONS

1. Controlled potential electrolytic initiation of anionic vinyl polymerization by direct electron transfer is feasible under appropriate conditions.
2. The reaction of the tetrabutylammonium cation with carbanions derived from vinyl compounds plays an important role in inhibiting these electro-initiated polymerizations.
3. The unusual variation in voltammetric peak heights with monomer concentration may be qualitatively explained in terms of protonation, dimerization and polymerization reactions following the electron transfer step. Thus, for styrene, as the ratio of monomer to tetrabutylammonium salt is increased, the reaction products change from ethylbenzene to 1,4-diphenylbutane, and then to polystyrene. These results are confirmed by controlled-potential electrolysis and coulometry.
4. The results obtained with diphenylpicrylhydrazyl show that cyclic voltammetry at a stationary platinum electrode is a very useful method for the study of electron transfer processes in tetrahydrofuran. Diphenylpicrylhydrazyl forms five relatively stable ionic and radical species in solution. The results also show that care is needed in interpreting the effect of free radical inhibitors on electro-initiated polymerizations.
5. The most useful aspect of cyclic voltammetry is that the fate

of the species formed by electron transfer from the electrode may be investigated. By this means, the relative reactivities of the radical anions, dianions and carbanion reduction products of acenaphthylene, acenaphthene, acenaphthylene dimers, and of five phenyl-substituted ethylenes were qualitatively determined. This application of cyclic voltammetry has not been reported previously.

6. The results for several of the phenyl-substituted ethylenes in tetrahydrofuran - $N(Bu)_4ClO_4$ solution indicate that their radical-anions are protonated in this medium, and are therefore stronger nucleophiles than the polycyclic aromatic hydrocarbons. However, preliminary voltammetric experiments in hexamethylphosphoramide with tetramethylammonium tetraphenylboride as electrolyte suggest that radical anion protonation is less important in this system. This solvent and electrolyte are therefore eminently suitable for electrochemical studies of organic anions, and also for electropolymerizations.

7. The results presented in this thesis show that in principle, cyclic voltammetry may be used to determine quantitatively the rate of the fast homogeneous reactions undergone by the reduction products. In practice, the high solution resistance caused distortion of the voltammograms at higher scan rates, so that the range of scan rates available was generally too small to allow quantitative deductions. The recent development of electronic resistance compensators may eliminate this problem.

8. The experimental methods are also applicable to a study of the mechanism of electrolyte discharge and of the electrolytic reactions associated with the formation of poly-p-xylenes.

REFERENCES.

1. Funt, B.L., Macromol. Revs., 1, 35 (1967).
2. Arnaud, P., J. Four. Elec., 71, 189 (1966).
3. Asahara, T. and M. Seno, Yuki Gasei Kagaku Kyokai Shi, 25, 719 (1967). C.A., 67: 109014s.
4. Fioshin, M.Ya. and A.P. Tomilov, Plast. Massy, 10, 2 (1960).
5. Ukida, J., S. Usami and T. Kominami, Talanta, 12, 1163 (1965).
6. Bezuglyi, V.D., E.K. Saliichuk, T.A. Alekseeva and A.I. Karamysheva, Vysokomol. Soedin, Ser. A, 9, 1867 (1967).
7. Goldschmidt, S. and E. Stockl, Chem. Ber., 85, 630 (1952).
8. Smith, W.B. and H.G. Gilde, J. Amer. Chem. Soc., 82, 659 (1960).
9. Smith, W.B. and D.T. Manning, J. Polymer Sci., 59, S45 (1962).
10. Porejko, S. and L. Perec, Polimery, 11, 68 (1966).
11. Funt, B.L. and K.C. Yu, J. Polymer Sci., 62, 359 (1962).
12. Tsvetkov, M.S. and E.P. Koval'chuk, Visn. L'viv Derzh. Univ., Ser. Khim., 8, 24 (1965). C.A., 66: 65878z.
13. Shapoval, G.S., Ukr. Khim. Zh., 33, 946 (1967). C.A., 67:117370v.
14. Elbersen, L., Electrochim. Acta, 12, 1473 (1967).
15. Vijh, A.K. and B.E. Conway, Chem. Revs., 67, 623 (1967).
16. Das, M.N. and A.R. Palit, Sci. Cult. (Calcutta), 16, 34 (1950).
17. Tidswell, B.M., Soc. Chem. Ind., Monograph 20, 130 (1966).
18. Dineen, E., T.C. Schwann and C.L. Wilson, J. Electrochem. Soc., 96, 226 (1949).
19. Parravano, G., J. Amer. Chem. Soc., 73, 628 (1951).
20. Kern, W. and H. Quast, Makromol. Chemie, 10, 202 (1953).
21. Tsvetkov, N.S., Vysokomol. Soedin, 3, 549 (1961); Polymer Sci. USSR, 3, 570 (1962).

22. Tsvetkov, N.S. and Z.F. Glotova, Vysokomol. Soedin, 5, 997 (1963); Polymer Sci. USSR, 5, 49 (1964).
23. Tsvetkov, N.S. and E.P. Koval'chuk, Visn. L'viv Derzh. Univ., Ser. Khim., 7, 32 (1964). C.A., 64: 15989g.
24. Fedorova, A.I., I.V. Shelepin and N.B. Moiseeva, Dokl. Acad. Nauk SSSR, 138, 165 (1961).
25. Fedorova, A.I., K. Li and I.V. Shelepin, Zh. Fiz. Khim., 38, 1685 (1964); Russian J. Phys. Chem., 38, 920 (1964).
26. Fedorova, A.I. and S. Ya. Vashina, Elektrokimiya, 3, 742 (1967).
27. Kolthoff, I.M. and L.L. Ferstandig, J. Polymer Sci., 6, 563 (1951).
28. Breitenbach, J.W. and Ch. Srna, Pure Appl. Chem., 4, 245 (1962).
29. Murphy, M., M.G. Carangelo, M. B. Ginaine and M.C. Markham, J. Polymer Sci., 54, 107 (1961).
30. Funt, B.L. and F.D. Williams, J. Polymer Sci. A, 2, 865 (1964).
31. Shapoval, G.S. and V.I. Shapoval, Ukr. Khim. Zh., 31, 1080 (1965).
32. Baizer, M.M., Tetrahedron Letters, 973 (1963).
33. Baizer, M.M., J. Electrochem. Soc., 111, 215 (1964).
34. Baizer, M.M. and J.D. Anderson, J. Org. Chem., 30, 1351 (1965).
35. Feoktistov, L.G., A.P. Tomilov and I.G. Sevast'yonova, Elektrokimiya, 1, 1300 (1965).
36. Tomilov, A.P. and V.A. Klimov, Elektrokimiya, 3, 232 (1967).
37. Arad, Y., M. Levy, I.R. Miller and D. Vosfi, J. Electrochem. Soc., 114, 899 (1967).
38. Lazarov, S., A. Trifonov and T. Vitanov, Z. Phys. Chem., 226, 221 (1964).
39. Funt, B.L. and S.W. Laurent, Can. J. Chem., 42, 2728 (1964).
40. Funt, B.L. and S.N. Bhadani, Can. J. Chem., 42, 2733 (1964).
41. Funt, B.L. and S.N. Bhadani, J. Polymer Sci. A, 3, 4191 (1965).
42. Gilch, H. and D. Michael, Makromol. Chemie, 99, 103 (1966).
43. Yamazaki, N., S. Nakahama and S. Kambara, J. Polymer Sci. B, 3, 57 (1965).

44. Szwarc, M., Fortschr. Hochpolymer Forsch., 2, 275 (1960).
45. Funt, B.L., S.N. Bhadani and D. Richardson, Can. J. Chem., 44, 711 (1966).
46. Funt, B.L., S.N. Bhadani and D. Richardson, J. Polymer Sci. A-1, 4, 2871 (1966).
47. Funt, B.L. and H. Kubota, unpublished results.
48. Laurin, D. and G. Parravano, J. Polymer Sci. B, 4, 797 (1966).
49. Gilch, H.G., J. Polymer Sci. A-1, 4, 1351 (1966).
50. Covitz, F.H., J. Amer. Chem. Soc., 89, 5403 (1967).
51. Ross, S.D. and D.J. Kelley, J. Appl. Polymer Sci., 11, 1209 (1967).
52. Conway, B.E., "Theory and Principles of Electrode Processes", Ronald Press, New York, 1965.
53. Frank, H.S. and R.T. Thompson in "The Structure of Electrolytic Solutions", W.J. Hamer, Ed., Wiley, New York, 1959, Chapter 8.
54. Riddiford, A.C., in "Advances in Electrochemistry and Electrochemical Engineering", P. Delahay and C.W. Tobias, Eds., Wiley, New York, Volume 4, 1966, p. 47.
55. Delahay, P., "Double Layer and Electrode Kinetics", Interscience, New York, 1965.
56. Kortum, G., "Treatise on Electrochemistry", 2nd English ed., Elsevier, New York 1965.
57. Delahay, P., "New Instrumental Methods in Electrochemistry", Interscience, New York, 1965.
58. Ives, D.J.G., and G.J. Janz, "Reference Electrodes", Academic Press, New York, 1961.
59. Meites, L., in "Technique of Organic Chemistry", Volume 1, 3rd ed, A. Weissberger, Ed., Interscience, New York, 1960, p 3281.
60. Rechnitz, G.A., "Controlled-Potential Analysis", Pergamon Press, London, 1963.
61. Lingane, J.J., "Electroanalytical Chemistry", 2nd ed, Interscience, New York, 1958, p 222.

62. Delahay, P., "New Instrumental Methods in Electrochemistry",
p 283.
63. Nernst, W., Z. Phys. Chem., 47, 52 (1904).
64. Bauer, H.H., J. Electroanal. Chem., 16, 419 (1968).
65. Randles, J.E.B., Trans. Faraday Soc., 44, 327 (1948).
66. Sevcik, A., Collect. Czech. Chem. Commun., 13, 349 (1948).
67. Nicholson, M.M., J. Amer. Chem. Soc., 76, 2539 (1954).
68. Reinmuth, W.H., Anal. Chem., 33, 185 (1961).
69. Delahay, P., J. Amer. Chem. Soc., 75, 1190 (1953).
70. Matsuda, H., Z. Elektrochem., 61, 489 (1957).
71. Nicholson, R.S. and I. Shain, Anal. Chem., 36, 706 (1964).
72. Polcyn, D.S. and I. Shain, Anal. Chem., 38, 370 (1966).
73. Polcyn, D.S. and I. Shain, Anal. Chem., 38, 376 (1966).
74. Nicholson, R.S., Anal. Chem., 37, 1351 (1965).
75. Saveant, J.M., Electrochim. Acta, 12, 999 (1967).
76. Matsuda, H. and Y. Ayabe, Z. Elektrochem., 59, 494 (1955).
77. Nicholson, R.S., Anal. Chem., 37, 667 (1965).
78. Saveant, J.M. and E. Vianello, Electrochim. Acta, 12,
1545 (1967).
79. Saveant, J.M., Electrochim. Acta, 12, 753 (1967).
80. Wopschall, R.H. and I. Shain, Anal. Chem., 39, 1514 (1967).
81. Dolinski, J. and K. Dziewonski, Berichte, 48, 1917 (1915).
82. Bourne, B.E., Canadian Electronics Engineering, 6, 42 (1962),
Nat. Research Council, Publication NRC 6710.
83. "Organic Reagents for Organic Analysis", Hopkin and Williams
Ltd., Essex, England, 2nd ed. (1950), p 171.
84. American Petroleum Research Institute Project, Hydrocarbon
Infrared Spectra, Serial no. 2151.

85. Bhadani, S.N., M.Sc. Thesis, University of Manitoba, 1964.
86. Gray, D.G., M.Sc. Thesis, University of Manitoba, 1965.
87. Funt, B.L. and D.G. Gray, *Macromol. Chem.*, 1, 625 (1966).
88. Graham, R.K., D.L. Dunkelberger and W.E. Goode, *J. Amer. Chem. Soc.*, 82, 400 (1960).
89. Peover, M.E., *Electroanalytical Chemistry*, 2, 1 (1967),
A.J. Bard, Ed., Dekker, New York.
90. Hoijsink, G.J., J. van Schooten, E. de Boer and W.V. Aalbersberg,
Rec. Trav. Chim., 73, 355 (1954).
91. Badoz-Lambling, J. and M. Sato, *Acta Chim. Hung.*, 32, 191 (1962).
92. Perichon, J. and R. Buvet, *Electrochim. Acta*, 9, 587 (1964).
93. Solon, E. and A.J. Bard, *J. Amer. Chem. Soc.*, 86, 1926 (1964).
94. Anson, F.C., *Anal. Chem.*, 33, 939 (1961).
95. Kemula, W. and R. Sioda, *Bull. Acad. Pol. Sci., Ser. Sci. Chim.*, 11, 394 (1963).
96. Reinmuth, W.H., *Anal. Chem.*, 33, 1793 (1961).
97. Grodzka, P.G. and P.J. Elving, *J. Electrochem. Soc.*, 110,
231 (1963).
98. Streitwieser, A., "Molecular Orbital Theory for Organic Chemists",
p 178, Wiley, New York, 1961.
99. Dietz, R. and M.E. Peover, *Trans. Faraday Soc.*, 62, 3535 (1966).
100. Streitwieser, A. and S. Suzuki, *Tetrahedron*, 16, 153 (1961).
101. Iwaizumi, M. and T. Isobe, *Bull. Chem. Soc. Japan*, 37, 1651 (1964).
102. Wawzonek, S., E.W. Blaha, R. Berkey and M.E. Runner, *J. Electrochem. Soc.*, 102, 235 (1955).
103. Saveant, J.M. and E. Vianello, *Compt. Rend.*, 256, 2597 (1963).
104. Maricle, D.L., *Anal. Chem.*, 35, 683 (1963).
105. Moacanin, J. and A. Rembaum, *J. Polymer Sci. B2*, 2, 979 (1964).
106. Marcus, R.A., *J. Chem. Phys.*, 43, 679 (1965).

107. Johnson, C.S., "Advances in Magnetic Resonance", Academic Press, New York, 1965, 1, p 33.
108. Chang, R. and C.S. Johnson, Jr., J. Chem. Phys., 46, 2314 (1967).
109. Baizer, M.M., Central Research Laboratories, The Monsanto Company, Private communication, 1967.
110. Cuvigny, T., J. Normant and H. Normant, Compt. Rend., 258, 3502 (1964).
111. Fraenkel, G., S.H. Ellis and D.T. Dix, J. Amer. Chem. Soc., 87, 1406 (1965).
112. Dubois, J.E. and H. Viellard, J. Chim. Phys., 62, 699 (1965).
113. Bhadani, S.N., State College of Forestry, Syracuse, N.Y., Private communication, 1967.
114. Lee, C.L., J. Smid and M. Szwarc, J. Phys. Chem., 66, 904 (1962).
115. Coulson, C.A. and A. Streitwieser, Jr., "Dictionary of π -electron Calculations", W.H. Freeman, San Francisco, 1965.